EFFECT OF STRAIN RATE ON THE SHEAR STRENGTH OF QUESTA ROCK PILE MATERIALS

by

Kojo Anim

Submitted in partial fulfillment of the requirements for the Degree of Master of Science in Mineral Engineering with Specialization in Geotechnical Engineering

New Mexico Institute of Mining and Technology
Department of Mineral Engineering

Socorro, New Mexico
May, 2010

This thesis is dedicated to God for allowing His beauty to be seen in me. And also to my lovely wife Olivia Anim for her continual love, I would say there is no force which is more potent than love.

"Success is not measured by what you accomplish but by the opposition you have encountered, and the courage with which you have maintained the struggle against overwhelming odds." ***Orison Swett Marden***

Abstract

In order to investigate the strain rate (creep) effect on shear resistance of rock pile materials at the Questa molybdenum mine in New Mexico**,** samples from Spring Gulch rock-pile were collected for laboratory experimental analyses. A comprehensive understanding of the creep phenomenon requires testing of soil samples from the rock pile for both dry and moist conditions at different rates of shear displacement. Understanding the creep movement in rock piles under both dry and moist conditions will help to evaluate long-term stability of rock piles.

To perform these analyses, seventy two (72) direct shear strength tests on dry and moist samples from Spring Gulch rock pile were conducted using a direct shear test box with dimensions of 6 cm × 6 cm × 2.54 cm. The soil sample was prepared quantitatively by separating the soil fines, i.e. the material passing the sieve number 200, from the coarser portion by wet sieving as well as the sieve analysis of the oven-dry coarser portion. The materials left on different sieves were stored in different containers.

To prepare a sample, appropriate portions of these stored materials were mixed together to result in the gradation curve corresponding to the scalped material passing sieve number 6. The effect of rate of deformation on dry Spring Gulch rock pile material was investigated with a compaction density of 1850 kg/m^3 at four different rates, 0.5 mm/min, 0.05 mm/min, 0.0275 mm/min and 0.005 mm/min.

The effect of compaction densities (1700 kg/m^3 and 1850 kg/m^3) on moist (8% water content) samples were also investigated for all shearing rates. Normal stresses of 160 kPa, 480 kPa and 750 kPa were used. Three shear tests for each normal stress were

conducted to investigate the reproducibility of the test results. During the shear test, the shear stress, the shear displacement and the normal displacement were measured concurrently. The obtained internal friction angles versus rate of shear deformation were plotted in a semi-logarithmic format and the data show a fairly consistent linear trend.

For both the dry and the moist Spring Gulch rock pile materials, the shear strain rates used in this study show no major effect on the shear strength of the material, even though the friction angle and cohesion intercept are affected by the deformation rate. The internal friction angle of the rock pile materials in moist conditions decreases with increasing compaction density. In addition, cohesion increases with increasing the compaction density by keeping the water content unchanged.

ACKNOWLEDGEMENTS

I am heartily thankful to my supervisor, Dr. Ali Fakhimi, whose encouragement and guidance from the initial to the final level enabled me to develop an understanding of the subject. I also thank the members of my thesis committee: Dr. Virginia McLemore, Dr. Navid Mojtabai and Dr. Mehrdad Razavi for their guidance and suggestions. My special thanks go to Dr. Virginia McLemore for her support and guidance throughout my studies here in New Mexico Tech. I acknowledge the following institutions for their financial support: Chevron Mining Inc., Shell Oil Company, and New Mexico Institute of Mining and Technology.

I especially want to thank Dr. Shari Kelley for choosing me as her research assistant on the Shell Oil Company project. Thank you for your financial support and patience as I went through this journey. I would like to formally thank Dr. Julianne Newmark for assisting me in putting my research study into words and for her helpful writing expertise.

I would like to express my deepest gratitude to the Ghanaian community on campus for all their support, especially Samuel Nunoo, Prosper Felli, Enoch Adogla and Frank Lloyd-Mills for assisting in my laboratory work. The last two years have been quite an experience and you have all made it a memorable time of my life. I will miss all of you. Good luck to each of you in your future endeavors.

I learned about the strength you can get from a close family life. I learned to keep going, even in bad times. I learned not to despair, even when my world was falling apart. I learned that there are no free lunches. And I learned the value of hard work. My

guidance (Madam Akosua Frema and Mr. Osei Yaw Ampomah) taught me how to live by those words. I am also grateful to your never-ending love and support in all my efforts and for giving me the foundation to be who I am now.

Thank you my lovely sister (Betty Agyemang) and Osei Frempong Brown, for supporting and encouraging me to pursue this degree. Lastly, I offer my regards and blessings to all of those who supported me in any respect during the completion of the project.

TABLE OF CONTENTS

LIST OF TABLES----------VI

LIST OF FIGURES ---------- VII

1. INTRODUCTION.....1

1.1. Statement of the Problem.....1

1.2. Objective and Scope of Study.....2

1.3. Site Description and Background 2

1.4. Rock Piles Construction History.....5

1.5. Organization of Thesis.....7

2. MINED ROCK-PILE SHEAR STRENGTH AND LITERATURE REVIEW ...9

2.1. Shear Strength of Soil 9

2.2. The Strength of Questa Rock Piles 13

2.2.1. In-situ direct shear testing..... 14

2.2.2. Conventional laboratory direct shear tests..... 15

2.3. Previous Studies on Creep Settlement of Questa Rock Piles 16

2.4. Soil Creep.....18

2.4.1. Methods of Measuring Soil Creep in the Field..... 19

2.4.2. The Oldest Method of Laboratory Creep Measurement..... 23

2.5. Rock Pile Deformation and Failure 24

2.6. Previous studies on strain rate effect on soil strength.....25

2.7. Effect of Moisture on Creep and Shear Strength of Soils.....26

3. METHODOLOGY 32

3.1. Sample Description.....32

3.1.1. Location 32

3.1.2. Visual Description 32

3.1.3. Petrographic Description 33

3.1.4. Laboratory Analyses 35
3.2. Experimental Tests and Procedures 37
3.2.1. Sieve Analysis 37
3.2.2. Wet Sieving 37
3.2.3. Dry Sieving 38
3.3. Experimental Setup and Shear Test Procedures 40
3.4. Degree of Saturation of Samples 43
4. TEST RESULTS AND DISCUSSION 44
4.1. Introduction 44
4.2. Results of Direct Shear Tests on Air-dried Samples 44
4.3. Direct shear tests on moist samples 49
4.4. Comparison of the shear strength of moist and dry samples 59
5. CONCLUSIONS AND RECOMMENDATIONS 66
5.1. Conclusions 66
5.2. Recommendations for Future Work 67
REFERENCES 69
APPENDIX A - Combined plot of normal displacement versus shear displacement for bulk densities of 1700 kg/m^3 and 1850 kg/m^3 for moist (8% water content) spring gulch samples for different shearing rates **76**
APPENDIX B - Grain size distribution summary table **78**
APPENDIX C - Results of direct shear tests on air-dry samples with bulk density of 1850 kg/m^3 (averages from the three test results) **81**
APPENDIX D - Results of direct shear tests on moist (8% water content) samples with bulk density of 1850 kg/m^3 (averages from the three test results) **83**
APPENDIX E - Results of direct shear tests on moist (8% water content) samples with bulk density of 1700 kg/m^3 (averages from the three test results) **85**

LIST OF TABLES

Table 1.1: Features of the Questa mine rock piles (URS Corporation, 2000; Norwest Corp., 2005). URS Corporation (2000) used the Revised Universal Soil Loss Equation (RUSLE) to estimate soil loss rates of the Questa rock piles (McLemore et al. 2008) ..... ……..7

Table 2.1: Summary of settlement evaluation estimation (in URS, 2003)...……..18

Table 3.1: Various laboratory analyses for sample SPR-SAN-0001 from Spring Gulch rock pile. QMWI and SWI are weathering indices described in McLemore et al (2009) ……35

Table 3.2: Chemical and mineralogical analysis for sample SPR-SAN-0001(McLemore et al. 2009) ...……36

Table 3.3: Determination of degree of saturation and void ratio as compaction density increases…….43

Table 4.1: Direct shear test results conducted on air-dry Spring Gulch rock pile material with varying rate of shear deformation.. ……...49

Table 4.2: Direct shear test results for moist samples with a compaction dry density of 1700 kg/m^3 and varying rate of shear deformation……55

TABLE 4.3: Direct shear test results for moist samples with a compaction dry density of 18500 kg/m3 and varying rate of sheardeformation……..56

LIST OF FIGURES

Figure 1.1: Location of the Questa molybdenum mine, northern Taos County, New Mexico (McLemore et al., 2007). 4

Figure 1.2: Location of the Questa molybdenum mine within the Red River basin. Green line delineates the Red River watershed (Molycorp Inc., 2002)..... 4

Figure 1.3: Configuration of rock piles depending on topography: (a) valley-fill, (b) ridge, (c) cross-valley, (d) heaped, (e) side-hill (Zahl et al., 1992). 6

Figure 2.1: The strength characteristics of soils with different compaction densities..... 10

Figure 2.2: Vertical displacement of soil measured during shearing (for a single test) .. 11

Figure 2.3: Strength Envelop from Direct Shear Tests..... 12

Figure 2.4: Set-up of in situ test using the bucket of an excavator to support the hydraulic jack (Boakye, 2008). 15

Figure 2.5: Examples of Soil Creep Monitoring System Application (Selby, 1968) 22

Figure 2.6: Mine Waste Embankments possible Failure Modes (After Caldwell and Moss, 1981)..... 24

Figure 2.7: Creep test on dense air-dry Antioch sand (After Lee and Seed, 1967)..... 30

Figure 2.8: Creep test on dense-oven dry Antioch sand (After Lee and Seed, 1967) 30

Figure 3.1: Photograph of sample location (SPR-SAN-0001) (McLemore et al., 2008). 32

Figure 3.2: Photograph of washed rock fragments from hand sample (SPR-SAN-0001) (Nunoo, 2009) 33

Figure 3.3: Electron microprobe image of rock fragments with soil matrix adhering to the larger rock fragments (McLemore et al, 2009). 34

Figure 3.4: Electron microprobe image of a rock fragment with a Fe-oxide (goethite) coating. A small rounded jarosite grain can be seen in the matrix. The jarosite and Fe-oxides are the brighter hues (McLemore et al, 2009). 34

Figure 3.5: Electron microprobe image displaying relict pyrite crystals (completely oxidized) that are being replaced by jarosite and Fe-oxides (McLemore et al, 2009)..... 34

Figure 3.6: Wet sieve analysis 38

Figure 3.7: Diagram illustrating the stacking of sieves. (Asphalt Handbook, 1989) 39

Figure 3.8: Mechanical shaker..... 39

Figure 3.9: Gradation curves (in-situ and lab materials) of the Spring Gulch material used for the experimental. 40
Figure 3.10: Direct shear test setup procedure 42
Figure 4.1: A plot of shear stress versus shear displacement curve for air-dry samples with bulk density of 1850 kg/m^3 for four different shearing rates 45
Figure 4.2: A plot of normal displacement versus shear displacement for air-dry samples with bulk density of 1850 kg/m^3 for four different shearing rates 46
Figure 4.3: Peak shear stress versus rate of shear deformation for air-dry samples with bulk density of 1850 kg/m^3 for four different shearing rates 46
Figure 4.4: Failure envelopes for air-dry Spring Gulch rock pile material for different shearing rates with compaction density of 1850 kg/m^3. 48
Figure 4.5: Effect of rate of shear deformation (RSD) on peak friction angle of dry samples with compaction density of 1850 kg/m^3. 48
Figure 4.6: A plot of shear stress versus shear displacement with bulk density of 1700 kg/m^3 for moist (8% water content) Spring Gulch samples at four different shear rates. 50
Figure 4.7: A plot of shear stress versus shear displacement with bulk density of 1850 kg/m^3 for moist (8% water content) Spring Gulch samples at four different shearing rates. 50
Figure 4.8: Combined plot of shear stress versus shear displacement for bulk densities of 1700 kg/m^3 and 1850 kg/m^3 for moist (8% water content) Spring Gulch samples at 0.5 mm/min shearing rate. 51
Figure 4.9: Combined plot of shear stress versus shear displacement for bulk densities of 1700 kg/m^3 and 1850 kg/m^3 for moist (8% water content) Spring Gulch samples at 0.05 mm/min shearing rate. 51
Figure 4.10: Combined plot of shear stress versus shear displacement for bulk densities of 1700 kg/m^3 and 1850 kg/m^3 for moist (8% water content) Spring Gulch samples at 0.0275 mm/min shearing rate. 52
Figure 4.11: Combined plot of shear stress versus shear displacement for bulk densities of 1700 kg/m^3 and 1850 kg/m^3 for moist (8% water content) Spring Gulch samples at 0.005 mm/min shearing rate 52

Figure 4.12: A plot of peak shear stress versus rate of shear deformation for moist samples..... 54
Figure 4.13: Failure envelopes for the moist samples with bulk density of 1700 kg/m^3. 54
Figure 4.14: Failure envelopes for the moist samples with bulk density of 1850 kg/m^3. 55
Figure 4.15: A plot of normal displacement versus shear displacement for moist samples with a dry bulk density of 1700 kg/m^3 at four different shearing rates. 57
Figure 4.16: A plot of normal displacement versus shear displacement for moist samples with a dry bulk density of 1850 kg/m^3 at four different shearing rates. 57
Figure 4.17: Effect of rate of shear deformation on friction angle of moist Spring Gulch rock pile material with different compaction densities..... 59
Figure 4.18: A plot of shear stress versus shear displacement of dry and moist Spring Gulch samples at 0.5 mm/min shearing rate and bulk density of 1850 kg/m^3..... 60
Figure 4.19: A plot of shear stress versus shear displacement of air-dry and moist samples at 0.05 mm/min shearing rates and bulk density of 1850 kg/m^3..... 60
Figure 4.20: A plot of shear stress versus shear displacement of air-dry and moist samples at 0.0275 mm/min Shearing rate and bulk density of 1850 kg/m^3..... 61
Figure 4.21: A plot of shear stress versus shear displacement of air-dry and moist samples at 0.005 mm/min shearing rate and bulk density of 1850 kg/m^3. 61
Figure 4.22: A plot of normal displacement versus shear displacement for air-dry and moist samples for 0.5 mm/min shearing rate and a bulk density of 1850 kg/m^3..... 62
Figure 4.23: A plot of normal displacement versus shear displacement for air-dry and moist samples for 0.05 mm/min shearing rate and a bulk density of 1850 kg/m^3..... 62
Figure 4.24: A plot of normal displacement versus shear displacement for air-dry and moist samples for 0.0275 mm/min shearing rate and a bulk density of 1850 kg/m^3..... 63
Figure 4.25: A plot of normal displacement versus shear displacement for air-dry and moist samples for 0.005 mm/min shearing rate and a bulk density of 1850 kg/m^3..... 63
Figure 4.26: A plot of peak shear stress versus rate of shear deformation for air-dried and moist samples compacted at a dry density of 1850 kg/m^3 64
Figure 4.27: Effect of rate of shear deformation on friction angle of air-dried and moist samples..... 65

This thesis is accepted on behalf of the
Faculty of the Institute by the following committee:

_____
Research Advisor

_____
Academic Advisor

_____
Committee Member

_____
Committee Member

_____
Date

I release this document to the New Mexico Institute of Mining and Technology.

_____
Student's Signature Date

1. INTRODUCTION

1.1. Statement of the Problem

The purpose of this thesis is to determine the strain rate effect on shear strength of Spring Gulch rock-pile material at the Questa molybdenum mine in New Mexico. The shear failure of a mass of soil does not merely plummet to a constant residual rate, but to a certain extent depends on the degree and rate of displacement. The effect of the strain rate (creep) on the shear strength of rock piles is essential for long-term stability analysis. The strength of rock piles is governed by the frictional resistance between soil particles in contact and the cohesion between them. This project is therefore sought to study the long-term effect of strain rate on friction angle in both dry and moist conditions.

Sharpe (1938) defined creep as the "slow down-ward movement of superficial soil or rock debris, usually imperceptible except to observations of long duration." Creep measurement is very important to establish the amount of soil displacement with time. Deformation can take place in a slope as a result of stresses and shear displacements in the mass of material forming the slope. The rate of deformation is a good indicator of the behavior of the rock piles.

Seasonal variation of moisture content is a common observation in poorly drained slopes of cohesive soils. An increase in moisture content, usually observed after rainfalls, decreases soil shear strength and thus reduces slopes safety (Farrag 1995; Gregory 1998; Zhang et al. 2003). For long-term stability of the rock piles, the effect of strain rate on the

strength of the rock piles needs to be studied. The strength of Questa rock-pile material is affected by strain rate, but there is still very little information available on the time-dependent behavior of Questa rock piles. A comprehensive understanding of this phenomenon therefore requires the testing of soil samples at different rates of displacement using a digital direct shear machine.

1.2. Objective and Scope of Study

The objective of the study is to investigate the effect of strain rate on shear strength of Spring Gulch rock pile under different shearing rates. The test is performed by deforming a specimen at a controlled strain rate on a horizontal shear plane.

The purpose of this research work is:

- To perform direct shear tests on samples from Spring Gulch rock-pile using different shearing rates.
- To evaluate the effect of strain rate on the shear strength of the rock pile material.
- To evaluate the effect of combined moisture content and strain rate on the shear strength.
- To evaluate the role of compaction density on the shear strength of the rock-pile material under different shear strain rate.

1.3. Site Description and Background

The Questa molybdenum mine, owned and operated by Chevron Mining Inc. (Formerly Molycorp Inc.), is located 5.8 km east of the town of Questa in Taos County, New Mexico. From 1965 to 1983 large-scale open-pit mining at the Questa mine

produced over 300 million tons of mine rock, which was end-dumped into various steep valleys adjacent to the open pit (URS Corporation, 2000) (Figure 1.1). As a result, the mine rock piles are typically at an angle of repose (35º to 40º) and have long slope lengths (up to 600 m) and comparatively shallow depths (~ 30 - 60 m). Molycorp Inc. initiated a comprehensive characterization program in 1998 for the mine rock piles in order to provide a basis for the development of a closure plan (Shaw et al., 2002). This characterization program included field reconnaissance and sampling of mine rock, physical and geochemical testing in the laboratory, as well as test plot and numerical model studies (Robertson GeoConsultants Inc., 2000, URS 2003, Norwest 2004).

The climate in Questa, New Mexico is a semi-arid with mild summers and cold winters (Wels et al., 2002). The average monthly temperature is below freezing for five months of the year (November through to March). The rainy season is during July and August. Heavy localized rainfalls during July and August often cause flash floods and mudflows, which sometimes block the highway between the Village of Questa and the Town of Red River (Molycorp Inc., 2002). Figure 1.2 shows the location of Questa molybdenum mine within the Red River basin. Lake evaporation (large free-water surface) and actual evapotranspiration (land surface including transpiration from vegetation) on site are estimated to be 1000 mm (39.4 inches) and 400 mm (15.8 inches), respectively (Robertson GeoConsultants Inc., 2000).

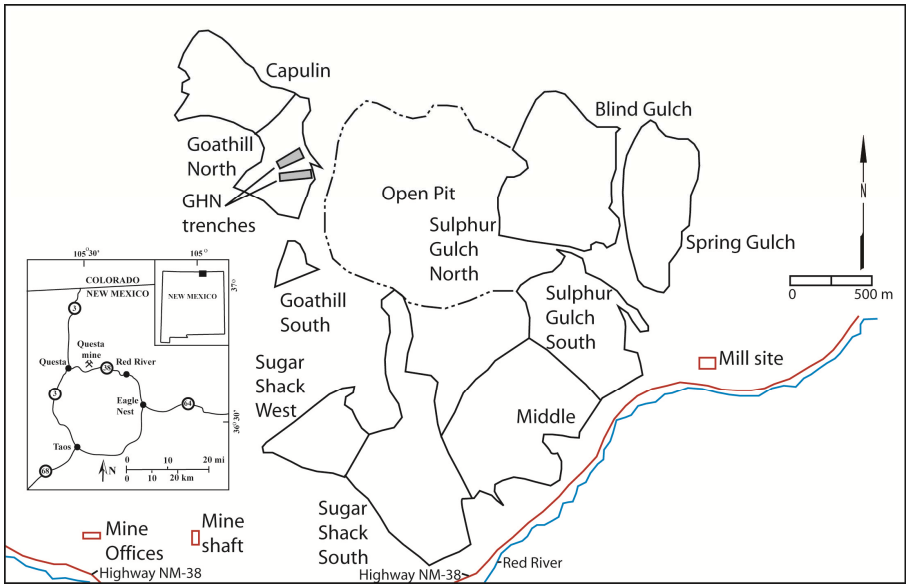

Figure 1.1: Location of the Questa molybdenum mine, northern Taos County, New Mexico (McLemore et al., 2007).

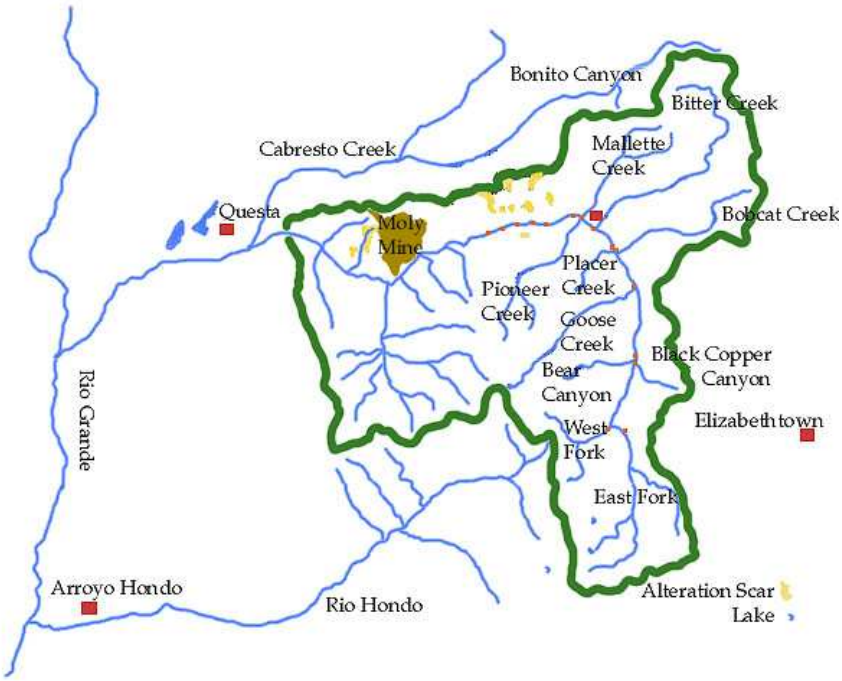

Figure 1.2: Location of the Questa molybdenum mine within the Red River basin. Green line delineates the Red River watershed (Molycorp Inc., 2002).

1.4. Rock Piles Construction History

The nature of the location and the topography determine the shape of mine rock piles. Mine rock piles can take the shape of one of, or a combination of many different configurations, such as valley-fill, cross-valley, side-hill, ridge, and heaped, depending on the topography of the area (Figure 1.3; Zahl et al., 1992). The dumping method of rock-pile material can be used to classify rock piles into five basic methods of rock-pile construction (Nichols, 1987; Moran et al., 1991; Quine, 1993; Shum, 1999; Tran, 2003):

- end dumping (dumping rock over dump face resulting in some particle size segregation down slope towards the toe of the rock pile, with particle size generally increasing)
- push dumping (dumping from trucks then leveling by pushing by tractor and shovel resulting in particle-size segregation; finer at the top, coarser at the toe of the rock pile)
- free dumping or plug dumping (dumping in small piles on the surface of the rock pile, grading the material, and compacting in layers or lifts resulting in dense layers with no real particle size segregation)
- drag-line spoiling (deposited on the surface without construction of lifts and minimal compaction resulting in dense layers with no real particle size segregation because of the relatively low overall height of the spoil piles; typically used in coal mining)
- mixing of waste rock with tailings.

The Questa rock piles were constructed predominantly by end-dumping as side-hill or valley-fill configurations at locations providing the shortest haul distance and least

elevation change from the area being mined at the time. End-dumping generally results in the segregation of materials with the finer-grained material at the top and coarser-grained material at the base, because the finer-grained material moves down a slope more slowly than the coarser-grained material. As the rock-pile face advances, the heterogeneity within the pile gradually increases.

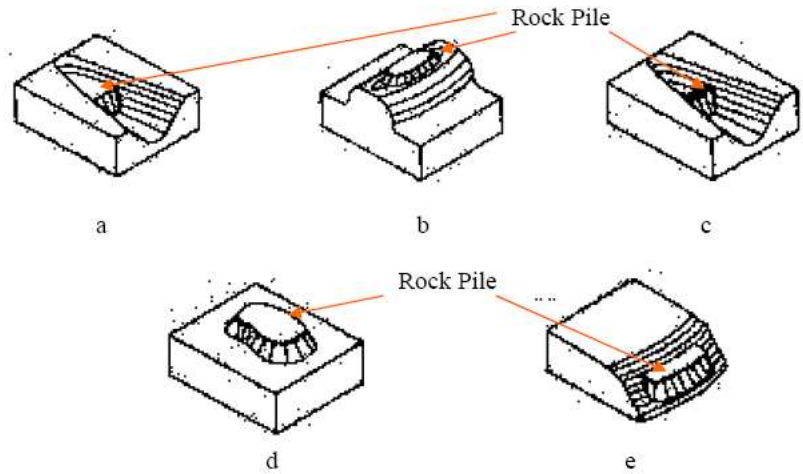

Figure 1.3: Configuration of rock piles depending on topography: (a) valley-fill, (b) ridge, (c) cross-valley, (d) heaped, (e) side-hill (Zahl et al., 1992).

The upper portion of the Questa rock piles tends to be more soil-like (matrix-supported), whereas the lower portions tend to be rock-like (cobble-supported) (McLemore et al., 2008). The underlying base of the Questa rock piles is coarse rock and typically is cobble-supported. As shown in Table 1.1, nine different rock piles were constructed during the open pit mining operation. This thesis studies the effect of creep, compaction density, and moisture content on the shear strength of the material collected from the Spring Gulch rock pile.

Table 1.1: Features of the Questa mine rock piles (URS Corporation, 2000; Norwest Corp., 2005). URS Corporation (2000) used the Revised Universal Soil Loss Equation (RUSLE) to estimate soil loss rates of the Questa rock piles. (McLemore et al. 2008)

Rock pile	Maximum height (ft)	Maximum thickness (ft)	Footprint (acres)	Slope area (acres)	Slope	Overall slope	Quantity of rock (million tons)	Area (acres)
Sugar Shack West	980	200	43	50.7	1.7 to 1.5H:1V	1.6H: 1V. 32°	31	
Sugar Shack South	1640	400	128.4	151.4	2.1 to 1.4H:1V	1.6H:1V 32°	53	87
Middle	1170	500	140	155.76	1.1 to 1.4H:1V	2.1H:1V 26°	46	133
Sulphur Gulch South	1200	400	70.9	75	3.3H:1V	2.9H:1V 19°	80	149
Spring Gulch	770	325	84.9	89	2.0 to 1.6H:1V	3.0H:1V	31	
Blind Gulch Sulphur Gulch South	740	375	128.3	134	2H to 1.4H:1V	3.7H:1V 15°	36	
Spring Gulch	770	325	84.9	89	2H to 1.6H:1V	3H:1V 18°		
Capulin	450	225	44.4	47.6	3.7H to 1.3H:1V	1.7H:1V 30°	26	
Goathill North	600	200	56.8	59	5.7H to 1.4H:1V	2.3H:1V 23°	16	
Goathill South	500	75	8.8	10	1.9H to 1.5H:1V	1.6H:1V 32°	9	

Rock pile	Years placed on benches	Years placed on slopes	Soil loss (tons/acre/year)	Annual soil loss (tons/year)
Sugar Shack West		1969, 1973, 1974, 1976, 1977	32	1376
Sugar Shack South	1974	1973, 1974, 1976, 1979	34.7	4442
Middle	1974, 1979, 1991	1974, 1976, 1077	31.9	4466
Spring Gulch	1969, 1973, 1974, 1976, 1977, 1991	1976	8	680
Capulin	1964-1977	1974, 1976, 1977	22	968
Goathill North	1964-1974		22.8	1300
Goathill South		1969	21	189
Suphur Gulch Nouth/Blind	1973, 1974, 1991, 1997	1976, 1977	12.7	1626
Sulphur Gulch South			34.7	2464

1.5. Organization of Thesis

This thesis is divided into five chapters. This first chapter provides an introduction, the objectives and scope of the project, a site description and background, information on rock piles construction history and an overview of the thesis. Chapter 2 is a literature review of published examples of previous studies on the strength of mine rock piles, the rate of deformation in soils mass, and shear strength behavior of saturated soil.

Chapter 2 includes insight gained from creep settlement estimated for Questa rock piles by different researchers. Chapter 3 describes the laboratory testing program developed to produce strain rate effects on the shear strength of the Spring Gulch rock pile. Background information for each test as well as detailed descriptions of the apparatus and testing procedure are described. The results of the testing program are presented and discussed in Chapter 4. Finally, conclusions of this research are presented in Chapter 5, along with applications of this work for geotechnical engineering practice and recommendations for future research.

2. MINED ROCK-PILE SHEAR STRENGTH AND LITERATURE REVIEW

2.1. Shear Strength of Soil

The shear strength of a soil is its resistance to deformation by continuous shear displacement of the soil particles upon the action of shear stress. When the maximum shear stress is reached, the soil is regarded to have failed. The failure conditions of a soil may be expressed in terms of limiting shear stress, called shear strength, or as a function of principal stresses. The shearing resistance of soil is constituted of the following main components (Kumari, 2009):

- The structural resistance to displacement of the soil because of the interlocking of the particles.
- The frictional resistance to translocation between the individual soil particles at their contact points.
- Cohesion or adhesion between the surfaces of the soil particles.

The shear strength in cohesionless soil results from inter-granular friction alone, while in cohesive soils it results both from internal friction as well as cohesion. Figure 2.1 shows the strength characteristics of soil with different compaction densities.

Strength is the measure of the maximum stress state that can be induced in a material without it failing. The shear strength of a soil is indicative of the stability and strength of the soil under various conditions of loading, compaction, and moisture content. However, the shear strength value determined experimentally is not an exceptional constant, which is the characteristic of the material, but can vary with the

method of testing. Shear strength parameters are crucial for stability analyses against slope failures and landslides. Soils with high shear strength will be able to support structures without failing. Otherwise, the structure will not be stable and side effects will occur, either, in the short term or long term depending on the shear strength.

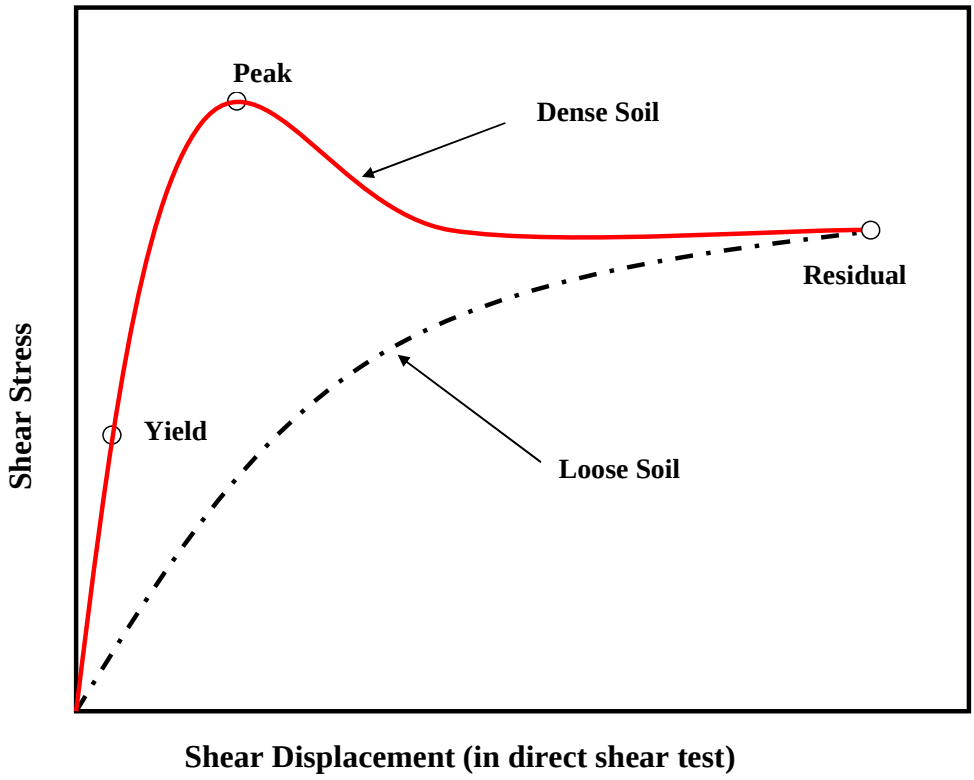

Figure 2.1: The strength characteristics of soils with different compaction densities

When shear stress is applied, the resulting deformation is always accompanied by a volume change, which is known as dilatancy. This shear-induced volume change accrues as a result of two competing modes of particle movement, namely, slip-down and roll-over (Dafalias, 1993). Figure 2.2 illustrates vertical displacement of soil measured during direct shear test. The slip-down movement of grains tends to reduce the volume by repacking the soil into a denser state. This mechanism is activated largely in loose

deposits of soil. The roll-over mechanism tends to increase the volume which is characteristic in the behavior of dense soil.

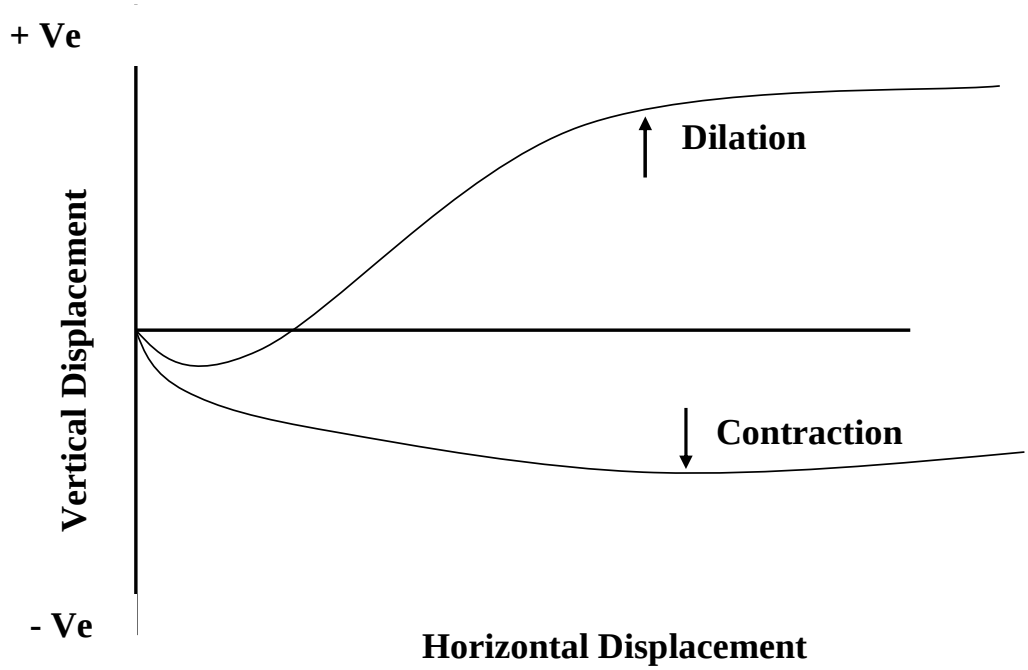

Figure 2.2: Vertical displacement of soil measured during shearing.

When the slip-down takes place, particles are filling gaps in the void and not moving largely in the direction of shearing. Therefore, the slip-down movement can occur rather easily without mobilizing a large amount of shear strain and the volume reduction is generally observed at an early stage of loading in the tests on sands with a wide range of density. A larger movement is always required for particles to roll over neighboring ones and hence the volume increase or dilation is generally induced at a later stage of shear stress application where the soil is largely deformed.

For soil with high density, the soil tends to exhibit strain hardening accompanied with dilatational behavior. The shear stress goes up initially, passes a peak stress and then

softening behavior starts, leading to a residual strength. However, for soil with low density, the strain-hardening behavior is exhibited with no post-peak softening (See Figure 2.1).

The stress on the shear plane can be resolved into the effective normal stress, σ_n', which acts perpendicularly to the surface and the shearing stress, τ, which acts along the surface. At failure, the relationship between shear (τ) and normal (σ_n') stresses are given by the Mohr-Coulomb criterion as follows (See figure 2.3):

$$\tau = c' + \sigma_n' \tan \phi' \tag{1.1}$$

Where: c' = effective cohesion and

ϕ' = effective friction angle

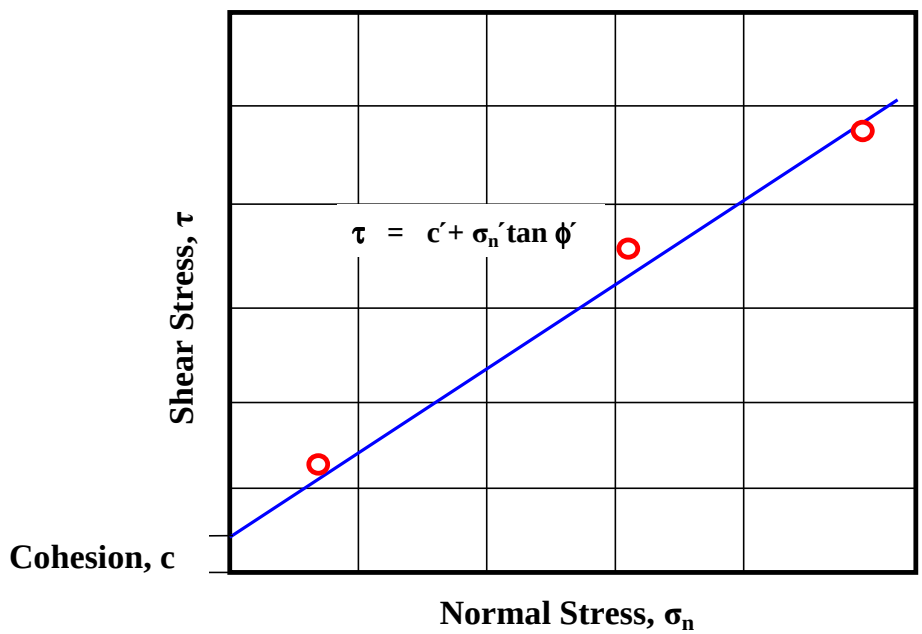

Figure 2.3: Strength envelop from direct shear tests.

2.2. The Strength of Questa Rock Piles

Some extensive studies for determining the strength parameters of rock piles have been performed in laboratories. Gutierrez (2006), Norwest Corporation (2005), URS Corporation (2000) and Robertson GeoConsultants (2000) performed geotechnical characterizations of the Questa mine rock piles. The geotechnical studies included laboratory particle size distribution, Atterberg limits, dry unit weight, specific gravity, moisture content, and shear strength. The shear strength properties of the Goathill North rock pile at the Questa molybdenum mine, New Mexico, was investigated by Gutierrez (2006).

Gutierrez (2006) investigated the shear strength of the air dried soil samples using a 5 cm × 5 cm shear box in the laboratory. Norwest (2005) concluded based on their results that a constant volume friction angle of 36° is the preferred angle for design to guarantee stability of the rock piles. Evaluation of erosion stability of the mine rock piles at Questa was also conducted by URS Corporation (2003). They studied the shear strength of these rock piles by laboratory direct shear tests using two types of shear boxes, a smaller direct shear box of size 6 cm × 6 cm and a relatively large 30 cm × 30 cm shear box.

Material passing through the No. 4 sieve was used for the 6 cm × 6 cm shear box test. For material less than 1.5 inch in size, 30 cm × 30 cm shear box was used for the direct shear testing. For the 6 cm by 6 cm shear box, the material was compacted to dry densities between 1500 kg/m^3 and 2300 kg/m^3 at moisture content between 10 to 14 percent. The 30 cm × 30 cm shear box samples were also compacted to a dry density

ranging from 1500 kg/m^3 to 1700 kg/m^3 at a moisture contents ranging from 8 to 11 percent.

Nunoo (2009) concluded that the shear strength of Questa mine material is affected by the particle size and shape during his investigation on the geotechnical properties of Questa rock piles and their natural analogs. Nunoo (2009) added that, larger samples contain less fines that result in higher friction angles.

Boakye (2008) performed in-situ direct shear tests to measure the cohesion of the Questa rock pile materials in order to investigate the intensity of cementation between particles. Boakye (2008) found out that Questa rock pile materials show no strong linear correlation between cohesion and the index parameters of the rock piles.

2.2.1. In-situ direct shear testing

Fakhimi et al. (2007) and Boakye (2008) designed a modified in-situ direct shear apparatus to determine in-situ shear strength and cohesion of Questa rock piles (Figure 2.4). Cohesion of the rock pile was addressed and investigated to determine the strength of cementation between soil particles. They conducted several tests at different locations within rock piles. The laboratory friction angle together with the Mohr-Coulomb failure envelope was used to determine the in-situ cohesion. The friction angles were obtained by conducting laboratory direct shear tests on dry specimens compacted to the in-situ dry density using low normal stresses in the range of 20 to 110 kPa. The applied normal stress for the in-situ tests ranges from 15 to 75 kPa.

One dial gauge was used to measure shear displacement, while two normal dial gauges attached to the lateral sides of the top platen were used to measure normal displacement of the rock pile block. The shear load was gradually increased. The

hydraulic jack loads and dial gauges reading were recorded after each 0.51 mm (20/1000 inch) of shear displacement. The average shear displacement rate was approximately 0.025 mm/s. Each in-situ shear test was normally continued for a shear displacement of 7.5 cm. Averaged in-situ cohesion of approximately 10 kPa for the rock pile material was obtained based on these field tests. The purpose of the in-situ test was to evaluate the effect of weathering on cohesion and friction angle of Questa rock piles.

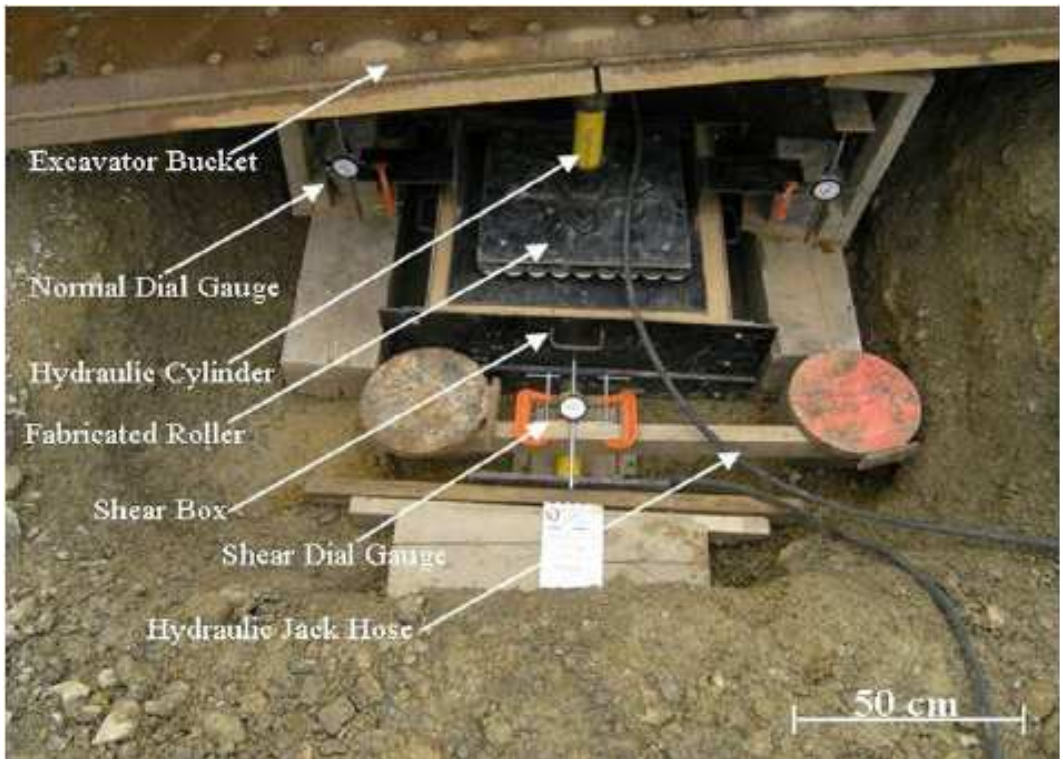

Figure 2.4: Set-up of in situ test using the bucket of an excavator to support the hydraulic jack (Boakye, 2008).

2.2.2. Conventional laboratory direct shear tests

Boakye (2008) performed laboratory direct-shear tests on the air-dried samples collected from the in-situ test sites. A 5 cm × 5 cm shear box was used to determine the strength of the soil in the laboratory. The tests were performed on reconstructed rock-pile

samples collected from each location of in-situ direct shear tests. This was to make sure that the corresponding conventional laboratory direct shear test was performed on the same material as tested in-situ so that a consistent comparison could be made between the two methods. The rock pile material passing through the No. 6 sieve was used for the laboratory direct shear testing. Each sample's in situ dry density was calculated using the sand replacement method (a standard sand cone method) and the measured moisture content. The dry density ranged from 1400 to 2680 kg/m^3 with a standard deviation of ±290 kg/m^3. The normal stresses used for the laboratory shear tests ranged between 20 kPa to 800 kPa.

The maximum horizontal or shear displacement was 12 mm. He reported a peak friction angles for air-dried Spring Gulch rock pile samples in a range of 37.6° to 46.6° for high normal stress between 120 kPa and 650 kPa.

2.3. Previous Studies on Creep Settlement of Questa Rock Piles

The estimated settlement for metal mine rock piles based on previous literature is about 5 percent (URS, 2003). Approximately the same 5 percent settlement was estimated from the topography at the Questa Molybdenum Mine rock piles. The weight of the rock piles during dumping imposes settlement of about 3 percent the height of the rock pile. Also, after five years of emplacement, an additional 1 percent settlement can take place. This estimation was based on Parkin's (1977) logarithmic form, a time-dependent settlement relationship that was used to estimate settlement in rock piles and rockfill.

Literature reviews by Naderian and Williams (1996) and Naderian (1997) show that creep persists for more than 10 years after construction. Questa mine rock piles should experience settlement of about 0.01 percent per year base on Parkin's time-dependent settlement relationship. This settlement would be about 10.2 mm per year for the Middle rock pile (one of the Questa rock piles), where the mine rock thickness is 82.3 m. Parkin's relationship for creep movement estimation is for vertical settlement.

The extent of horizontal and vertical components of the creep settlement may also be related to the foundation contact at the base of the rock piles (URS, 2003). In May 2001, the surface movements located on the lower bench (elevation 8680 ±) of the Middle pile have shown from 0 to 0.06 m of movement. This corresponds to a settlement rate of up to 0.034 m/yr or about 0.05 percent per year.

Installed inclinometers through the rock piles into the underlying bedrock show clearly that creep settlement is presently occurring within the rock piles at the Questa Mine (URS, 2003). Readings from two inclinometers also suggest the possibility that down-slope creep is occurring. To correct the errors during measurements, additional inclinometer readings might be useful in estimating creep in the rock piles.

The above evaluations are summarized in Table 2.1. Questa rock piles are estimated to have average settlement base on the evaluations of about 5 percent (URS, 2003). A 5 percent settlement implies that for rock pile of 61 to 122 m thick, vertical settlement of up to about 3 to 6 m has been occurred since the rock piles were emplaced (URS Corporation, 2000).

Table 2.1: Summary of settlement evaluation estimation of Questa rock piles (URS, 2003)

Settlement Evaluation	Estimated Settlement (Percent)
Historic Rock Pile Topography	3 to 7
Middle Rock Pile Survey Monuments	5.6
Pressuremeter Test Results	3.0 to 4.6
Parkin's Method (1977)	1.7
Literature Review (Naderian and Williams, 1996 and Naderian, 1997)	0.3 to 7
Current Creep Middle	0 – 0.05% per year
Current Creep Estimate (Parkin, 1977)	0.01% per year

2.4. Soil Creep

Terzaghi (1950) reported two different types of creep movements, namely seasonal creep which affects only shallow surface layers during seasonal change in moisture and temperature, and the "mass creep" or "continuous creep." The "mass creep" or "continuous creep" is a consequence of the ground stresses (gravitational force) and is controlled largely by the rheological behavior of slope materials. Slope movements of varying magnitude occur at shear stresses which are well below failure stresses (Chowdhury, 1978). Ter-Stepanian (1963) studied the long-term stability of slopes using a quantitative approach by considering the zone of soil creep and its rate in simple natural slopes. He reported that, "creep is the rate of relative shear deformation reached at a certain time after the application of shear stress."

Creep is the continuous deformation with time under some applied load. Landslide displacement and slope stability of cohesive soils are correlated to the creep deformation and creep strength behavior of the soil (Shimokawa, 1979). Shimokawa (1979) studied creep deformation on cohesive soil to forecast landslide movement. The

main focus was on creep deformation and creep failure. Shimokawa (1979) performed four different experiments consisting of undrained triaxial compression creep test, undrained strain-controlled triaxial compression test, drained triaxial compression creep test, and direct shear creep test. For the undrained strain-controlled triaxial compression test, five loading speeds were used in the experiment: 0.0014, 0.011, 0.016, 0.032 and 0.096 percent per 1 minute. After Shimokawa's experiment, creep deformation curves for cohesive soils were grouped into four with respect to the strain-logarithmic time. From the results, he concluded that the creep strain versus logarithmic time were linear for all the tests.

Paritzek and Woodruff (1957) suggested that the term soil creep includes down-slope processes which are not readily recognizable, but which are deduced as being present.

The rates of soil creep were studied for a 30-year period in southeastern Utah on Mancos Shale badland slopes averaging 35 degrees by Godfrey (1997). He noted that the average rate of movement was 2.71 cm per year on 35 degree slope. In summary, Godfrey (1997) work reveals the downward slope creep rate increases as the slope angle increases.

2.4.1. Methods of Measuring Soil Creep in the Field

In order to know the amount of movement that is likely to occur, it is necessary to make frequent monitoring of creep movement in the field. The soil material forming the rock pile slope, the slope angle and the dump height determine the extent of the creep

movement. Despite the 28 years lapse, the measuring techniques of soil deformation identified by McCarthy (1981) still prevail:

A. Surveying
    I. Leveling
    II. Electronic distance measurement
    III. Location by intersection
B. On-site inspections
C. Photogrammetry
D. Extensometers
    I. Above surface
    II. Buried
E. Acoustic emission
F. Laser beacon
G. Settlement cells
H. Inclinometers
    I. Surface or buried tiltmeters
    II. Borehole inclinometers

The rock pile materials, the height and construction method of rock pile materials determine which technique is applicable (McCarthy (1981)).

Selby (1966) reported that Kirkby (1965) (Figure 2.5A) used a tilt bar made up of steel rod 9 or 15 inches long with ¼ inches square-section mild steel. It had a crosspiece of steel with a brass strip attached and parallel to the crosspiece, on which is mounted a sensitive spirit level. At one end of the brass strip was an adjusting screw which was used

to set the bubble after each measurement. Each graduation on the level shows a tilt of 10 sec. of arc and tilts of ± 50 sec. of arc can be observed directly. The tilt bars were inserted in the soil to depths of 6 and 12 inches and were placed in pairs. Measurements were made at three-day intervals. Its design involves the supposition that the rate of shear is average over the length of the tilt bar.

Dury (1959) (Figure 2.5B) measured the inclination of a metal tube by lowering into it a glass container of hydrofluoric acid. He allowed the container to remain stationary at a given depth while the acid etches a horizontal ellipse inside it. The angle between the plane of the ellipse and the side of the container gives the angle of slope of the metal tube at a particular depth. A series of measurements gives the profile of each tube and the rate of creep at varying depths.

Williams (1957) (Figure 2.5C) working in periglacial environments used plastic tubes, of 1.5 cm intervals diameter and 0.15 cm wall thickness, which were buried in the ground with the top of the tube exposed. The curvature of the tube resulting from soil movements was determined at intervals by the insertion of a specially constructed probe. The bottom of the plastic tube was at a depth greater than that of soil movement, and the top located by survey.

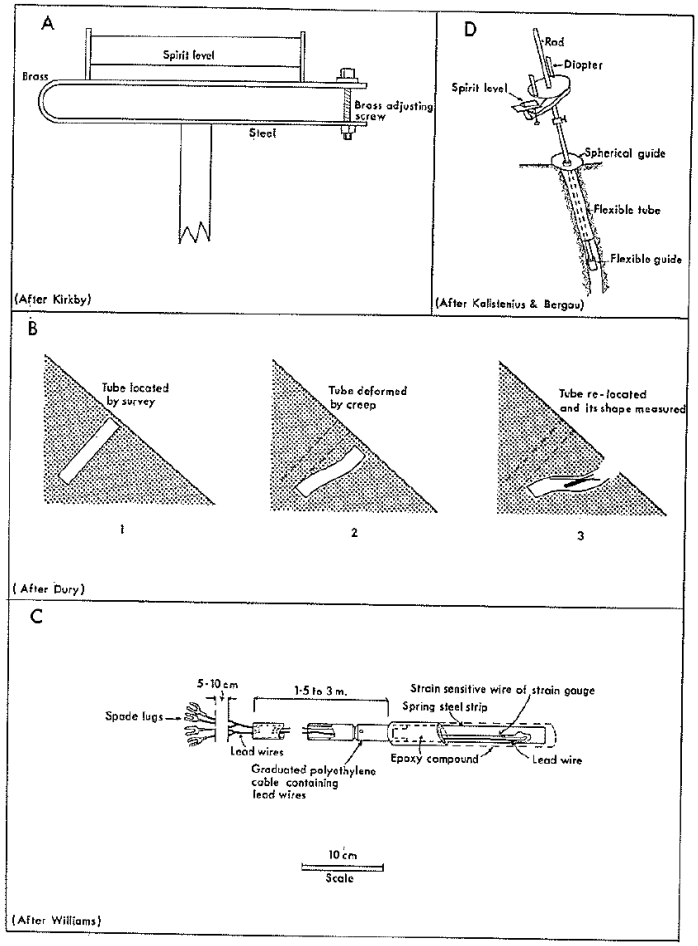

Figure 2.5: Examples of soil creep monitoring system application (Selby, 1968)

Kallstenius and Bergau (1961) (Figure 2.5D) found out that the workers at the Swedish Geotechnical Institute (SGI) have devised an inclinometer, which has some of the properties of Kirkby's and Williams's instruments. This rod inclinometer was placed inside a flexible tube which is inserted vertically into the ground to a maximum depth of 4 m. The inclinometer consists of a straight rod with a flexible guide which follows the bends of the tube. Where the rod enters the tube it was centered by means of a disc and a spherical guide. The inclination and length of the rod between the guides determines the position of the center of the lower guide in relation of the center of the spherical guide.

The direction and angle of the inclination were measured by means of an instrument mounted on the rod. The instrument consists of a diopter and a spirit level which can be adjusted to give an indication of the position and inclination of the rod. To take a measurement the rod is inserted to the required depth for readings to be taken. The SGI has developed two other instruments for use at depths of up to 90 m and for giving warning of dangerous earth movements.

Everett (1962, 1963) has used small aluminum pressure plates anchored vertically in the soil and connected to the shaft of a potentiometer by an aluminum rod. He measured the displacement caused by soil movement against the plate of the potentiometer shaft and a resistance change which was modified with Wheatstone bridge. According to Selby (1966), Ohio and Alaska used Everett's instrument to record soils movement during freezing and thawing and wetting and drying.

2.4.2. The Oldest Method of Laboratory Creep Measurement

Davison (1889) measured soil movements in the laboratory conditions. He set a tray of soil at an angle with a pointer mounted on the soil. He noted the position of the pointer before and after night frost, and determined that the surface of the soil had risen vertically during the freezing and fallen at an angle in a down-slope direction during the thawing. Young (1958) and Kirkby (1965) also conducted laboratory experiments to determine the creep behavior of soils. They used soil blocks in inclined troughs with glass sides. Metal pins were pushed into the sides of the blocks and their positions measured at intervals for about 40 days, during which the soil was wetted and dried. The pins were generally found to move both down-slope and vertically downwards.

2.5. Rock Pile Deformation and Failure

As a result of stresses and shear displacements, deformation can occur in the mass of material forming the rock piles. Figure 2.6 shows various failure modes that can occur in rock piles (Caldwell and Moss 1981). Questa rock piles were constructed as a result of end-dumping and may result in surface slides as the rock pile material moves down the slope. The rock pile material forming the slope has both frictional strength and cohesion, which determine the strength of the rock pile. The methods of failure mode depend on the topographic location of the dump site. When the base area for end-dumping of rock piles is inclined, failure is more likely to occur in the future.

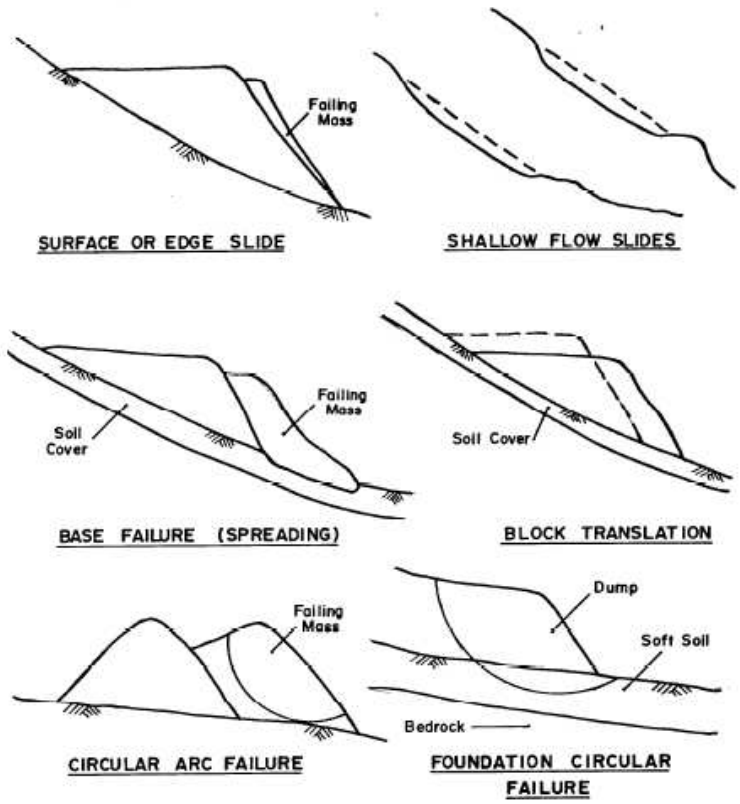

Figure 2.6: Mine waste embankments possible failure modes (from Caldwell and Moss, 1981)

2.6. Previous studies on strain rate effect on soil strength

Al-Mhaidib (2005) studied the effect of shearing rate on interface friction angle between sand and steel to investigate the loading rate effect on pile bearing capacity. He mentioned that soil and material surface properties affect the interfacial friction angle. The shear strength of soil depends on the rate of loading and therefore, the pile capacity will depend on the rate of loading into the soil. Three normal stresses were used for the test on smooth and rough surfaces: 50 kPa, 100 kPa, and 150 kPa. Al-Mhaidib (2005) sheared the samples using five different rates: 0.9 mm/min, 0.4 mm/min, 0.08 mm/min, 0.048 mm/min, and 0.0048 mm/min. Conventional direct shear test with dimensions of 100 mm × 100 mm was used for the experiments. Al-Mhaidib (2005) noted in his experiment that the maximum shear stress of the sand increases as the rate of shearing increases; the internal friction angle of sand increases with increasing rate of shearing.

The effect of loading rate on sand was investigated by Al-Mhaidib (2004). The main purpose of the research was to determine loading rate influence on the axial capacity of the pile groups. A normal load at a constant rate of loading was used on the model piles. Concurrently, the load and the pile displacement were measured using a proving ring and a deformation dial gauge. From the results, he concluded that compressive capacity of the pile group rooted in sand increases as the rate of loading increases.

Díaz-Rodríguez et al. (2009) studied strain-rate effects on Mexico City soil. Their research aimed at strain rate effects on load-deformation and yield stress of Mexico City soil. They performed undrained triaxial compressive test on undisturbed soil samples. They concluded that Mexico City soil shows considerable time-dependent stress-strain

characteristics. The axial strain at peak deviatoric stress is independent of the strain rate. Additionally, increasing strain rates increase the undrained strength of the soil. Berre and Bjerrum 1973; Vaid and Campanella (1977) stated that all previous studies by Casagrande and Wilson (1951) found out that Mexico City soils recognized a lower limit for the undrained compressive strength of 45 and 55 kPa at very low strain rates. Alberro and Santoyo (1973) also found (assuming zero cohesion) an increase in the effective stress friction angle of 2°–3° per log cycle of strain rate with the same soil. Alberro and Santoyo (1973) and Casagrande and Wilson (1951) also found out that, strain-rate is an independent value of the strain at the peak deviatoric load.

The effect of strain rate on effective friction angle remains uncertain, according to Bjerrum et al. (1958). Crawford (1959) attributed it to experimental difficulties and conflicting data, changes in failure mode (Richardson and Whitman 1963), and data interpretation (Kenney, 1951). From a broad perspective, higher strain rate leads to a higher effective strength envelope (Lo and Morin (1972); Tavenas et al. (1978); Vaid et al. (1979); Leroueil and Tavenas (1979)).

2.7. Effect of Moisture on Creep and Shear Strength of Soils

Yoshida et al. (1991) found a decrease in shear strength of soil as a result of an increase in the degree of saturation. Bishop and Bright (1963) attributed the strength reduction to the effective stress existing in partially saturated soils. They collected soils samples from several landslide sites to ascertain the reduction of shear strength of partially saturated soils as a result of increase in saturation ratio. They performed laboratory triaxial test with water content attuned to have the same values ranging from 5

to 15% for each test. The samples were compacted to in-situ compacted density equal to the field density measurement. After the test, they noted that the strength of soil decreases as the degree of saturation increases. In addition, the strength of the soil decreases drastically as the degree of saturation changes from 80% to 100%, which is fully saturated. They also noted that both cohesion intercepts and internal friction decrease as the degree of saturation increases.

Lemos (1986) and Tika (1989) studied the changes in residual strength with the rate of displacement using IC/NGI ring shear apparatus (Bishop et al., 1971). The shear strength of a soil sample, which was sheared at a slow rate of displacement until a residual value was reached, increased to a peak strength higher than that of the slow residual when the rate of displacement was increased suddenly. The shear strength either remained constant at an elevated strength or fells below that of the slow residual strength.

They named the constant strength that was achieved after a large displacement "fast residual." One of the problems with the tests that were carried out by Lemos (1986) and Tika (1989) was that they were unable to maintain the high shear velocities for sufficient magnitudes to ensure that stabilization had occurred.

Hence, Parathiras (1994) designed a new set of rings that used ball bearings to maintain a constant gap between the upper and lower confining rings and hence reduce the amount of soil loss through the gap. Parathiras (1994) investigated the effect of different rates of displacement on the residual strength of plastic soil. He used his modified IC/NGI ring shear apparatus with a new set of confining rings to determine the residual strength of plastic soils. All the experiments show a residual structure which ended after the soil has reached its ultimate strength.

Parathiras (1994) compared the fast and the slow strength of the soil. At the fast shearing rates, the strength of plastic soils is governed by the shape of their shearing surface and the amount of water in the environment. The strength of the soil decreases as the water content increases. Higher excess pore pressure is generated at low strain rate undrained loading, and is more pronounced in extension than compression loading (Casagrande and Wilson 1951; Bjerrum et al., 1958; Crawford, 1959; Richardson and Whitman, 1963).

Sasaki et al. (1999) noted the process of soil creep (strain rate) by monitoring slope movements in Japan. They reported that, the amount of creep due to one rainfall event is greater than creep due to the cumulative amount of rainfall and the reduction of suction became greater. The speed of creep on the slope surface is several millimeters a year. The estimated annual amount of soil movement by creep is similar to the general amount of soil moved by debris flows in Japan. After their studies, they concluded that soil creep increases with increasing soil moisture content. In addition, the amount of creep caused by one rainfall has a positive correlation with the amount of rain and increases in soil moisture. Soil creep continues during and after a rainfall.

Nash (1953) found no difference in the strength between dry and wet conditions after performing a series of direct shear test on fine clean quartz. To the contrary, Bishop and Eldin (1953) conducted drained triaxial compression test on medium to clean sand in both dry and saturation conditions with confining pressure of 5 psi. They performed the test on different range of densities. At the end of the test they found out that the internal friction angle was constantly higher for dry sand than the saturated sand. To support the claim that water has an effect on the friction of soil, Tschebotarioff (1951) performed

sliding frictional test on block samples of different materials. Tschebotarioff's (1951) test was established by Horn and Deere (1962). Both studies found out that water reduces the friction between smooth blocks of layer- lattice minerals such as mica. The internal friction angle of powdered mica is reduced by the addition of water during a direct shear test.

Lee and Seed (1967) performed triaxial tests on Antioch sand at a confining pressure of 1.0 kg/cm^2 using an oven dried sample, air dried sample, and saturated sample. The strength of the samples increases in the order of saturation, air-dry, and oven-dry, respectively. Lee and Seed (1967) also found that the rate of strain increases strength for each confining pressure and moisture condition.

The behavior of air dried and oven dried Antioch sand samples were further investigated (Lee and Seed, 1967). The applied load was constant for a long period without injecting water into the sample. After some days of constant load, it was found that long-term creep was often extensively large, and shattering shear failure was also found in all cases (Figure 2.7 and Figure 2.8). They also performed a series of tests on air-dried and oven-dried Antioch sand by gravitationally injecting water into the sample through the bottom drainage line. Lee and Seed (1967) added water to the samples while the test was in session and after the axial strains had reduced to a very slow rate. The sample failed immediately after the water was initiated (Figures 2.7 and 2.8). A series of tests was also performed in which the applied load was constant for one day before water was initiated. Failure occurred 1 hour after the water was initiated. The mode of failure was almost the same for all the tests.

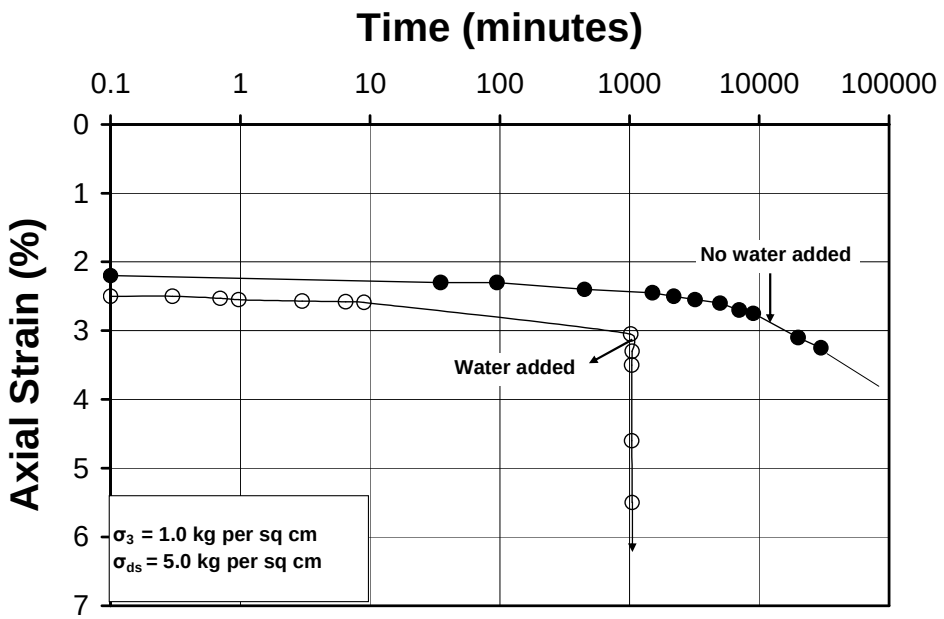

Figure 2.7: Creep test on dense air-dry Antioch sand (After Lee and Seed, 1967)

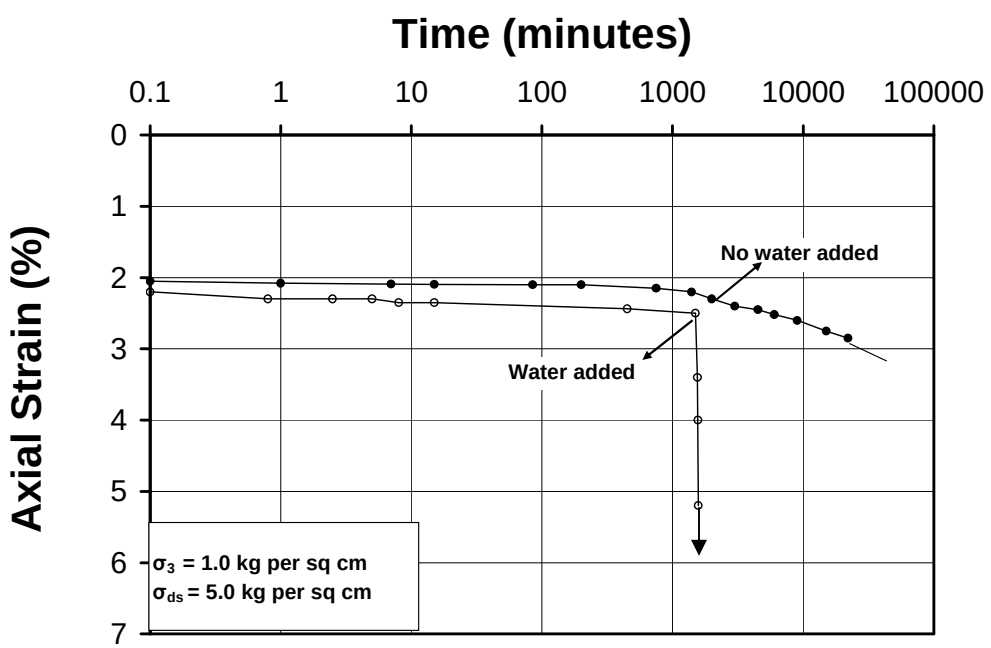

Figure 2.8: Creep test on dense oven-dry Antioch sand (After Lee and Seed, 1967)

Settlements of fourteen rockfill dams were studied by Sowers, Williams, and Wallace (1965). During the studies, the Dix River Dam was deliberately flooded for 8-day period. Settlement measured during the flood period increased from 0.32% to 0.74%. The rate of settlement during the flood was found to be greater than the rate before and after flooding.

In summary, it appears that the shear strength of some soils decreases with increasing water content.

3. METHODOLOGY

3.1. Sample Description

3.1.1. Location

The material for the laboratory analysis for this project was taken from the top of the Spring Gulch rock pile at UTM coordinates 13N4062285, 455255E zone 13 (NAD 27) and elevation of 9414 ft (2838.9 m) (Figure 3.1).

Figure 3.1: Photograph of sample location (SPR-SAN-0001) (McLemore et al., 2008).

3.1.2. Visual Description

The sample is brown, well graded with poor sorting and consists of andesite. The particle size for the rock fragments ranges from cobble to clay, the fragments are sub-angular, and there appears to be minor oxide staining on the outside of some fragments (Figure 3.2). The sample has some plasticity. In hand sample, the sample is brown in color and after washing, the hand sample is dark brown in color. The clays in this sample have cemented rock fragments.

Figure 3.2: Photograph of washed rock fragments from hand sample (SPR-SAN-0001) (Nunoo, 2009)

3.1.3. Petrographic Description

In thin section, the sample is brown to grey in color, has clay or silt- to gravel-sized particles that are sub-angular and sub-discoidal in shape (Nunoo, 2009). The lithology is 100% andesite with 35% quartz-sericite-pyrite (QSP) and 7% propyllitic alteration. The rock is composed of ~80% rock fragments, ~15% iron oxides, ~4% clay, ~1% gypsum, with trace amounts of pyrite and epidote. Epidote is found in trace amounts on rock surfaces, chlorite is described as soapy green grains, and 98% of the gypsum crystals are clear and authigenic. The primary cement in this sample is Fe-oxides with minor amounts of clay and jarosite. Pyrite crystals have numerous small inclusions of apatite and quartz, and many pyrite crystals display eroded and scalloped grain edges, oxidized rims, and goethite replacement (Figures 3.3 to 3.5).

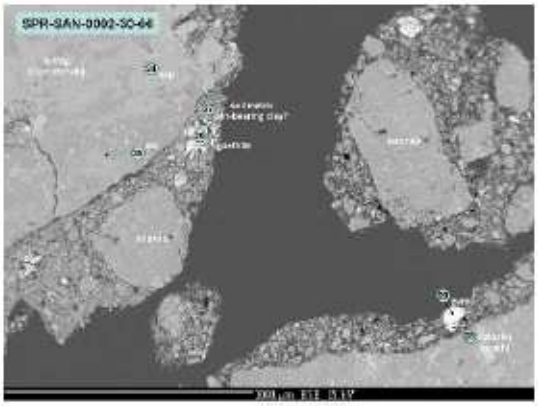

Figure 3.3: Electron microprobe image of rock fragments with soil matrix adhering to the larger rock fragments (McLemore et al, 2009).

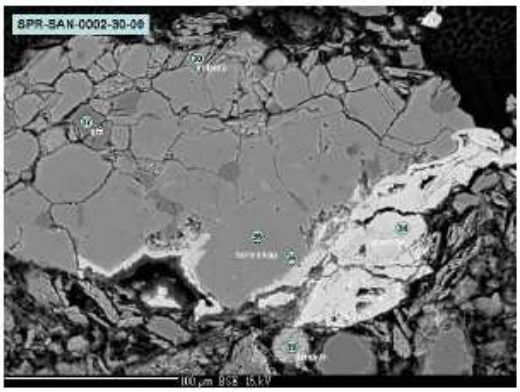

Figure 3.4: Electron microprobe image of a rock fragment with a Fe-oxide (goethite) coating. A small rounded jarosite grain can be seen in the matrix. The jarosite and Fe-oxides are the brighter hues (McLemore et al, 2009).

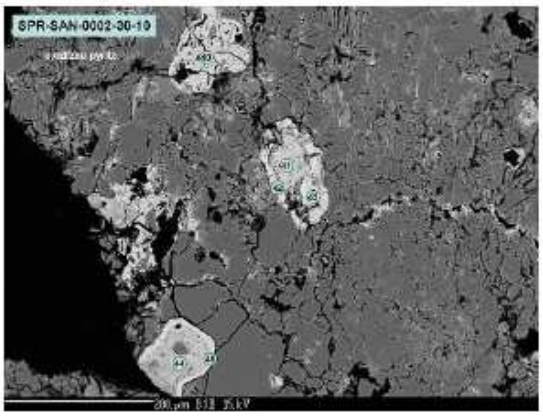

Figure 3.5: Electron microprobe image displaying relict pyrite crystals (completely oxidized) that are being replaced by jarosite and Fe-oxides (McLemore et al, 2009).

3.1.4. Laboratory Analyses

Summarized laboratory results for mineralogy and chemistry for the Spring Gulch rock pile material are in Tables 3.1 and 3.2. These tables indicate the various laboratory analyses on the Spring Gulch sample.

Table 3.1: Various laboratory analyses for sample SPR-SAN-0001 from Spring Gulch rock pile (McLemore et al., 2009). QMWI and SWI are weathering indices described in McLemore et al. (2009).

pastepH	4.22
pasteCond (mS/cm)	3.98
pasteTDS	1.71
AP	5.63
NP	18.96
netNP	-13.33
NPAP	13.33
QMWI	7
SWI	2

Table 3.2: Chemical and mineralogical analysis for sample SPR-SAN-0001(McLemore et al., 2009)

Chemistry	**Wt. % SPR-SAN-0001**	**Mineralogy**	**%**
SiO_2	59.74	Quartz	25
TiO_2	0.73	K-spar/orthoclase	21
Al_2O_3	14.39	Plagioclase	18
Fe_2O_3T	5.9	Albite	-
FeOT	5.36	Anorthite	-
FeO	3.27	Biotite	-
Fe_2O_3	2.3	Clay	-
MnO	0.11	Illite	14
MgO	2.96	Chlorite	8
CaO	2.31	Smectite	3
Na_2O	2.79	kaolinite	0.9
K_2O	3.5	mixed layered	-
P_2O_5	0.38	Epidote	2
S	0.18	Magnetite	-
SO_4^{2-}	0.46	Fe oxides	4
C	0.05	Goethite	-
LOI	4.22	Hematite	-
Total	97.72	Rutile	0.5
Trace elements (ppm)		Apatite	0.9
Pb	20.7	Pyrite	0.3
Th	8	Calcite	0.4
U	3	Gypsum	2
Sc	13.8	detrit gypsum	-
V	122	auth gypsum	-
Ni	62.8	Zircon	0.03
		halerite	-
		Molybdenite	-
		Fluorite	0.5
		Jarosite	-
		Copiapite	-
		Chalcopyrite	-

3.2. Experimental Tests and Procedures

3.2.1. Sieve Analysis

The Spring Gulch soil sample was prepared by separating the soil fines (that is the material passing the sieve # 200) from the coarser portion by wet sieving. After wet sieving, the coarser portion of the soil sample was then oven-dried for about 24 hours. The oven-dried coarser portion of the total sample was then used for sieve analysis. Sieve analysis provides a way of separating bulk materials into size fractions allowing us to ascertain the particle size and distribution through weighing the distinct fractions. Usually, sieving processes are carried out on dry material. However, when dry sieving cannot produce an adequate degree of separation between the individual fractions, wet sieving is required (such as in this case).

3.2.2. Wet Sieving

Wet sieving (Figure 3.6) was performed to obtain the basic index parameters of the soil that can be used to estimate the strength of the rock pile. The soil sample was placed in a dish and allowed to dry for two days at 70 °C – 100 ºC. The whole dry sample was then weighed and recorded. Tap water was added and mixed thoroughly to loosen the clumped fine materials from coarser portion and then the whole sample was soaked for about 24 hours. The fine materials was washed through sieves #6, #10 and #200. The fines removed during washing were retained. The coarse fractions of the soil remained on the surface of the sieves and the silt/clay fraction passed through sieve #200. The weight of the silt/clay fraction is obtained by difference between the whole sample and the

coarser fraction weights. The purpose of the washing of the soil on the #200 sieve is to ensure that all the fines and surface coatings are washed off of the granular soil particles.

Figure 3.6: Wet sieve analysis

3.2.3. Dry Sieving

The dried and weighed coarser fraction was sieved through a stack of sieves consisting of the following: 3 in, 2 in, 1.5 in, 1 in, ¾ in, 3/8 in, #4, #6, #10, #16, #30, #40, #50, #100, #200 and a pan. The stacked column of sieves (Figure 3.7) was then transferred to an automatic sieve shaker for a period of 30-45 minutes (Figure 3.8). The materials retained on each sieve were weighed and recorded and stored in separate bags. The fines (minus #200 sieve) were stored in a separate container too. The materials retained on the stacked sieves were combined together to obtain the wet-dry gradation curve (Figure 3.9). The materials retained on sieve numbers 10, 16, 30, 40, 50, 100, 200 and the fines (minus #200 sieve) were mixed together according to the gradation curve of

Figure 3.9 (lab) to provide samples for the direct shear testing. Therefore, scalped material is used for direct shear testing.

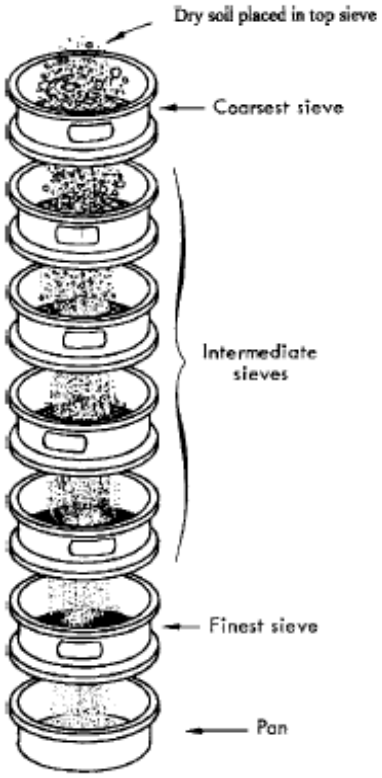

Figure 3.7: Diagram illustrating the stacking of sieves. (Asphalt Handbook, 1989)

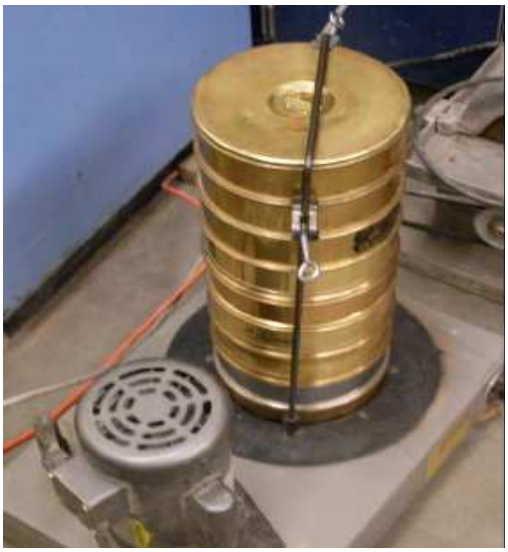

Figure 3.8: Mechanical shaker

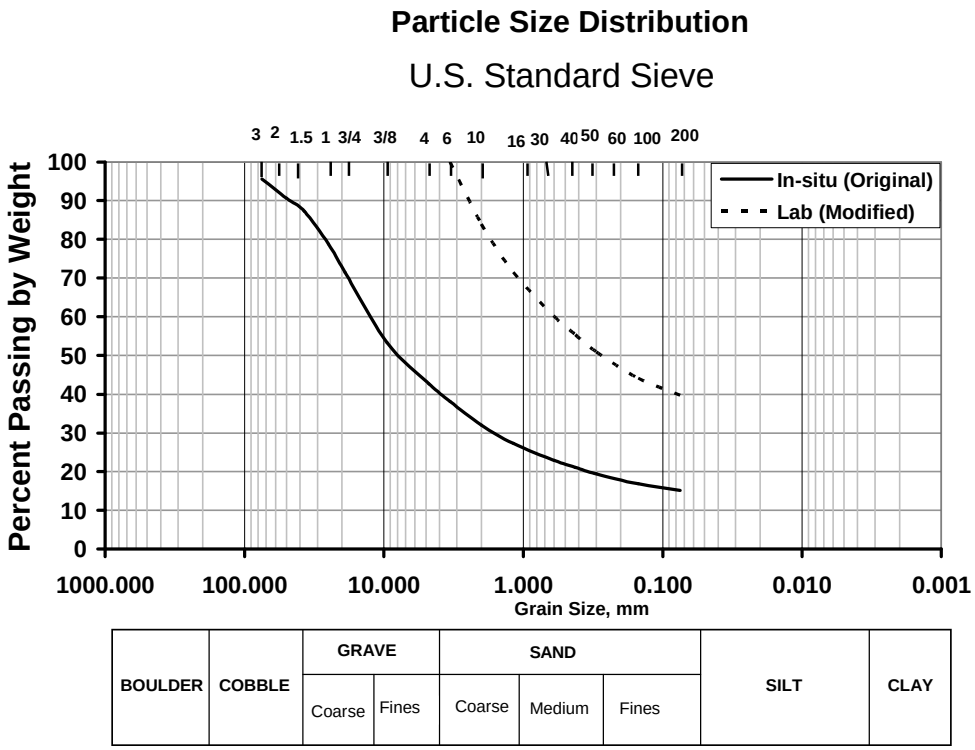

Figure 3.9: Gradation curves (in-situ and lab materials) of the Spring Gulch material.

3.3. Experimental Setup and Shear Test Procedures

The mass of the soil sample corresponding to the volume of the shear box and the required compaction density was quantitatively measured. The shear box used is 6 cm × 6 cm in size (Figure 3.10A). The shear box alignment screws are removed to separate the shear box halves (Figure 3.10B). The bottom plate and the porous stone are placed in the bottom of the lower shear box half. The top half is then replaced and fastened together with the two shear box alignment screws. The soil sample is then placed into the shear box and tampered in three layers (Figure 3.10C). The shear box is then placed in the shear test device. The U-shaped cutout extending from the shear box must fit tightly onto the extension from the shear force load cell. The shear box restraining screws are tightened to secure the shear box (Figure 3.10D). The LVDTs for measuring the soil

vertical and shear deformations are adjusted so that the sensors can measure at least 10 mm of deformation (Figure 3.10E). The LVDTs are secured firmly by tightening the locking screw.

To run the test, there are four stages: initialization, consolidation, shearing, and measurement. The unsaturated soil sample is allowed to consolidate for about 30 minutes. The transducer operation tab is checked to ensure that the computer was reading the LVDT and load cell transducer signal conditioner readout correctly. The two shear box alignment screws (Figure 3.10F) are removed before the direct shear test was performed. The shearing motion is started and the run tab on the digital shear machine is also pushed to run the test. The test is allowed to run until either the shear force begins to fall or until it reaches the maximum shear displacement that the machine can handle. After completion of a shear test, the shearing motion is stopped and the normal load is removed from the shear box. The shear box is then carefully removed from the test machine. The shear box is emptied and is cleaned to be ready for the next shear test.

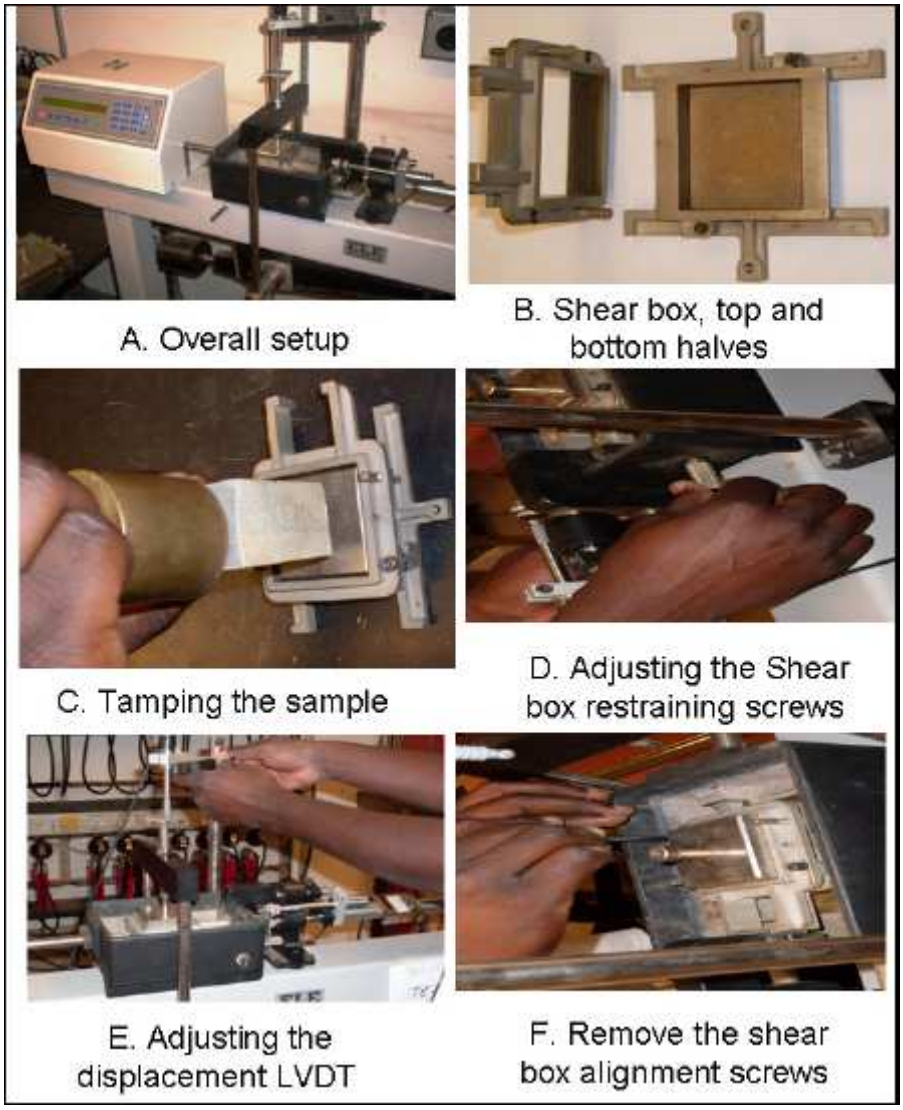

Figure 3.10: Direct shear test setup procedure

Dry compaction densities of 1700 kg/m^3 and 1850 kg/m^3 of the samples were tested. The compaction densities were chosen so that they were approximately in the range of in-situ values which were determined from the field in-situ measurements (Fakhimi et al. 2007). Air dried samples and samples with 8% water content were tested to study the effect of water on the behavior of the unsaturated soil samples. The effect of shear rate deformation was studied by using different deformation rates of 0.5 mm/min, 0.05

mm/min, 0.0275 mm/min and 0.005 mm/min. The duration of the shear load stage was defined by the maximum shear displacement of 10 mm. For example a test with the shear displacement rate of 0.005 mm/min took about 33 hours to finish. Normal stresses of 160 kPa, 480 kPa and 750 kPa were used. In general, more than one shear test was conducted for a given normal load and a shear displacement rate to ensure the repeatability of the test results. The shear and normal displacements of the soil sample together with the applied shear force were measured during each shear test.

3.4. Degree of Saturation of Samples

Increasing compaction density increases the degree of saturation of the soil sample with a constant water content (8%). This in effect reduces the void sizes in the soil sample. Table 3.3 shows compaction density, void ratio and degree of saturation for samples with 8 % water content. The specific gravity, G_s of the soil sample is 2.76.

Table 3.3: Determination of degree of saturation and void ratio as compaction density increases.

Compaction density (kg/m^3)	Void ratio, e	Degree of Saturation (%)
1700	0.624	35.4
1850	0.492	44.9

4. TEST RESULTS AND DISCUSSION

4.1. Introduction

This chapter presents and analyzes the results of direct shear tests with different rates of shear deformation on dry and moist (8% water content) Spring Gulch rock pile materials. The data obtained are plotted and discussed accordingly. A laboratory testing program was developed for this study that included a series of direct shear tests with four different rates of shear deformation varying from a lower value of 0.005 mm/min to the highest of 0.5 mm/min. Normal stresses of 160 kPa, 480 kPa and 750 kPa were used. To ensure the repeatability of the results for each normal stress, three direct shear tests were performed corresponding to a specific rate of shear deformation. Averages for the three tests performed are computed and used for discussion in this chapter.

4.2. Results of Direct Shear Tests on Air-dried Samples

The measured shear stress-shear displacement curves for dried samples compacted to a dry density of 1850 kg/m^3 using four different rate of shear deformation are shown in Figure 4.1. Figure 4.1 shows that the stress-displacement curves for the dry samples have peak values from which the shear stress reduces with further displacement. The dry samples show hardening in all samples followed by a softening behavior for some samples and normal stresses. A plot of normal displacement against shear displacement is used to identify the expansion or dilatation behavior of the rock pile

material during the direct shear test. Negative displacements indicate dilation of the material (Figure 4.2). As expected, as the applied normal stress increases, dilation of the material decreases during the shear test.

Figure 4.3 shows the peak shear stress as a function of the deformation rate. It appears that the shear strength of the rock pile material is not noticeably affected by the deformation rate. The Mohr-Coulomb envelopes for the shear tests are depicted in Figure 4.4. Even though the peak shear strength values are relatively insensitive to the deformation rate, it appears that the friction angle increases as the deformation rate increases (Figure. 4.5). A likely justification of this behavior is that at higher shearing rates, less time is allowed for rearrangement of particles inside the shear box, which results in a greater friction angle of the material (Al-Mhaidib 2005). Another possibility for higher friction angle is that the thickness of the soil that is mobilized upon shearing varies with strain rate and the amount of dilation in the mobilized zone increases as the strain rate increases (Figure 4.2).

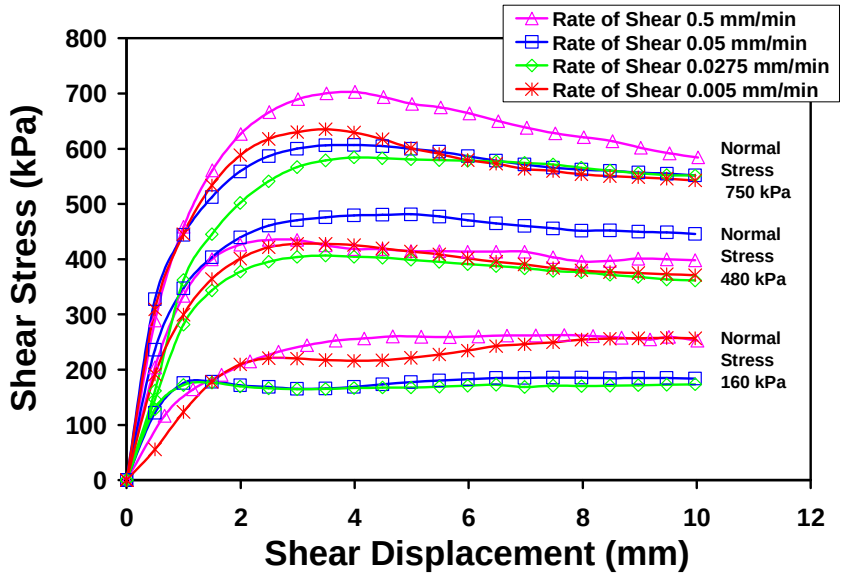

Figure 4.1: A plot of shear stress versus shear displacement curve for air-dry samples with dry density of 1850 kg/m^3 for four different shearing rates

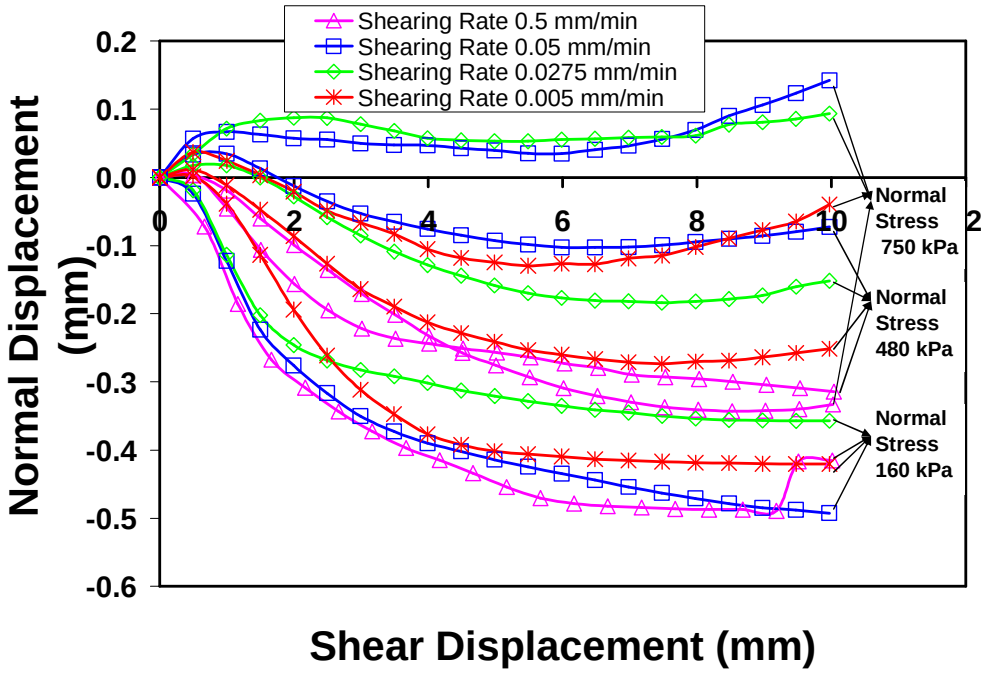

Figure 4.2: A plot of normal displacement versus shear displacement for air-dry samples with dry density of 1850 kg/m^3 for four different shearing rates

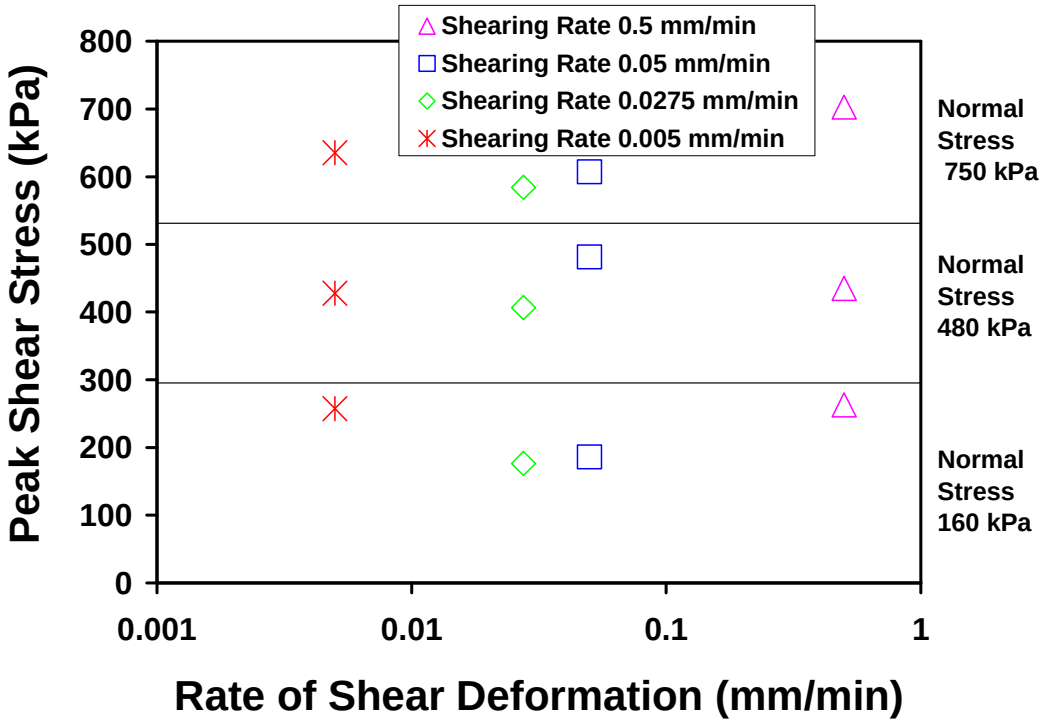

Figure 4.3: Peak shear stress versus rate of shear deformation for air-dry samples with dry density of 1850 kg/m^3 for four different shearing rates

The results of direct shear tests including the peak friction angles, residual friction angles (corresponding to a shear displacement of 10 mm), peak cohesions and residual cohesions from all the tests on dry Spring Gulch rock pile material are listed in Table 4.1. Table 4.1 also reveals that, the internal peak friction angle increases as the rate of shear deformation increases. Note that the peak internal friction angles versus the rate of shear deformation have been plotted in a semi-logarithm format in Figure 4.5. The plotted results show a moderately constant linear trend, which agrees with the results reported by Etsuro (1979). The relationships between the internal friction angle and rate of shear deformation of dry Spring Gulch rock pile materials with a compaction density of 1850 kg/m^3 is represented by the following equation:

$$\phi = 0.9755 \mathrm{Ln}\,(RSD) + 37.5 \qquad (2)$$

Where Ln stands for natural logarithm and

ϕ = internal friction angle of dry Spring Gulch rock pile material in degrees, and

RSD = Rate of Shear Deformation in mm/min.

The above equation is based on the test results and it can vary from rock pile to rock pile. Note that cohesion values do not show a specific trend as the shearing rate is changed. In general cohesion is a very sensitive parameter compared to friction angle. Literature review shows that cohesion can have a large scatter; a coefficient of variation of more that 50% has been reported for cohesion in the literature (Baecher and Christian, 2003).

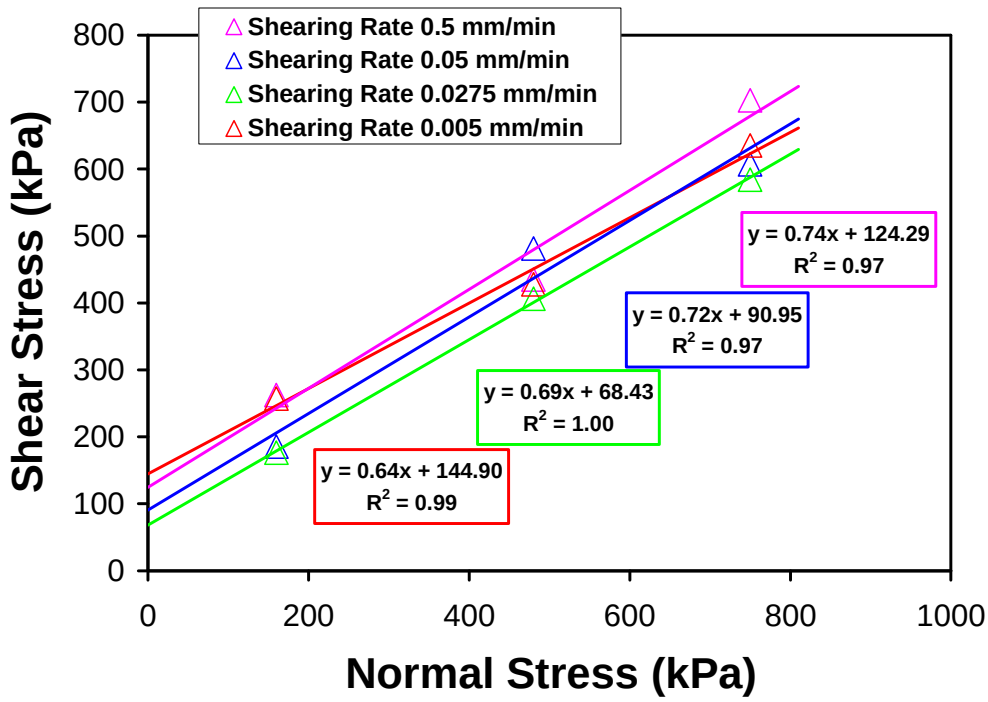

Figure 4.4: Failure envelopes for air-dry Spring Gulch rock pile material for different shearing rates with compaction dry density of 1850 kg/m^3.

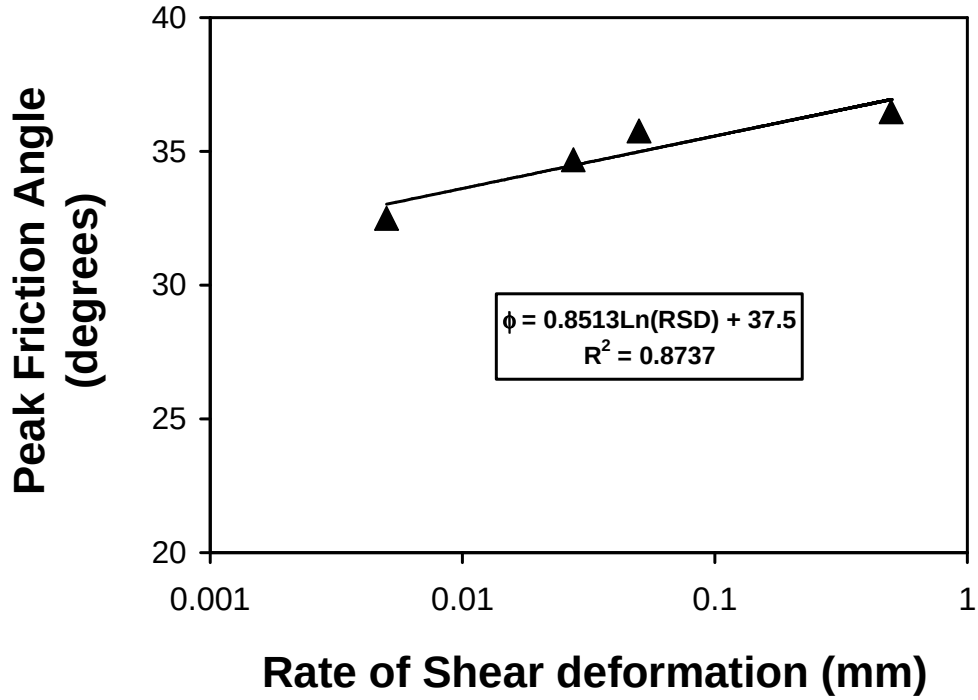

Figure 4.5: Effect of rate of shear deformation (RSD) on peak friction angle of dry samples with compaction dry density of 1850 kg/m^3.

Table 4.1: Direct shear test results conducted on air-dry (compaction density of 1850 kg/m^3) Spring Gulch rock pile material with varying rate of shear deformation.

Shearing Rate	Normal Stress	Peak Shear Stress	Peak Friction Angle	Peak Cohesion	Residual Shear Stress	Residual Friction Angle	Residual Cohesion
(mm/min)	(kPa)	(kPa)	(degrees)	(kPa)	(kPa)	(degrees)	(kPa)
0.5	160	262.8	36.5	125.0	252.3	29.2	152.4
0.5	480	435.0			398.1		
0.5	750	702.8			584.4		
0.05	160	185.8	35.8	91.0	183.8	32.2	102.0
0.05	480	481.3			445.7		
0.05	750	607.0			551.9		
0.0275	160	176.4	34.7	68.4	173.3	32.6	65.8
0.0275	480	406.6			361.2		
0.0275	750	584.2			551.5		
0.005	160	257.4	32.5	144.9	256.7	25.7	167.4
0.005	480	427.8			371.1		
0.005	750	635.3			542.7		

4.3. Direct shear tests on moist samples

Samples with moisture content of 8% were tested using dry compaction densities of 1700 kg/m^3 and 1850 kg/m^3. Plots of the shear stress versus shear displacement for the two densities at the same moisture content of 8% under different rates of shearing are shown in Figures 4.6 and 4.7. As expected the shear stress increased with increasing the normal stress but moist samples do not show post-peak softening behavior. Figures 4.8 to 4.11 show the role of compaction density and shear displacement rate on the material behavior. By increasing the compaction density, the overall rigidity of the specimens (initial slopes of the curves) increases, but the peak stresses are not necessarily increased. This observation could be due to the increased in fines material in the samples with greater density as in this situation greater compaction effort is used.

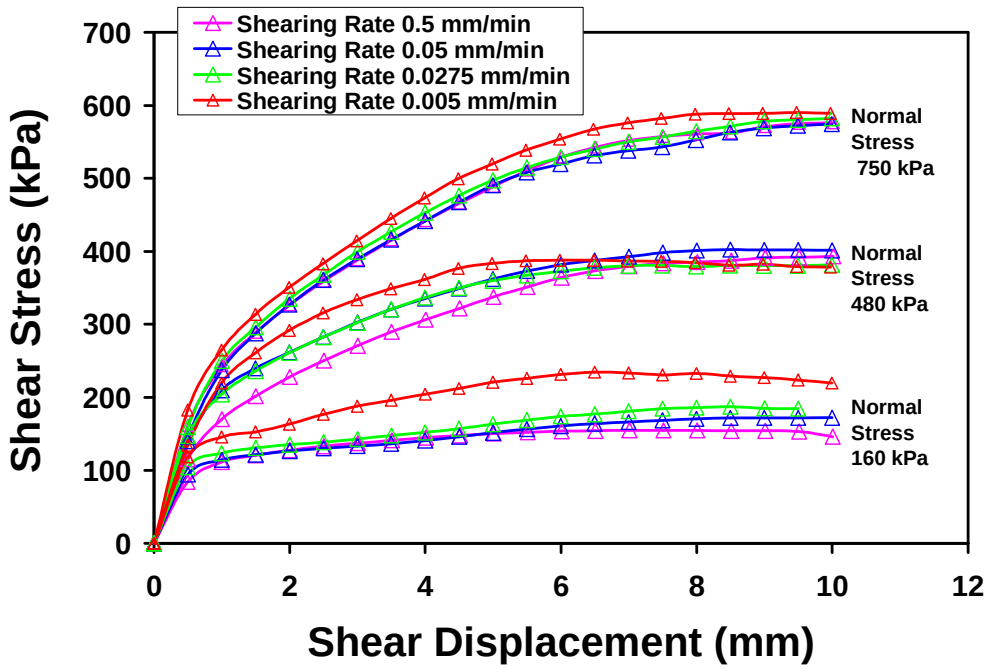

Figure 4.6: A plot of shear stress versus shear displacement with dry density of 1700 kg/m^3 for moist (8% water content) Spring Gulch samples at four different shear rates.

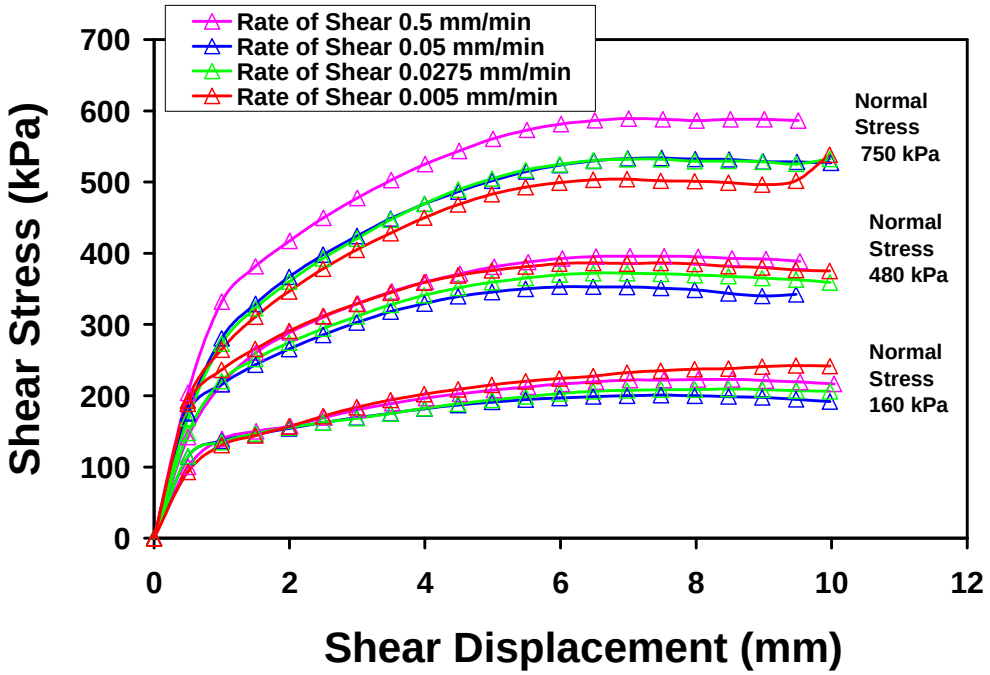

Figure 4.7: A plot of shear stress versus shear displacement with dry density of 1850 kg/m^3 for moist (8% water content) Spring Gulch samples at four different shearing rates.

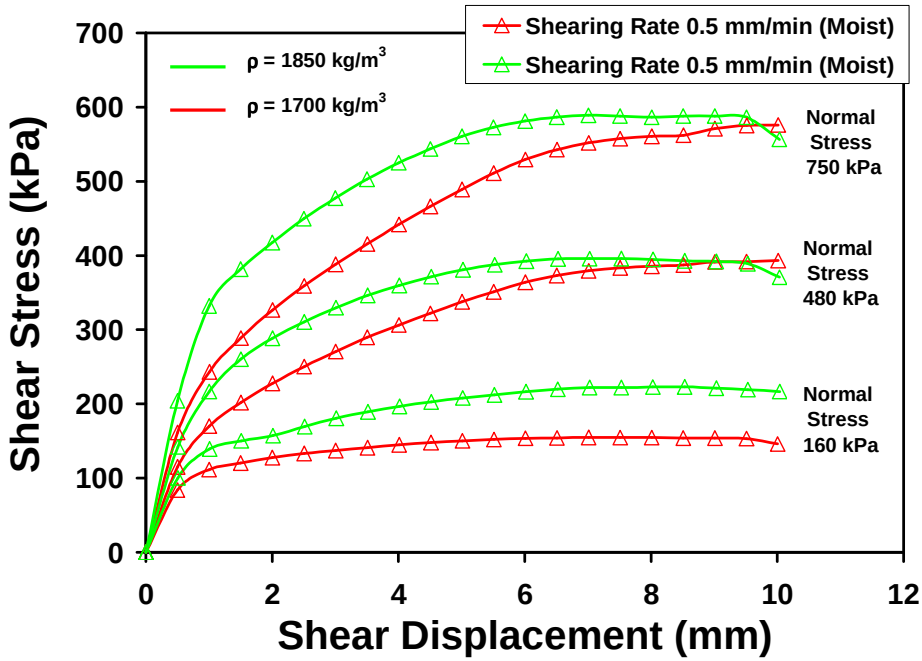

Figure 4.8: Combined plot of shear stress versus shear displacement for dry densities of 1700 kg/m^3 and 1850 kg/m^3 for moist (8% water content) Spring Gulch samples at 0.5 mm/min shearing rate.

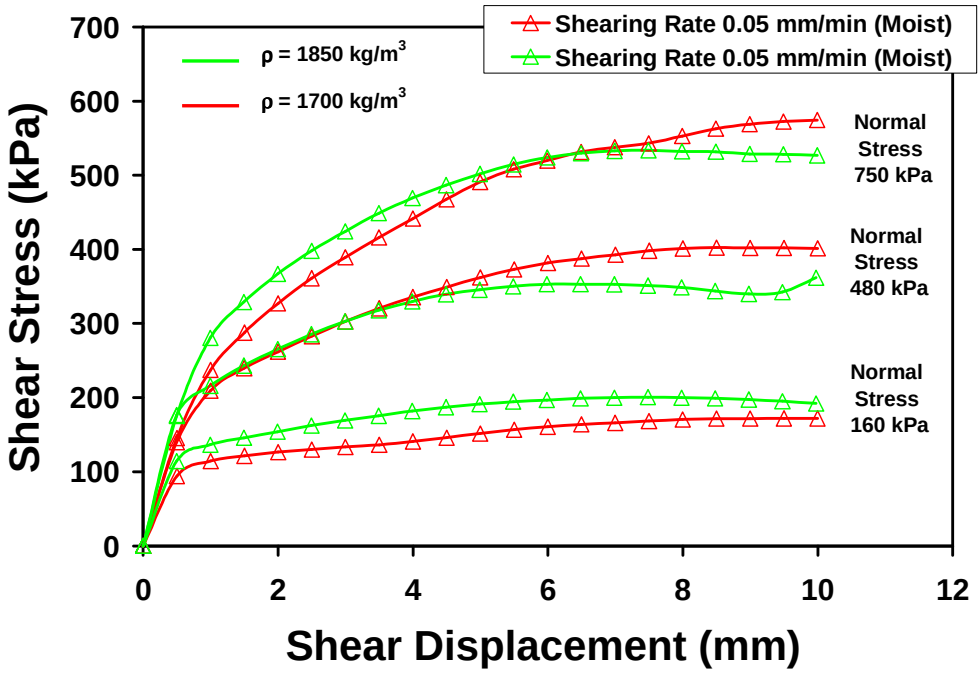

Figure 4.9: Combined plot of shear stress versus shear displacement for dry densities of 1700 kg/m^3 and 1850 kg/m^3 for moist (8% water content) Spring Gulch samples at 0.05 mm/min shearing rate.

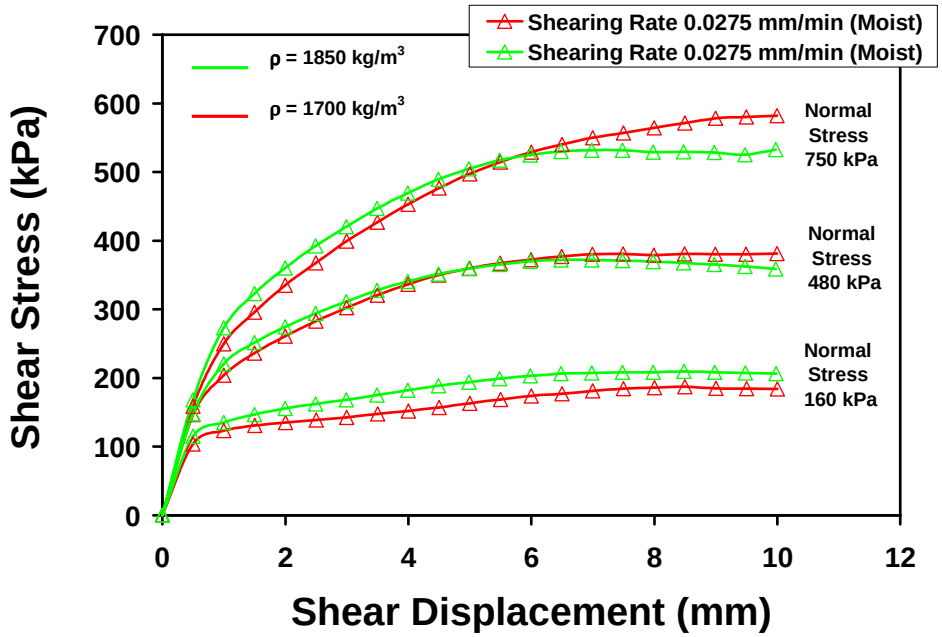

Figure 4.10: Combined plot of shear stress versus shear displacement for dry densities of 1700 kg/m^3 and 1850 kg/m^3 for moist (8% water content) Spring Gulch samples at 0.0275 mm/min shearing rate.

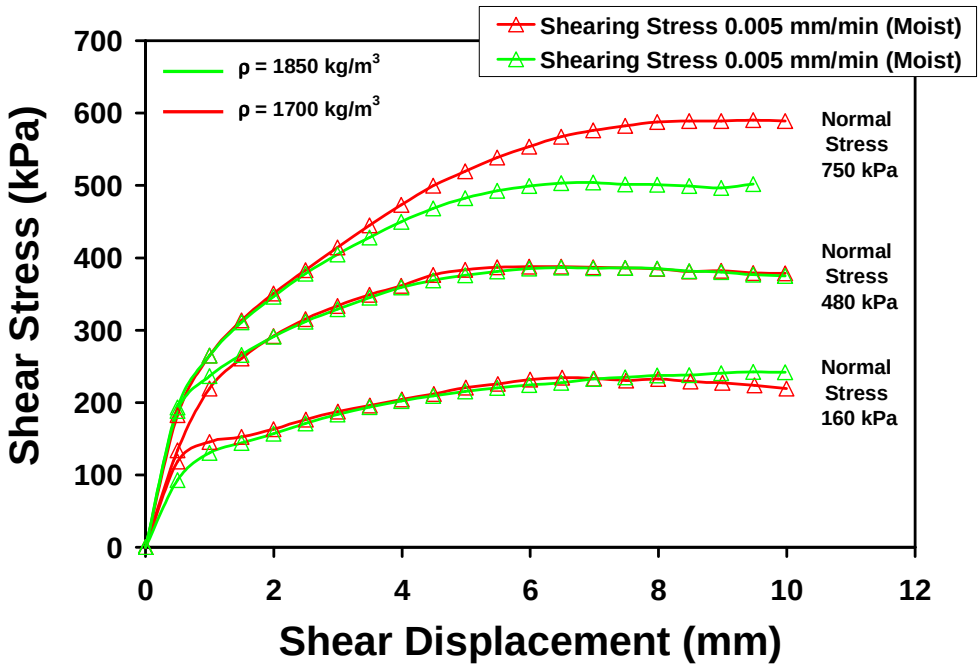

Figure 4.11: Combined plot of shear stress versus shear displacement for dry densities of 1700 kg/m^3 and 1850 kg/m^3 for moist (8% water content) Spring Gulch samples at 0.005 mm/min shearing rate

The peak shear stresses for different shearing rates and densities are shown in Figure 4.12. No general trend is observed as it appears that at least two competing components are involved with the shear strength. On one hand, greater density should cause an increase in shear strength. On the other hand, as mentioned above, greater compaction effort can create greater amount of fine material in the specimen. Greater compaction causes an increase in the degree of saturation of the sample, which could be responsible for strength reduction. This has been confirmed by other studies. For example, Yoshitada et al. (1991) reports that an increase in degree of saturation causes a decrease in soil strength. The degrees of saturation for the two densities are reported in Table 3.3 (chapter 3).

The Mohr-Coulomb diagrams for the moist samples are shown in Figures 4.13 and 4.14. From these figures, the friction angles and cohesion intercepts were obtained. These parameters are reported in Tables 4.2 and 4.3. Comparison of the friction angles and cohesion values in these tables suggests that moist sample with greater compaction density have smaller friction angles while their cohesion values are greater.

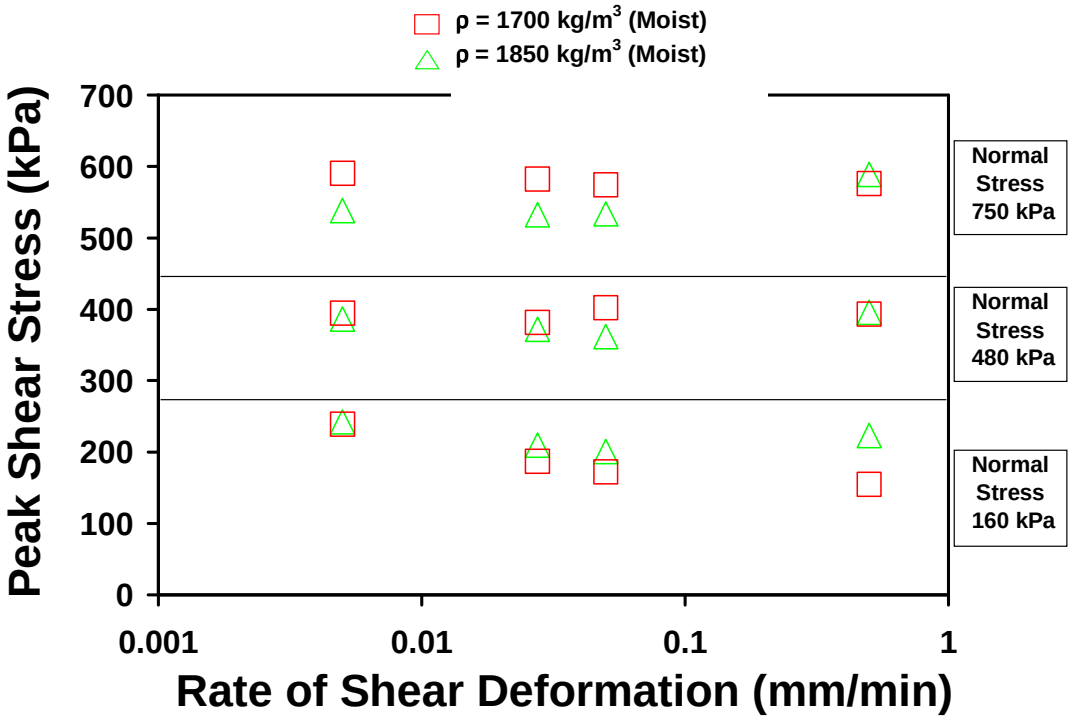

Figure 4.12: A plot of peak shear stress versus rate of shear deformation for moist samples.

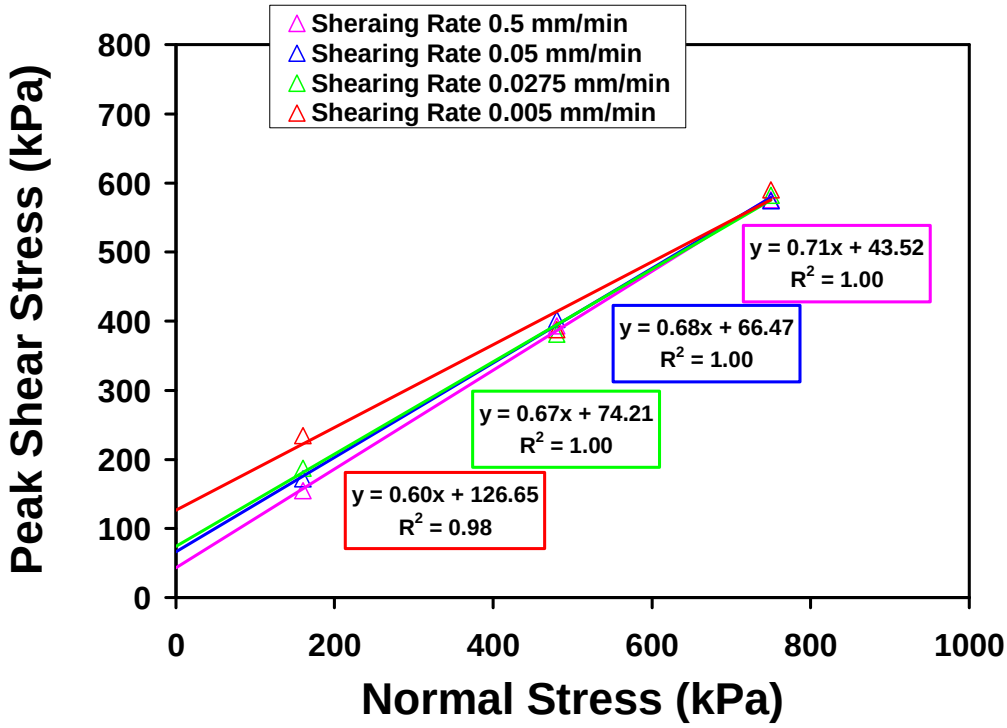

Figure 4.13: Failure envelopes for the moist samples with dry density of 1700 kg/m^3.

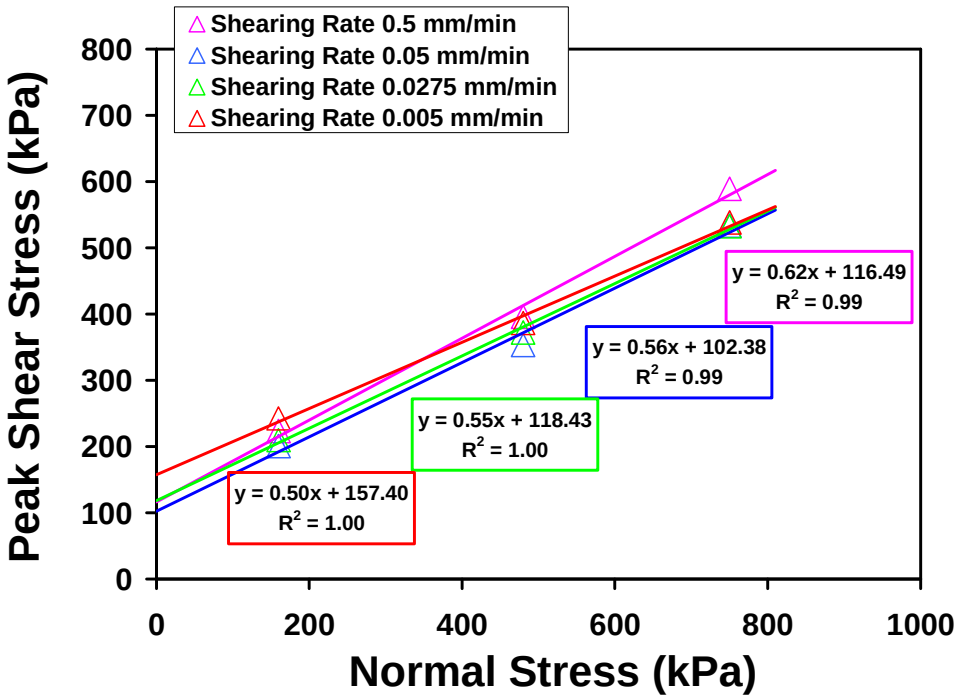

Figure 4.14: Failure envelopes for the moist samples with dry density of 1850 kg/m^3

Table 4.2: Direct shear test results for moist samples with a compaction dry density of 1700 kg/m^3 and varying rate of shear deformation.

Shearing Rate	Normal Stress	Peak Shear Stress	Peak Friction Angle	Peak Cohesion	Residual Shear Stress	Residual Friction Angle	Residual Cohesion
(mm/min)	(kPa)	(kPa)	(degrees)	(kPa)	(kPa)	(degrees)	(kPa)
0.5	160	154.9	35.6	43.5	146.1	36.1	33.6
0.5	480	393.1			393.1		
0.5	750	575.9			575.9		
0.05	160	172.0	34.3	66.5	172.0	34.3	66.2
0.05	480	402.4			401.4		
0.05	750	574.3			574.3		
0.0275	160	187.2	33.7	74.4	184.0	33.9	70.6
0.0275	480	381.2			381.22		
0.0275	750	582.1			582.1		
0.005	160	2391	30.6	133.8	238.1	30.5	129.6
0.005	480	394.5			382.2		
0.005	750	590.2			588.9		

Table 4.3: Direct shear test results for moist samples with a compaction dry density of 1850 kg/m^3 and varying rate of shear deformation.

Shearing Rate	Normal Stress	Peak Shear Stress	Peak Friction Angle	Peak Cohesion	Residual Shear Stress	Residual Friction Angle	Residual Cohesion
(mm/min)	(kPa)	(kPa)	(degrees)	(kPa)	(kPa)	(degrees)	(kPa)
0.5	160	223.1	31.7	116.5	216.8	29.8	115.9
0.5	480	395.9			388.9		
0.5	750	589.0			586.3		
0.05	160	200.8	29.2	104.9	192.1	29.5	97.9
0.05	480	353.0			342.3		
0.05	750	533.6			526.8		
0.0275	160	209.7	28.6	118.4	206.3	28.8	110.8
0.0275	480	372.1			358.9		
0.0275	750	532.6			532.6		
0.005	160	242.4	26. 6	157.4	241.8	26.6	153.5
0.005	480	386.5			375.0		
0.005	750	538.3			538.3		

The volumetric soil behavior during shear deformation needs to be discussed too. The normal displacement versus shear displacement for moist samples is shown in Figures 4.15 and 4.16. Notice that, as expected by reducing the normal stress, the dilation of the material increases. The effect of shearing rate is depicted in Figures 4.15 and 4.16 as well but no general conclusion can be made from these figures regarding the effect of shearing rate on the dilatational behavior of the material.

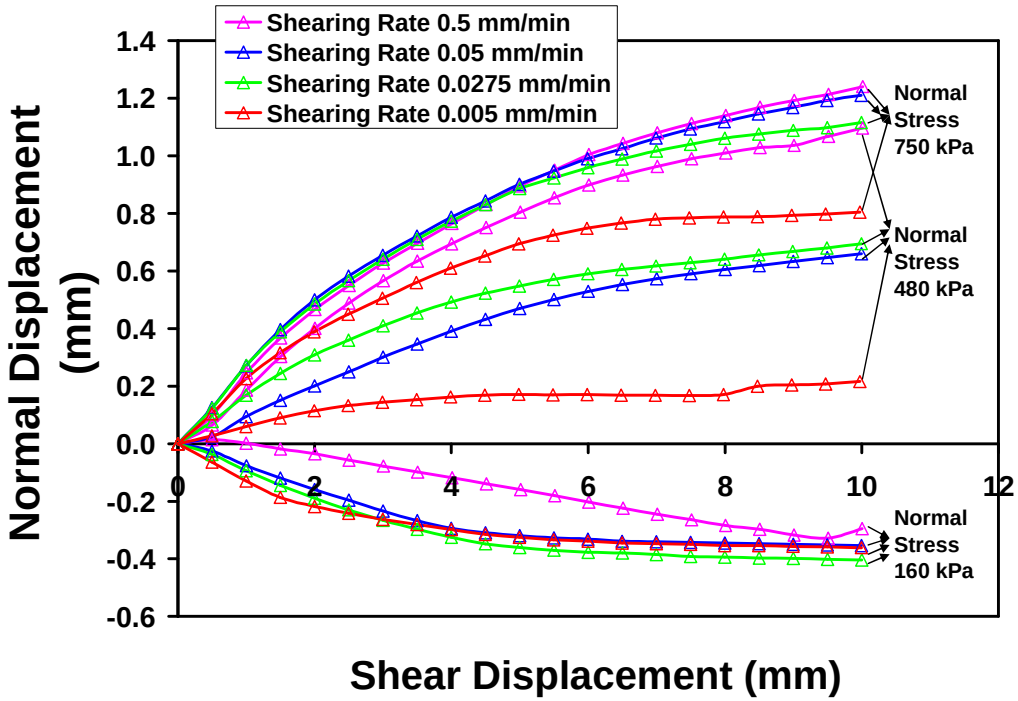

Figure 4.15: A plot of normal displacement versus shear displacement for moist samples with a dry density of 1700 kg/m^3 at four different shearing rates.

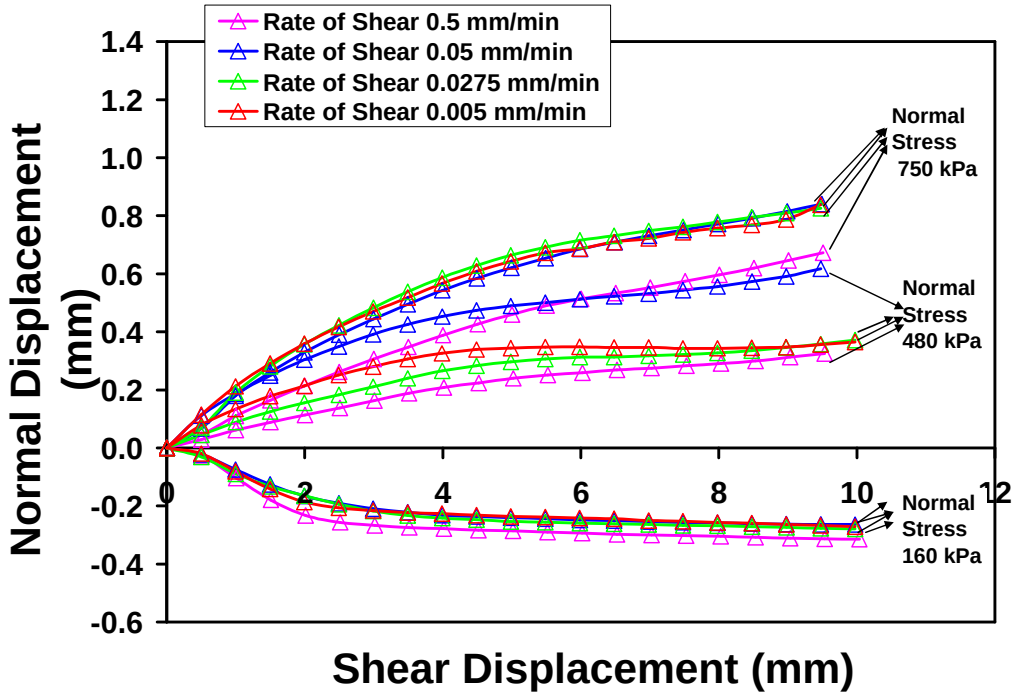

Figure 4.16: A plot of normal displacement versus shear displacement for moist samples with a dry density of 1850 kg/m^3 at four different shearing rates.

The influence of shearing at different rates on the peak friction angle is shown in Figure 4.17 for compaction densities of 1700 kg/m^3 and 1850 kg/m^3. The friction angle generally increases with the increase in shearing rate. As reported for the dry condition, a plot of peak internal friction angle against the rate of shear deformation on a semi logarithm graph shows a linear trend. Figure 4.17 also reveals that, as the compaction density increases, the friction angle of the moist Spring Gulch rock pile material decreases. Decrease in shear strength of soil as a result of increase in degree of saturation was reported by Yoshitada (1991). The reduction in friction angle can be attributed to the increase in the degree of saturation and possibly the generation of fine material due to the greater compaction effort.

The relationships between the internal friction angle and the rate of shear deformation of moist Spring Gulch rock pile materials with compaction densities of 1700 kg/m^3 and 1850 kg/m^3 are represented by the following equations:

$\phi = 0.9755\text{Ln (RSD)} + 36.7$ (for 1700 kg/m^3 density) and; (3)

$\phi = 1.1105\text{Ln (RSD)} + 32.5$ (for 1850 kg/m^3 density) (4)

In the above equations RSD (rate of shearing deformation) must be given in mm/min.

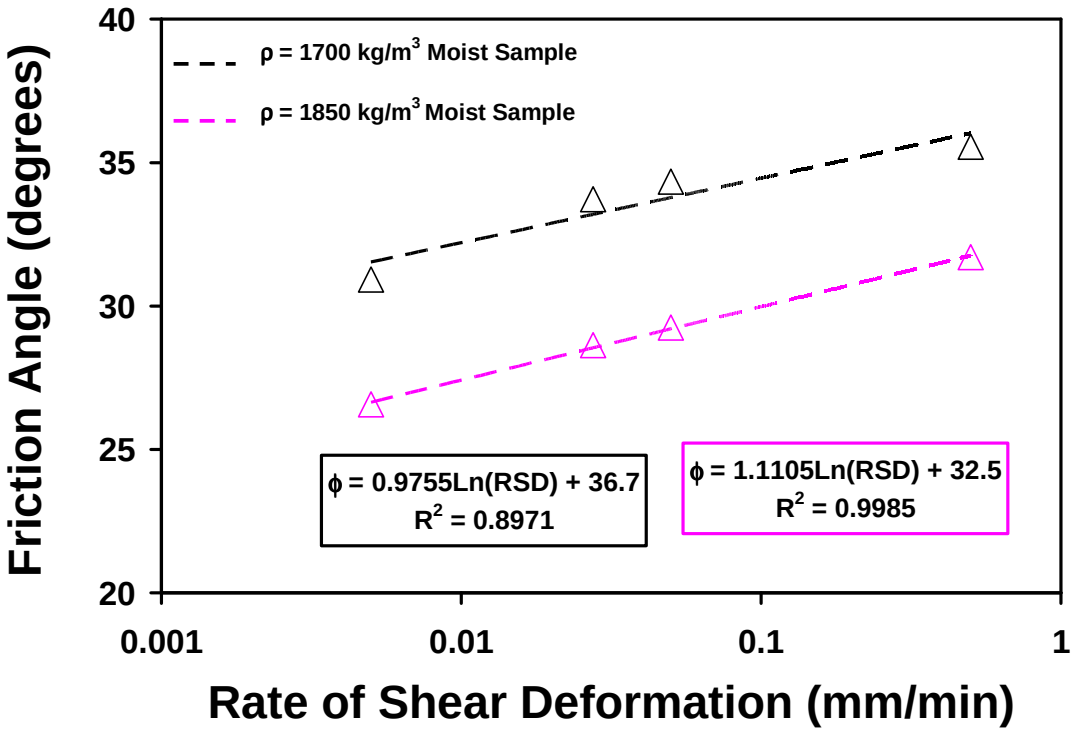

Figure 4.17: Effect of rate of shear deformation on friction angle of moist Spring Gulch rock pile material with different compaction densities.

4.4. Comparison of the shear strength of moist and dry samples

The effects of moisture on mechanical behavior of rock pile materials are discussed in this section. In Figures 4.18 to 4.21 the shear stress versus shear displacement is shown for different shearing rates with a dry compaction density of 1850 kg/m^3 for both dry and moist samples. As expected, the dry samples mostly show both hardening and softening behavior while the moist samples show no softening after the peak. The dry samples show greater rigidity too, which is expected. These behaviors are consistent with the greater dilatation behavior of the dry material compared to that of the moist samples (Figures 4.22 to 4.25).

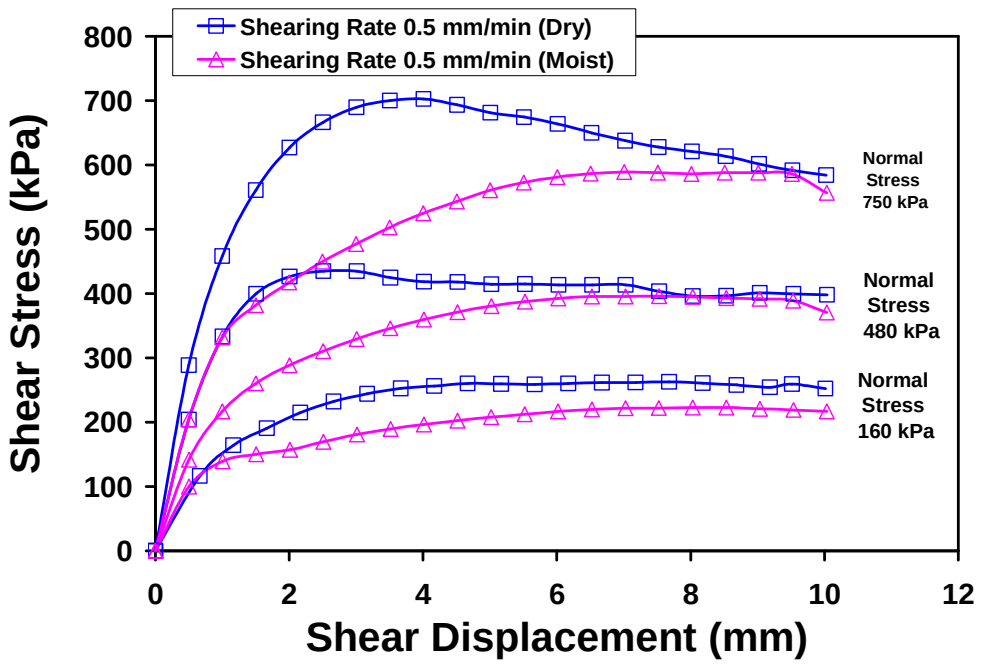

Figure 4.18: A plot of shear stress versus shear displacement of dry and moist Spring Gulch samples at 0.5 mm/min shearing rate and dry density of 1850 kg/m^3.

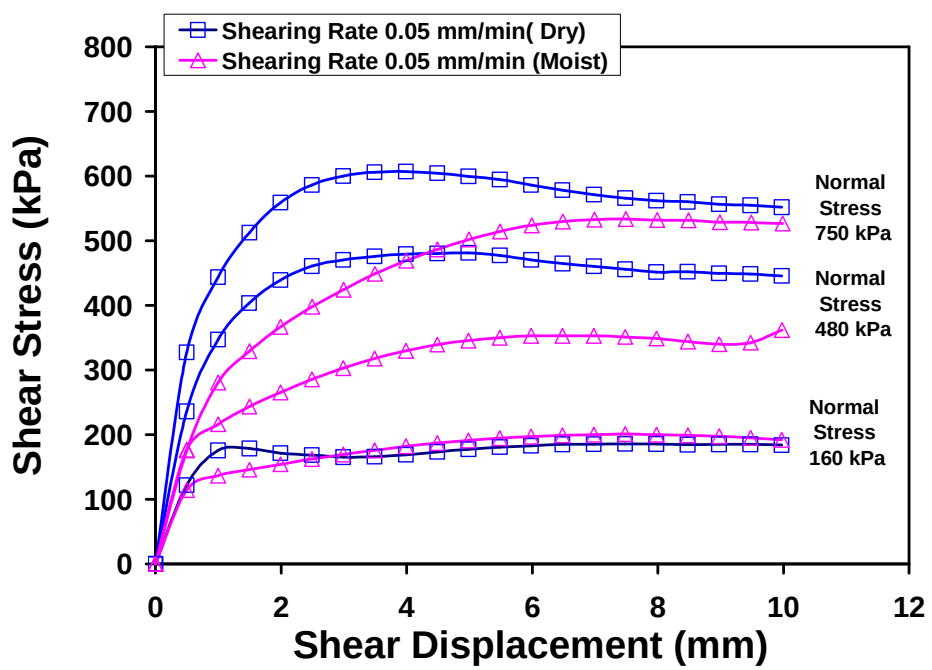

Figure 4.19: A plot of shear stress versus shear displacement of air-dry and moist samples at 0.05 mm/min shearing rates and dry density of 1850 kg/m^3.

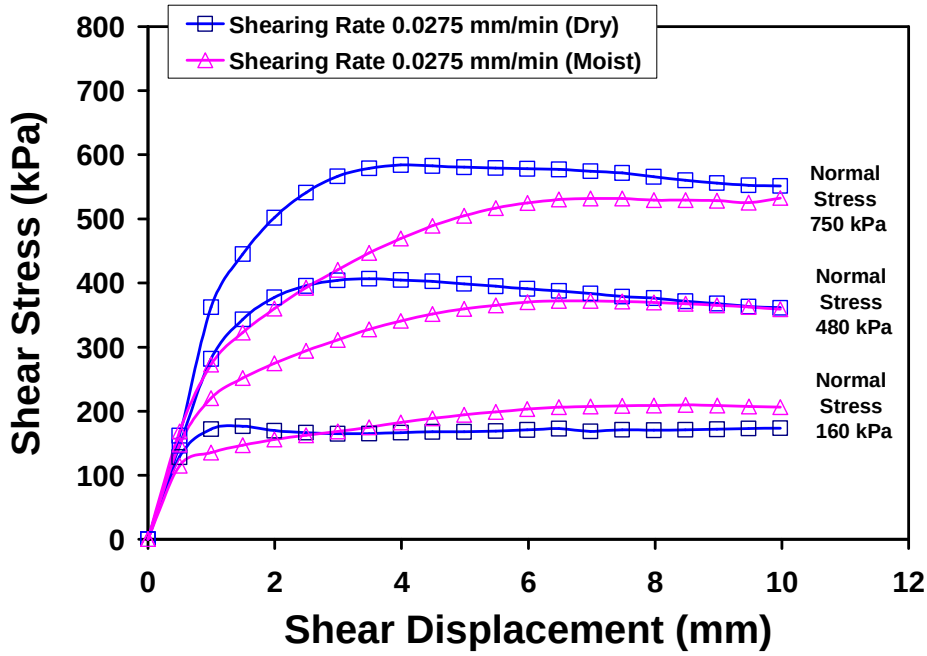

Figure 4.20: A plot of shear stress versus shear displacement of air-dry and moist samples at 0.0275 mm/min Shearing rate and dry density of 1850 kg/m^3.

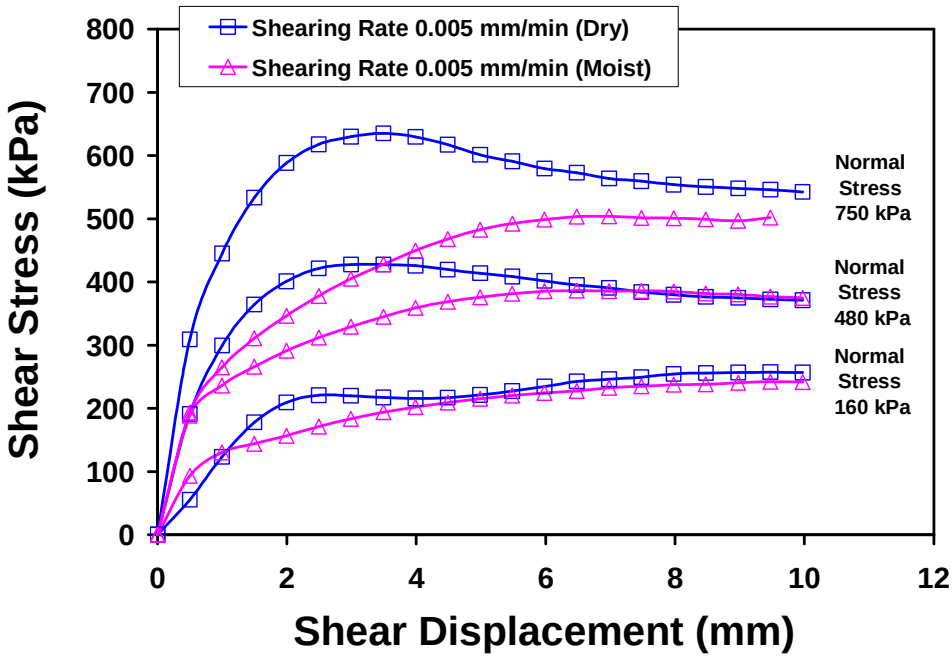

Figure 4.21: A plot of shear stress versus shear displacement of air-dry and moist samples at 0.005 mm/min shearing rate and dry density of 1850 kg/m^3.

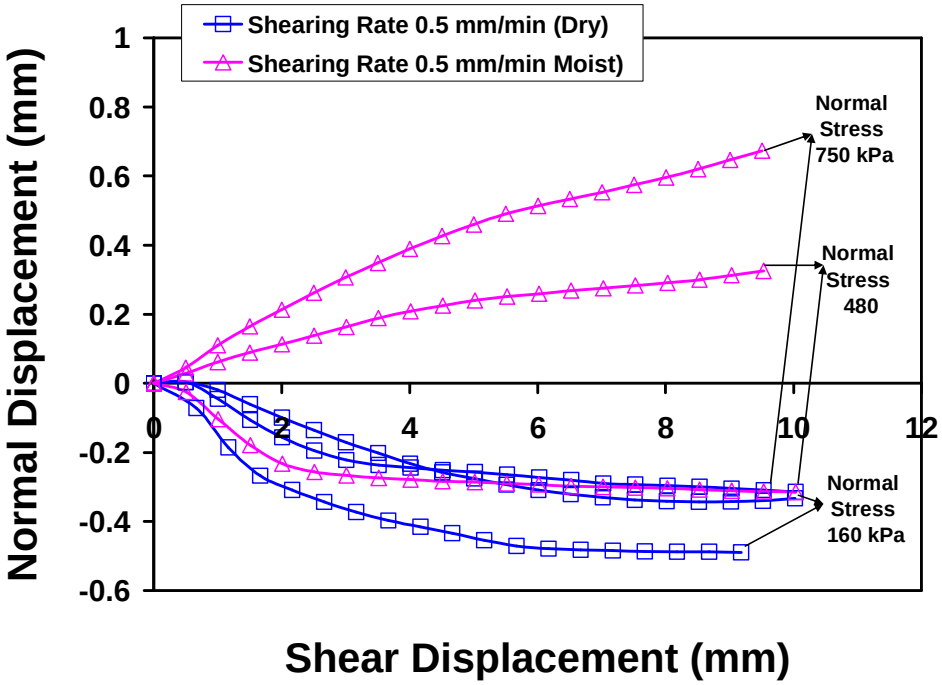

Figure 4.22: A plot of normal displacement versus shear displacement for air-dry and moist samples for 0.5 mm/min shearing rate and a dry density of 1850 kg/m^3.

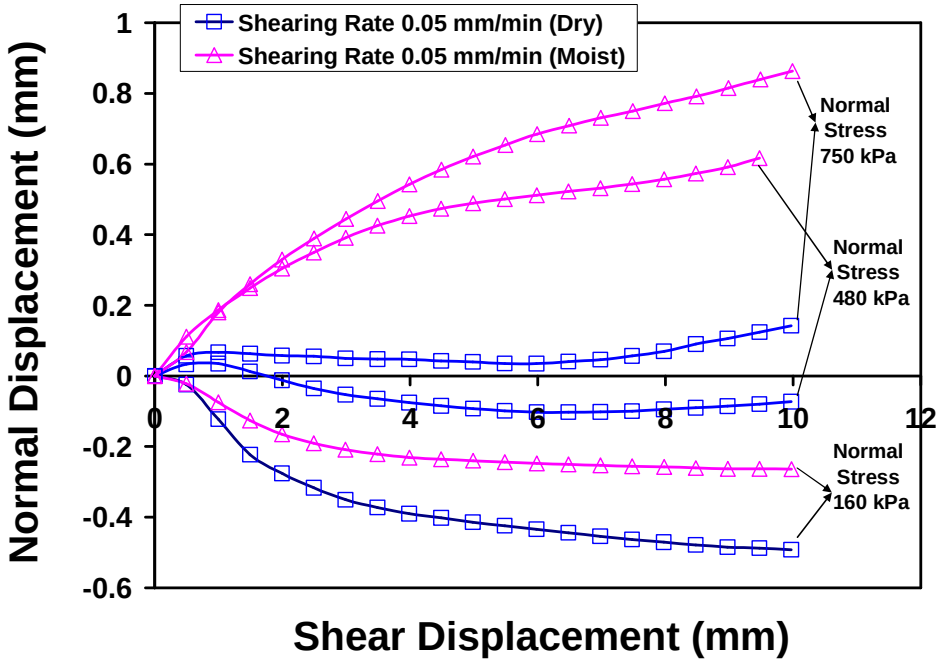

Figure 4.23: A plot of normal displacement versus shear displacement for air-dry and moist samples for 0.05 mm/min shearing rate and a dry density of 1850 kg/m^3

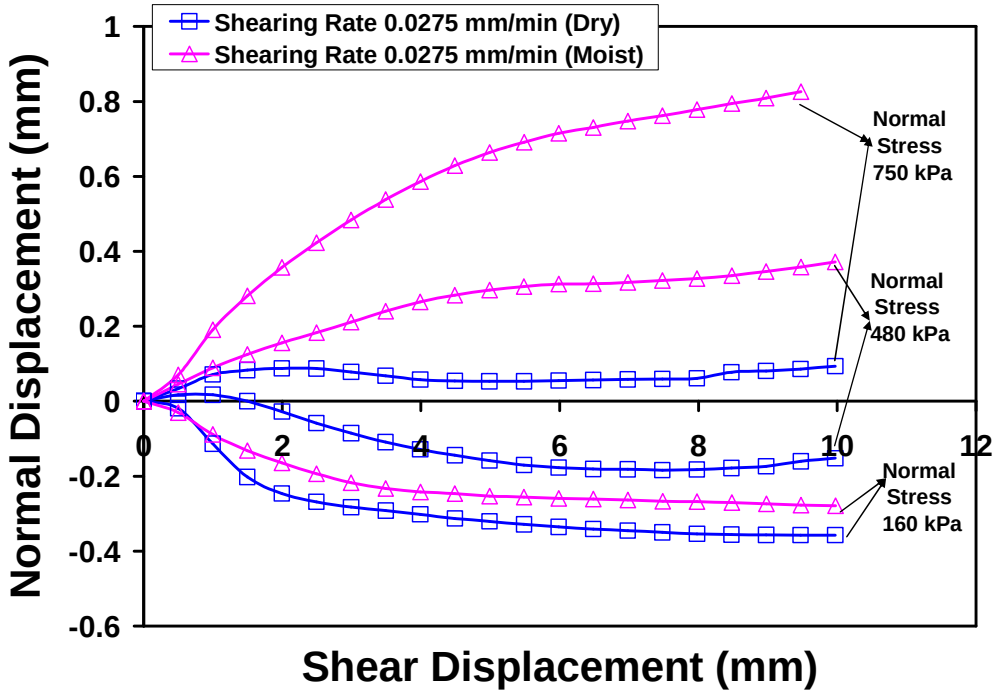

Figure 4.24: A plot of normal displacement versus shear displacement for air-dry and moist samples for 0.0275 mm/min shearing rate and a dry density of 1850 kg/m^3.

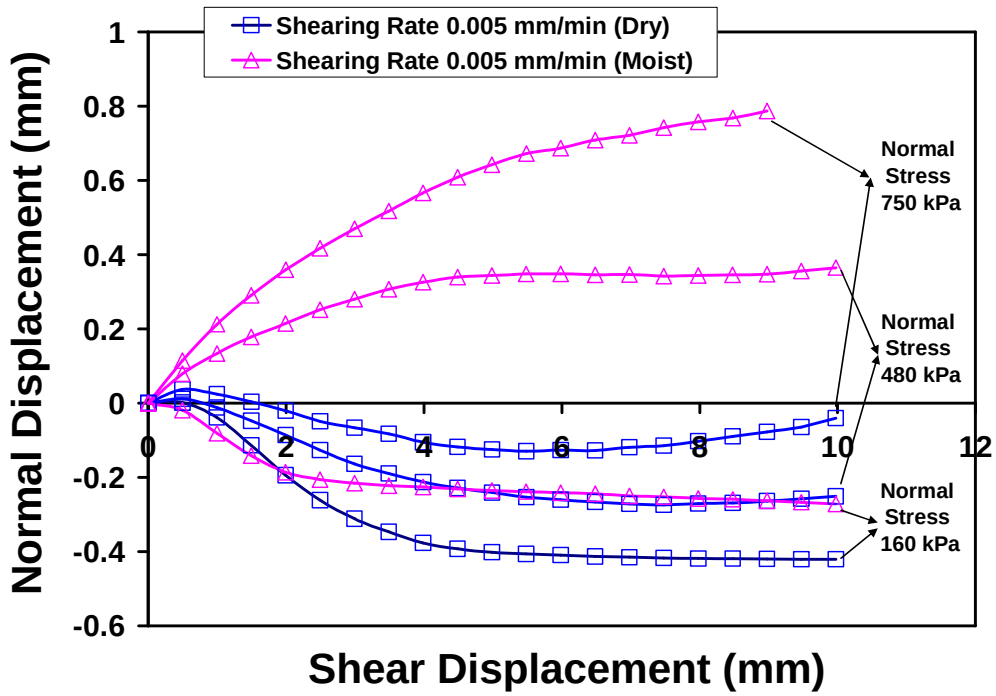

Figure 4.25: A plot of normal displacement versus shear displacement for air-dry and moist samples for 0.005 mm/min shearing rate and a dry density of 1850 kg/m^3.

The shear strengths of the rock pile material for different shear displacement rates are depicted in Figure 4.26. The dry samples are stronger than the moist ones which is consistent with the above discussions. This moisture softening was observed in previous studies that were conducted on Questa rock pile material (Nunoo, 2009).

In Figure 4.27, the effect of shear displacement rate on friction angle for moist and dry samples are shown. Two moist samples with dry compaction densities of 1700 and 1850 kg/m^3 are depicted in the figure. This figure suggests that irrespective of moisture content, the friction angle decreases by reducing the shearing rate. It also indicates that moist samples with higher density show lower friction angles for the reasons discussed before. Considering the equations for the best fit lines in Figure 4.26, it appears that the slope of the lines for moist samples is greater than that for dry samples; friction angle of moist samples is more sensitive to the shear displacement rate.

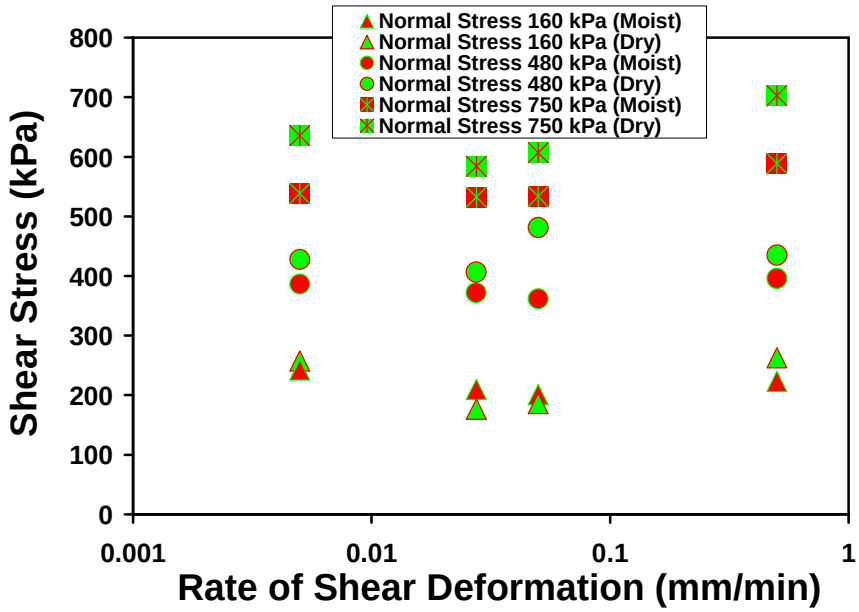

Figure 4.26: A plot of peak shear stress versus rate of shear deformation for air-dried and moist samples compacted at a dry density of 1850 kg/m^3

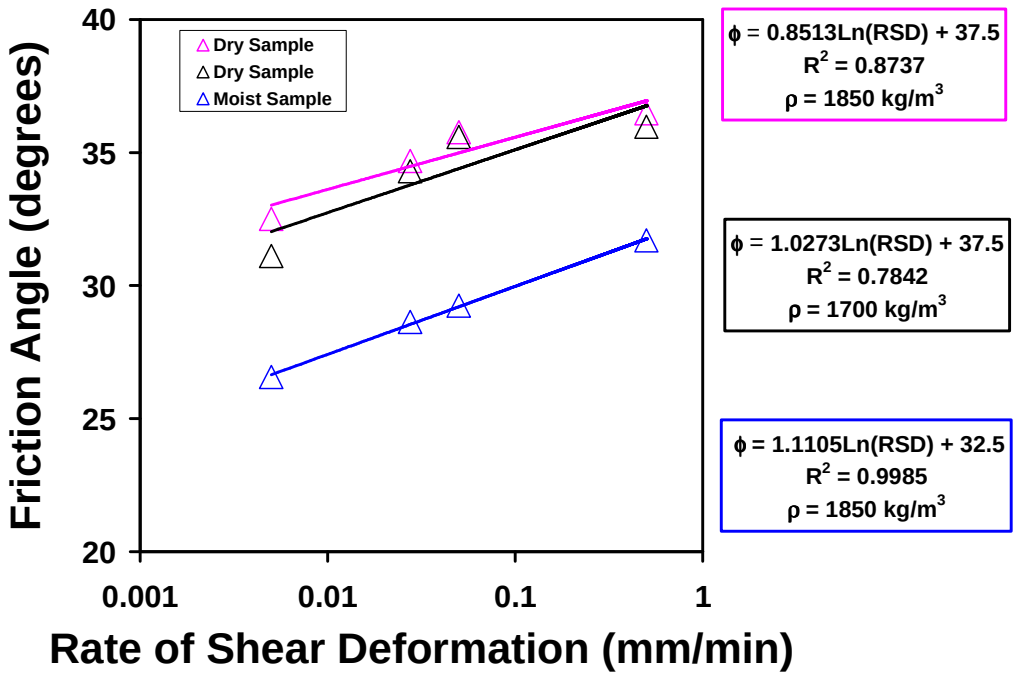

Figure 4.27: Effect of rate of shear deformation on friction angle of air-dried and moist samples.

The results of this study indicate that, knowledge of creep movement in rock piles under both dry and moist conditions is important for geotechnical stability analysis. For both dry and moist Spring Gulch rock pile materials, strain rate effects reported in this study show no drastic impact on the shear strength even though the friction angle and cohesion intercept are affected by the deformation rate. Another important finding is the role of moisture on rock pile stability. Consistent with previous studies (Nunoo, 2009), additional moisture causes reduction in shear strength and friction angle of the Questa rock pile material.

5. CONCLUSIONS AND RECOMMENDATIONS

5.1. Conclusions

This thesis examined the behavior of the Questa rock pile material under different shearing rates by performing direct shear tests on Spring Gulch rock pile materials. The soil specimens were subjected to three normal stresses of 160, 480 and 750 kPa at four different shearing rates of 0.5 mm/min, 0.05 mm/min, 0.0275 mm/min and 0.005 mm/min. At each normal stress, three tests of the same shearing rate were performed. The effect of rate of deformation on dry Spring Gulch rock pile material was investigated with a compaction density of 1850 kg/m^3 at four different rates of 0.5 mm/min, 0.05 mm/min, 0.0275 mm/min and 0.005 mm/min.

The effect of compaction densities 1700 kg/m^3 and 1850 kg/m^3 on moist (8 % water content) samples were also investigated using different shearing rates. The 8 % water content was chosen because it is close to the average in-situ water content of Questa rock piles. During the shear test, the shear stress, the shear displacement, and the normal displacement were measured concurrently. The obtained internal friction angles versus the rate of shear deformation were plotted in a semi-logarithmic format and the data show a fairly consistent linear trend.

Based on the results of this investigation, the following conclusions are drawn. The results are based on testing on scalped rock pile materials that may not represent the

true behavior of in situ material. Furthermore, the findings are restricted to the shearing rates, compaction densities and normal stresses used in this study.

- The internal friction angle of the rock pile material increases with increasing shearing rate for both dry and moist conditions.
- The internal friction angle of the rock pile materials in moist conditions decreases with increasing compaction density. Also, cohesion increases with increasing the compaction density by keeping the water content unchanged.
- For both dry and moist Spring Gulch rock pile materials, strain rate effect reported in this study shows no major impact on the shear strength even though the friction angle and cohesion intercept are affected by the deformation rate.
- The moist samples have smaller friction angle compared to those of dry samples.
- The shearing rates have greater effect on friction angle of the moist samples compared to the situation with dry samples.

5.2. Recommendations for Future Work

- Further laboratory direct shear tests are needed to determine the effect of adding water to loaded samples (during the course of the shear testing) of air-dry Spring Gulch rock pile materials.
- Further experimental work that covers large variations in shearing rate, water content, and compaction density is needed to get definitive results on the effects of strain rate on friction angle of rock piles.
- Evaluation of the rock pile creep model is needed based on the results obtained from these laboratory experiments.

- Laboratory tests on in situ materials using large shear boxes is recommended to obtain a more realistic picture of the effect of strain rate on shear strength of rock pile material.

REFERENCES

Alberro, J., and Santoyo, E., (1973). “Long term behavior of Mexico City clay.” Proc., 8th Int. Conf. on Soil Mechanics and Foundation Engineering, Vol. 1, pp. 1–9.

Al-Mhaidib , A. I., (2005), Shearing Rate Effect on Interfacial Friction between Sand and Steel, Proceedings of The Fifth International Offshore and Polar Engineering Conference, Department of Civil Engineering, King Saud University, pp. 633-639.

Al-Mhaidib, A. I., (2004), "Effect of Loading Rate on Pile Groups in Sand",proceedings of the International Conference on Geotechnical Engineering (ICGE-2004) , Sharjah, United Arab Emirates, pp. 62-67.

Baecher, G.B. and Christian, J.T., (2003), Reliability and Statistics in Geotechnical Engineering, John Wiley and Sons, London and New York.

Berre, T., and Bjerrum, L. (1973). “Shear strength of normally consolidated clays.” Proc., 8th Int. Conf. on Soil Mechanics and Foundation Engineering, Vol. 1, pp. 39–49.

Bishop, A.W. and Blight, G.E., (1963). Some aspects of effective stress in saturated and partly saturated soils. Géotechnique Vol. 13, pp. 177–197.

Bishop, A.W., Eldin, A. K. G., (1953). “The Effect of stress History on the Relation Between Friction Angle and Porosity in Sand.” Proceedings, 3rd International conference on Soil Mechanics and Foundation Engineering. Zurich, Vol. 1, 100-105.

Bishop, A. W., Green, G. E., Garga, V. K, Andersen, A. and Brown, J. D., (1971). A new ring shear apparatus and its application to the measurement of the residual strength. Géotechnique, The Institution of Civil Engineers. Vol. 21, No. 4, pp. 273-328.

Boakye, K., (2008). Large in Situ Direct Shear Tests on Rock Piles at the Questa Mine, Taos County, New Mexico, Master’s Thesis, New Mexico Institute of Mining and Technology Department of Mineral Engineering.

Bjerrum, L., (1972). “Embankments on soft ground.” ASCE Proc., Specialty Conference on Performance of Earth and Earth Supported Structures, Vol. 2, pp. 1–54.

Bjerrum, L., Simons, N., and Torblaa, I., (1958). “The effect of time on the shear strength of soft marine clay.” Proc., Brussels Conf. on Earth Pressure Problems, Vol. 1, pp. 148–158.

Caldwell, J. A., and Moss, A. S. E., (1981). The simplified Analysis of Mine Embankments, Denver USA, AIME Fall meeting.

Casagrande, A., and Wilson, S. D., (1951). “The Effect of rate of loading on the strength of clays and shales at constant water content.” Geotechnique, 2(3), pp. 251-263.

Chen, J. –W., and Lin, C. –Y., (2003). Dilative Behavior of Granular Materials, International Journal of Offshore and Polar Engineering, Vol. 13, No. 4, pp. 301-307

Chowdhury, R. N., (1978). Slope Analysis, Developments in Geotechnical Engineering. Elsevier Scientific publishing Co., New York, Vol. 22, p. 423.

Crawford, C. B., (1959), “The influence of rate of strain on effective stresses in sensitive clay.” ASTM Spec. Tech. Publ., 254, pp. 36–68.

Dafalias, Y. F., (1993). "Overview of constitutive models used in VELACS." Verification of Numerical Procedures for the analysis of soil liquefaction problems, 2, pp. 1293-1304.

Davison, C., (1889). On the Creeping of the Soil Cap through the Action of the frost, Geol. Mag., Vol. 6 pp 255-261.

Díaz-Rodríguez, J. A., Martínez-Vasquez, J. J., Santamarina, J. C., (2009). Strain-Rate Effects in Mexico City Soil, Journal of Geotechnical and Geoenvironmental Engineering. Vol. 135, No. 2, pp 300-305.

Dury, G. H., (1959). The Face of the Earth, Pelican, p. 223.

Everett, K. R. (1962). Quantitative measurement of soil movement. Geol. Soc. Amer. Special Paper 73, pp. 147-148.

Everett, K. R., (1963). Slope movement, Neotoma Valley, Southern Ohio. Inst. of Polar Studies (Ohio State Univ.) Report 6, 59 p.

Fakhimi A., Boakye K., Sperling D., and McLemore V., (2007). Development of a modified in situ direct shear test technique to determine shear strength of mine rock piles: Geotechnical Testing Journal, Vol. 31, No. 3, paper on line www.astm.org.

Farrag, K., (1995) “Effect of Moisture Content on the Interaction Properties of Geosynthetics,” Geosynthetics’95 Conference, Nashville, pp 1031-1041.

Godfrey, A.E., (1997), Mass movement of Mancos Shale crust near Caineville, Utah: a 30-year record. Geogr. Ann., 79 A (3), pp. 185-194.

Gregory, G. H., (1998), "Mechanism of shallow slope failures in clay" ASCE Texas Section Fall Meeting, Geotechnical section, Texas Section-ASCE, Dallas.

Gutierrez, L. A. F., (2006), "The Influence of Mineralogy, Chemistry and Physical Engineering Properties on Shear Strength Parameters of the Goathill North Rock Pile Material, Questa Molybdenum Mine, New Mexico," M. S. thesis, New Mexico Institute of Mining and Technology, Socorro, p. 201.

Gutierrez, L.A.F., Viterbo, V.C., McLemore, V.T., and Aimone-Martin, C.T., (2008), Geotechnical and Geomechanical Characterisation of the Goathill North Rock Pile at the Questa Molybdenum Mine, New Mexico, USA; in Fourie, A., ed., First International Seminar on the Management of Rock Dumps, Stockpiles and Heap Leach Pads: The Australian Centre for Geomechanics, University of Western Australia, pp. 19-32.
http://geoinfo.nmt.edu/staff/mclemore/Molycorppapers.htm, (accessed October 29, 2009).

Herasymiuk, G. M., (1996), Hydrology of a sulphide waste rock dump: MSc thesis, University of Saskatchewan, Saskatoon.

Horn, H. M., and Deere, D. U., (1962). "Frictional Characteristic of Minerals," Geotechnique, Vol. 12, No. 4, pp. 319-335.

Kallstenius, T., and Bergau, W., (1961). In situ determination of horizontal ground movements. Proc. 5 th Int. Conf. Soil Mechanics and Foundation Engineering, Vol. 1, pp 481-485.

Kenney, C. (1959), "Discussion." ASTM Spec. Tech. Publ., 254, 49–58. Kulhawy, F. H., and Mayne, P. W., (1990), Manual of estimating soil properties for foundation design, Geotechnical Engineering Group, Cornell Univ., Ithaca, N.Y.

Kirkby, M.J., (1959). A study of rate of erosion and mass movements on slopes with special reference to Galloway, Ph.D. Dissertation, University of Cambridge, p. 436

Kumari, D., (2009), Effect of Moisture on Strength Characteristics of river sand, Bachelor Thesis, Department of Civil Engineering, National Institute of Technology, Rourkela, p.11

Lee, K. L., Seed, H. B., (1967), Effect of Moisture on the Strength of a Clean Sand, Journal of the Soil Mechanics and Foundations Division: Proceedings of the American Society of Civil Engineers, pp. 17-20.

Lemos, L.J.L., (1986). The effect of the rate of shear on residual strength, PhD Thesis, Imperial College, University of London.

Leroueil, S., and Tavenas, F., (1979), "Discussion on 'Strain rate behaviour of Saint-Jean-Vianney clay' by Vaid et al." Can. Geotech. J., Vol. 16(3), pp. 616–620.

Lo, K. Y., and Morin, J.P., (1972). "Strength anisotropy and time effects of two sensitive clays." Can. Geotech. J., Vol. 9(3), pp. 261-277.

McCarty, M. K., (1981). Monitoring Stability of Waste Rock Dumps. Symposium on Design of Non-Impoundment Mine Waste Embankments, Denver, USA. AIME 1981 Fall meeting.

McLemore, V.T. et al., (2008), Evaluation of weathering indices for the Questa rock piles: unpublished report to Chevron, Task B1.1.

McLemore, V. T., Fakhimi, A., Zyl, D. V., Ayakwah G. F., Anim, K., Boakye, K., Ennin, F., Felli, P. Fredlund, D., Gutierrez. L. A.F., Nunoo, S., Tachie-Menson, S. and Viterbo, V. C., (2009). Literature Review of other Rock Piles: Characterization, Weathering, and Stability, Questa Rock Pile Weathering Stability Project http://geoinfo.nmt.edu/staff/mclemore/documents/ofr_517.pdf, (accessed October 29, 2009).

McLemore, V. T., Walsh, P., Donahue, K., Gutierrez, L., Tachie-Menson, S., Shannon, H. R., and Wilson, G. W., (2005), Preliminary Status Report On Molycorp Goathill North Trenches, Questa, New Mexico, in 2005 National Meeting of the American Society of Mining and Reclamation, Breckenridge, Colorado, p. 26.

Merril, G. P., (1921). A Treatise on Rocks, Rock Weathering and Soils. The MacMillan Company, NY, 400.

Molycorp Inc., (2002), Request for Letters of Intent. In: B. Walker (Editor), Questa, NM.

Moran, K. A., Gerencher, E., Jones, C. E., and Konasewich, D. E., (1991). Critical literature review of acid rock drainage from waste rock: MEND 1.11.1, 176.

Naderian, A., (1997). Characterisation of behaviour of open-cut coal mine back-fill. PhD Thesis, The University of Queensland, Australia.

Naderian, A.R. and Williams, D.J. (1996). Simulation of open-cut coal mine back-fill behaviour. Proceedings of National Symposium on the Use of Recycled Materials in Engineering Construction, May 1996, Sydney, Australia, 17-22. IEAust National Conference Publication no. 96/06, Cnaberra, Australia.

Nash, N. L., (1953). "The Shearing Resistance of a Fine Closely Graded Sand," Proceedings, 3rd International Conference of Soil Mechanics and Foundation Engineering, Zurich, Vol. 1, pp. 160-164.

Nichols, R. S., (1987), Rock segregation in waste dumps; in Flow-through rock drains: Proceedings of the International symposium convened at the Inn of the South, Cranbrook, B.C., September 8-11, 1986.

Norwest Corporation, (2004), Goathill North Slide Investigation, Evaluation and Mitigation Report: unpublished report to Molycorp Inc., Vol. 3, p. 99.

Norwest Corporation, (2005), Questa Roadside Rock piles 2005 Operation Geotechnical Stability Evaluation: unpublished report to Molycorp Inc., Vol. 3, p. 210.

Nunoo, S., (2009). Geotechnical Evaluation of Questa Mine Material, Taos County, New Mexico, Masters Thesis, New Mexico Institute of Mining and Technology Department of Mineral Engineering.

Parathiras, A.N., (1994), Displacement rate effects on the residual strength of soils, PhD Thesis, Imperial College, University of London.

Paritzek, E. J. and Woodruff, J. F., (1957). A clarification of the definition and classification of soil creep. J. Geol., Vol. 65(5), pp. 653-656.

Parkin, A. K., (1977). The compression of rockfill. Australia Geomech. J., G7 pp 33-39.

Quine, R. L., (1993) Stability and deformation of mine waste dumps in north-central Nevada: M.S. thesis, University of Nevada, Reno, 402 p.

Richardson, A. M., Jr., and Whitman, R. V., (1963), "Effect of strain-rate upon undrained shear resistance of a saturated remoulded fat clay." Geotechnique, Vol. 13(4), pp 310–324.

Richardson, A. M., Jr., and Whitman, R.V., (1963). "Effect of strain-rate upon undrained shear resistance of a saturated remoulded fat clay." Geotechnique, Vol. 13 (4), pp. 310-324.

Robertson GeoConsultants Inc., (2000), Interim Mine Site Characterization Study, Questa Mine, New Mexico, 052008/10, Robertson Geoconsultants Inc. Unpublished Report toMolycorp Inc.

Sasaki, Y., Fujii, A., and Asai, K., (1999), Soil creep process and its role in debris slide generation — field measurements on the north side of Tsukuba Mountain in Japan, Engineering Geology, Vol. 56, pp 163-183.

Selby, M. J., (1966), Methods of Measuring Soil Creep, NZ Journal Hydrology, vol. 5, pp. 54-63.
http://www.hydrologynz.org.nz/downloads/JoHNZ_1966_v5_2_Selby%282%29.pdf
(accessed on May 22, 2009)

Sharpe, C. F. S., (1938). Landslides and Related Phenomena, New York: Columbia University Press. p. 21.

Shaw, S. C., Wels, C., Roberston, A. and Lorinczi, G., (2002), Physical and Geochemical Characterization of Mine Rock Piles at the Questa Mine, New Mexico In: Overview, 9th International Conference on Tailings and Mine Waste '02. Balkema, Rotterdam, Netherlands.

Shimokawa, E., (1973), Creep Deformation of Cohesion Soils and its Relationship to Landslide, Mem. Faculty of Agriculture, Kagoshima University, 16, pp. 125-156

Shum, M. G. W., (1999), Characterization and dissolution of secondary weathering products from the Gibraltar mine site: M. S. thesis, University of British Columbia, Vancouver, 310 p.

Sowers, G. F., Williams, R.C. and Wallace, T.S. (1965), "Compressibility of Broken Rock and the Settlement of Rockfills," Proceedings of the Sixth International Conference of Soil Mechanics. Montreal, Canada, Vol. 1, pp. 561-565.

Tavenas, F., Leroueil, S., LaRochelle, P., and Roy, M., (1978), "Creep behaviour of an undisturbed lightly overconsolidated clay." Can. Geotech. J., Vol. 5(3), pp 402–423.

Ter-stepanian, G., (1963), On the long-term stability of slopes, Norwegian Geotechnical Institute, in Slope Analysis, developments in geotechnical engineering, v. 22, p. 298.

Terzaghi, K., (1950), Mechanics of landslides, Application of Geology to Engineering Practice, Geol. Soc. Am., Berkeley Volume, Harvard Soil Mechanics Series; 83 – 123 in: Slope Analysis, developments in geotechnical engineering, v. 22, p. 298.

Tika, T.M., (1989), The effect of the rate of shear on residual strength, PhD Thesis, Imperial College, University of London.

Tran, A. B., Miller, S., Williams, D. J., Fines, P., and Wilson, G. W., (2003), Geochemical and mineralogical characterization of two contrasting waste rock dumps—The INAP waste rock dump characterization project; in ICARD 2003—Proceedings from the 5th international conference on acid rock drainage: The Australasian Institute of Mining and Metallurgy, Melbourne, pp. 939-947.

Tschebotarioff, G. P., (1951). Soil Mechanics, Foundations, and Earth Structures. McGraw-Hill Book Co., Inc., New York, p. 123

URS Corporation, (2000), "Interim Mine Rock Pile Erosion and Stability Evaluations, Questa Mine," Unpublished report to Molycorp, Inc., 6800044388.00, December 1,

http://www.molycorp.com/hes/MolycorpQuestaReports/InterimReport052007_1.pdf (accessed on March 14, 2009).

URS Corporation, (2003) Mine Rock Pile Erosion and Stability Evaluations Questa Mine, Unpublished Report to Molycorp, Inc.

Vaid, Y. P., and Campanella, R. G., (1977). "Time-dependent behavior of undisturbed clay." Geotech. Engrg. Div., Vol. 103(7), 693-709.

Vaid, Y. P., Robertson, P. K., Vaid, Y. P., and Campanella, R. G., (1979). "Strain rate behavior of Saint-Jean-Vianney clay." Can. Geotech. J., Vol. 16 (1), pp. 34-42.

Wels, C.; Loudon, S.; Fortin, S., (2002), Factors influencing net infiltration into mine rock piles at Questa Mine, New Mexico; *in* Tailings and Mine Waste '02: proceedings of the Ninth International Conference on Tailings and Mine Waste: Fort Collins, Colorado, USA, pp. 469-477.

Williams, P. J., (1957). The direct recording of solifluction movements. Amer. J. Science, Vol. 255, pp. 705-715.

Yoshida, Y., Kuwano, J., and Kuwano, R., (1991), Effect of Saturation on the Shear Strength of Soils, Japanese Society of Soil Mechanics and Foundations Engineering. Vol. 31, pp 181-186.

Young, A., (1958). Some Field Observations of Slope Form and Regolith, and Their Relation to Slope Development. Ph.D. Dissertation, University of Sheffield.

Zahl, E. G., Biggs, F., Boldt, C. M. K., Connolly, R. E., Gertsch, L., and Lambeth, R. H., (1992) Waste Disposal and Contaminant Control, in Hartman, H. L., ed., SME Mining Engineering Handbook: Littleton, CO, Society for Mining, Metallurgy and Exploration Inc., p. 1170-1180.

Zhang, Z., Farrag, K., and Morvant, M., (2003). Evaluation of the effect of synthetic fibers and nonwoven geotextile reinforcement on the stability of heavy clay embankments. Rep. No. FHWA/LA.03/373, Louisiana Transportation Research Center, La.

Zhu, J., and Yin, J., (2000). "Strain-rate-dependent stress-strain behavior of overconsolidated Hong Kong marine clay." Can. Geotech. J., Vol. 37(6), pp. 1272-1282.

APPENDIX A

Combined plot of normal displacement versus shear displacement for dry densities of 1700 kg/m^3 and 1850 kg/m^3 for moist (8% water content) spring gulch samples for different shearing rates

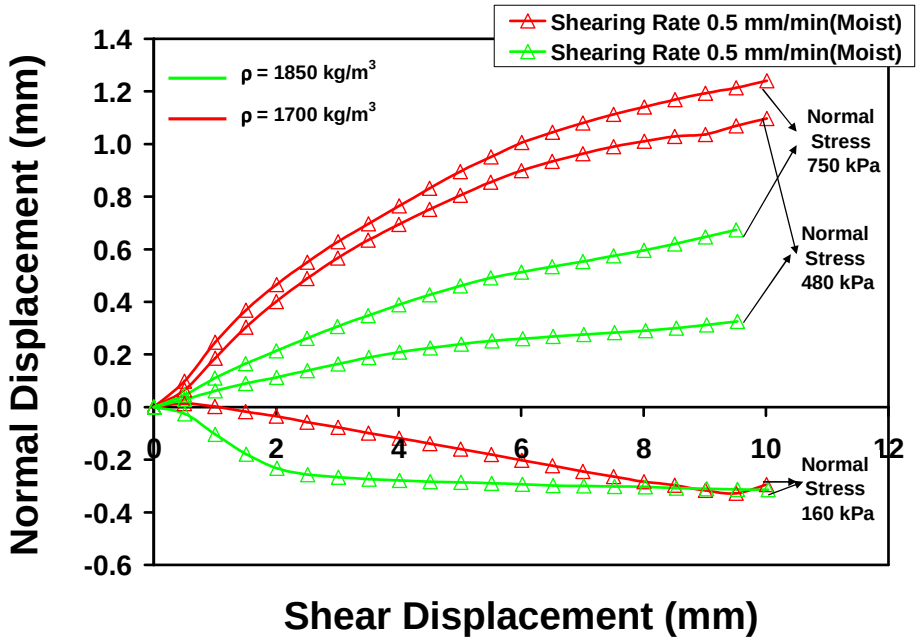

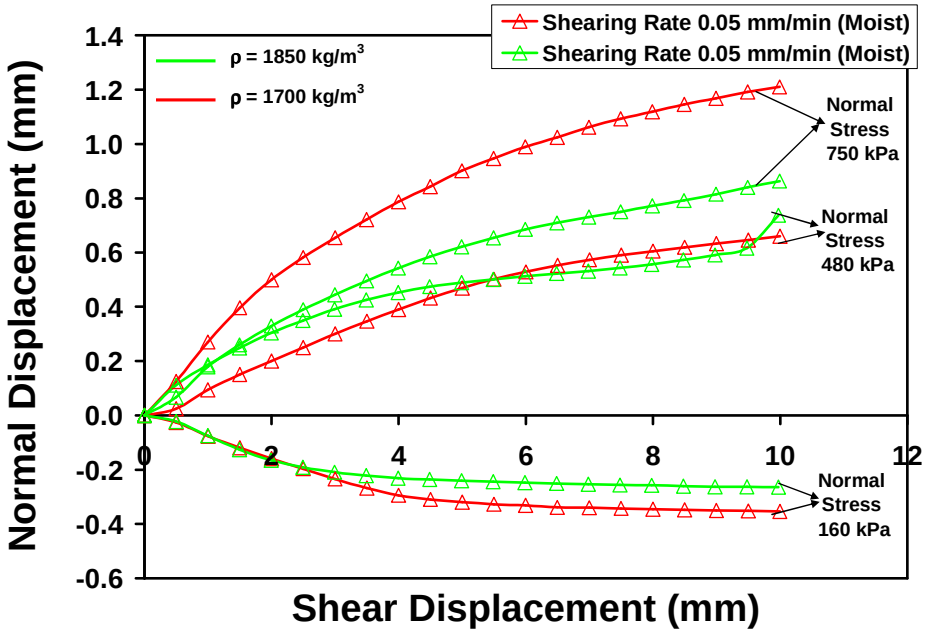

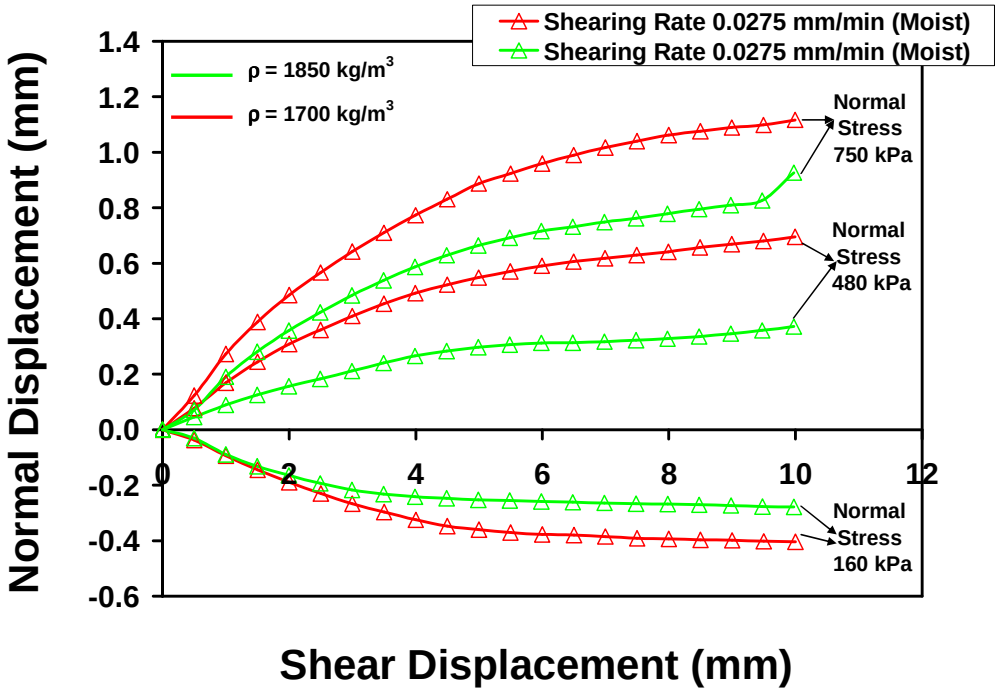
Shearing Rate 0.0275 mm/min (Moist)
Shearing Rate 0.0275 mm/min (Moist)
ρ = 1850 kg/m3
ρ = 1700 kg/m3
Normal Stress 750 kPa
Normal Stress 480 kPa
Normal Stress 160 kPa
Normal Displacement (mm)
Shear Displacement (mm)
1.4
1.2
1.0
0.8
0.6
0.4
0.2
0.0
-0.2
-0.4
-0.6
0
2
4
6
8
10
12

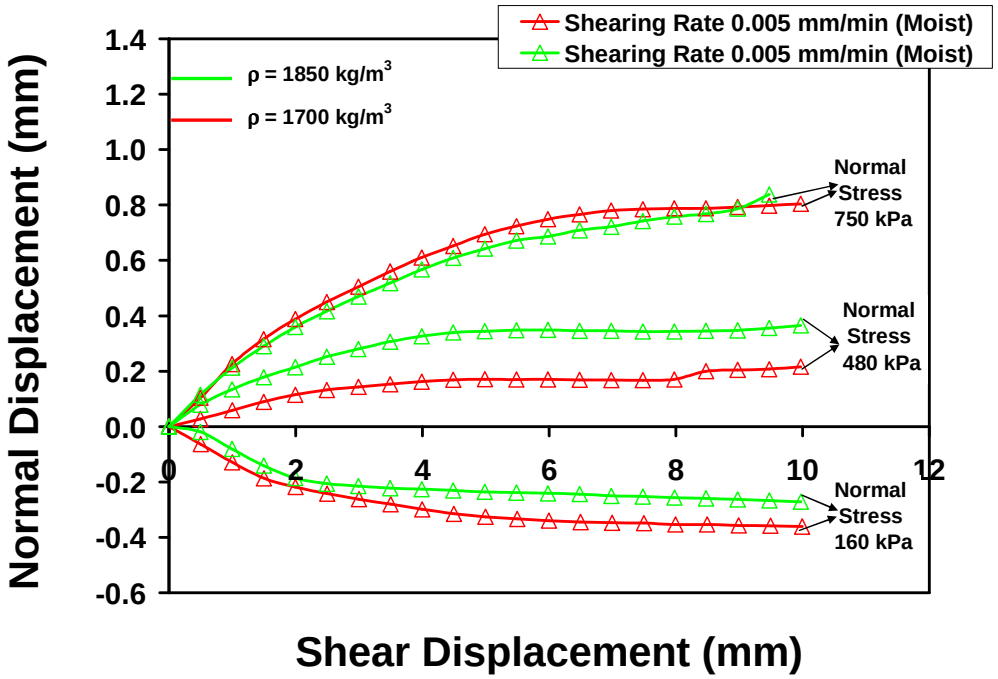
Shearing Rate 0.005 mm/min (Moist)
Shearing Rate 0.005 mm/min (Moist)
ρ = 1850 kg/m3
ρ = 1700 kg/m3
Normal Stress 750 kPa
Normal Stress 480 kPa
Normal Stress 160 kPa
Normal Displacement (mm)
Shear Displacement (mm)
1.4
1.2
1.0
0.8
0.6
0.4
0.2
0.0
-0.2
-0.4
-0.6
0
2
4
6
8
10
12

APPENDIX B

Grain size distribution summary table

Total mass of air-dried field sample (g) =	**40796.19**
Mass of air dried coarse aggregate in field sample before sieve analysis (g) =	**35080.55**
Mass of air dried coarse aggregate in field sample after sieve analysis (g) =	**34684.42**
Mass of oven dried fines (g) =	**5715.64**
Percent loss during sieve analysis (%) =	**0.97**

Grain size	**U.S. Standard**	**Mass Retained**	**% Retained**	**Cumulative % Retained**	**% Finer by weight**
(mm)	**Seive No.**	**(g)**	**R_n**	**ΣR_n**	**$100-\Sigma R_n$**
75	**3 in.**	1794.92	4.40	4.40	95.60
50	**2 in.**	2021.03	4.95	9.35	90.65
37.5	**1-1/2 in.**	1349.74	3.31	12.66	87.34
25	**1 in.**	3484.35	8.54	21.20	78.80
19	**3/4 in.**	2993.94	7.34	28.54	71.46
9.5	**3/8 in.**	7404.96	18.15	46.69	53.31
4.75	**4**	4335.89	10.63	57.32	42.68
3.36	**6**	1857.33	4.55	61.87	38.13
2	**10**	2486.55	6.10	67.97	32.03
1.18	**16**	1938.13	4.75	72.72	27.28
0.6	**30**	1784.34	4.37	77.09	22.91
0.425	**40**	726.85	1.78	78.88	21.12
0.3	**50**	694.62	1.70	80.58	19.42
0.15	**100**	1053.03	2.58	83.16	16.84
0.075	**200**	689.70	1.69	84.85	15.15
Pan	_	69.04	0.17	85.02	_

Modified soil weight passing sieve #6 (g)	15554.03

Grain size	U.S. Standard	Mass Retained	% Retained	Cumulative % Retained	% Finer by weight
(mm)	Sieve No.	(g)	R_n	ΣR_n	$100-\Sigma R_n$
3.36	6	0	0.00	0.00	100.00
2	10	2487.09	15.99	15.99	84.01
1.18	16	1938.03	12.46	28.45	71.55
0.6	30	1782.49	11.46	39.91	60.09
0.425	40	729.48	4.69	44.60	55.40
0.3	50	694.33	4.46	49.06	50.94
0.15	100	1052.39	6.77	55.83	44.17
0.075	200	689.04	4.43	60.26	39.74

Mass of Water added	14.63
Sample area, Ao (cm2)	36.00
Sample height (cm)	2.54
Moisture content (%)	8.00
compacted density (g/cm3)	2.00
Mass of air-dry soil for experiment (g)	182.88
Percentage by mass of coarse aggregate retained (g)	110.20
Mass of fines to be added (g)	72.68

U.S. Standard	% Retained	Proportion by weight
Sieve No.	Rn	(g)
6	0.00	0.0
10	15.99	29.2
16	12.46	22.8
30	11.46	21.0
40	4.69	8.6
50	4.46	8.2
100	6.77	12.4
200	4.43	8.1

	Mass of Water added	**13.53**
	Sample area, Ao (cm^2)	**36.00**
	Sample height (cm)	**2.54**
	Moisture content (%)	**8.00**
	compacted density (g/cm^3)	**1.85**
	Mass of air-dry soil for experiment (g)	**169.16**
	Percentage by mass of coarse aggregate retained (g)	**101.94**
	Mass of fines to be added (g)	**67.23**
U.S. Standard	**% Retained**	**Proportion by weight**
Sieve No.	**Rn**	**(g)**
6	0.00	0.0
10	15.99	27.0
16	12.46	21.1
30	11.46	19.4
40	4.69	7.9
50	4.46	7.6
100	6.77	11.4
200	4.43	7.5

APPENDIX C

Results of direct shear tests on air-dry samples with bulk density of 1850 kg/m^3
(Averages from the three test results)

Shearing Rate 0.5 mm/min											
Normal Stress 160 kPa				Normal Stress 480 kPa				Normal Stress 750 kPa			
Horizontal Displacement (mm)	Shear Force (kN)	Vertical Displacement (mm)	Shear Stress (kPa)	Horizontal Displacement (mm)	Shear Force (kN)	Vertical Displacement (mm)	Shear Stress (kPa)	Horizontal Displacement (mm)	Shear Force (kN)	Vertical Displacement (mm)	Shear Stress (kPa)
0.00	0.00	0.00	0.00	0.00	0.00	0.00	0.00	0.00	0.00	0.00	0.00
0.67	419.54	-0.07	116.54	0.50	734.64	0.00	204.07	0.50	1039.73	0.00	288.81
1.17	591.58	-0.19	164.33	1.00	1200.35	-0.05	333.43	1.00	1650.97	-0.02	458.60
1.67	686.37	-0.27	190.66	1.51	1439.44	-0.11	399.84	1.50	2019.61	-0.06	561.00
2.17	774.14	-0.31	215.04	2.01	1535.11	-0.16	426.42	2.00	2256.59	-0.10	626.83
2.66	835.75	-0.34	232.15	2.51	1565.83	-0.20	434.95	2.50	2398.43	-0.14	666.23
3.17	879.46	-0.37	244.30	3.01	1565.48	-0.22	434.86	3.01	2483.04	-0.17	689.73
3.67	909.31	-0.40	252.58	3.51	1529.85	-0.24	424.96	3.51	2520.78	-0.20	700.22
4.17	923.52	-0.41	256.53	4.01	1506.67	-0.24	418.52	4.01	2530.08	-0.23	702.80
4.67	937.39	-0.43	260.39	4.52	1505.27	-0.25	418.13	4.51	2497.08	-0.26	693.63
5.17	935.29	-0.45	259.80	5.02	1492.63	-0.26	414.62	5.01	2452.84	-0.28	681.35
5.67	932.13	-0.47	258.92	5.52	1492.98	-0.26	414.72	5.51	2428.62	-0.29	674.62
6.17	937.39	-0.48	260.39	6.03	1489.47	-0.27	413.74	6.01	2390.53	-0.31	664.04
6.67	941.78	-0.48	261.61	6.53	1489.12	-0.28	413.64	6.52	2339.97	-0.32	649.99
7.18	942.66	-0.48	261.85	7.03	1489.47	-0.29	413.74	7.02	2296.61	-0.33	637.95
7.68	946.17	-0.49	262.82	7.53	1452.78	-0.29	403.55	7.52	2260.10	-0.34	627.81
8.18	939.15	-0.49	260.87	8.03	1425.57	-0.30	395.99	8.02	2235.17	-0.34	620.88
8.68	928.62	-0.49	257.95	8.53	1428.03	-0.30	396.68	8.52	2209.19	-0.34	613.66
9.18	916.50	-0.49	254.58	9.03	1444.01	-0.30	401.11	9.02	2166.18	-0.34	601.72
9.51	933.44	-0.42	259.29	9.53	1438.56	-0.31	399.60	9.52	2130.20	-0.34	591.72
10.01	908.43	-0.42	252.34	10.04	1433.30	-0.31	398.14	10.02	2103.87	-0.33	584.41

Shearing Rate 0.05 mm/min											
Normal Stress 160 kPa				Normal Stress 480 kPa				Normal Stress 750 kPa			
Horizontal Displacement (mm)	Shear Force (kN)	Vertical Displacement (mm)	Shear Stress (kPa)	Horizontal Displacement (mm)	Shear Force (kN)	Vertical Displacement (mm)	Shear Stress (kPa)	Horizontal Displacement (mm)	Shear Force (kN)	Vertical Displacement (mm)	Shear Stress (kPa)
0.00	0.00	0.00	0.00	0.00	0.00	0.00	0.00	0.00	0.00	0.00	0.00
0.50	437.98	-0.02	121.66	0.50	850.15	0.03	236.15	0.50	1178.41	0.06	327.34
1.00	631.95	-0.12	175.54	1.00	1249.51	0.03	347.08	1.00	1597.43	0.07	443.73
1.50	642.48	-0.22	178.47	1.50	1453.13	0.01	403.65	1.50	1844.94	0.06	512.48
1.99	617.56	-0.28	171.54	1.99	1580.75	-0.01	439.10	1.99	2012.76	0.06	559.10
2.49	606.67	-0.32	168.52	2.49	1658.52	-0.04	460.70	2.49	2111.06	0.06	586.41
2.99	595.09	-0.35	165.30	2.99	1693.98	-0.05	470.55	2.99	2160.92	0.05	600.25
3.49	596.84	-0.37	165.79	3.49	1712.94	-0.06	475.82	3.49	2181.98	0.05	606.11
3.99	607.37	-0.39	168.72	3.99	1726.10	-0.08	479.47	3.99	2185.14	0.05	606.98
4.49	624.05	-0.40	173.35	4.49	1729.09	-0.08	480.30	4.49	2176.72	0.04	604.64
4.99	638.09	-0.41	177.25	4.99	1732.77	-0.09	481.33	4.99	2159.16	0.04	599.77
5.48	650.03	-0.42	180.56	5.49	1718.55	-0.10	477.38	5.48	2141.26	0.04	594.79
5.98	657.93	-0.43	182.76	5.98	1693.63	-0.10	470.45	5.98	2111.42	0.03	586.50
6.48	665.30	-0.44	184.81	6.48	1672.91	-0.10	464.70	6.48	2081.92	0.04	578.31
6.98	666.71	-0.45	185.20	6.98	1657.11	-0.10	460.31	6.98	2057.35	0.05	571.49
7.48	668.81	-0.46	185.78	7.48	1641.31	-0.10	455.92	7.48	2036.81	0.06	565.78
7.98	667.58	-0.47	185.44	7.98	1625.52	-0.09	451.53	7.98	2023.64	0.07	562.12
8.48	663.55	-0.48	184.32	8.48	1627.27	-0.09	452.02	8.48	2016.62	0.09	560.17
8.97	665.30	-0.48	184.81	8.98	1618.49	-0.09	449.58	8.98	2004.33	0.11	556.76
9.47	665.30	-0.49	184.81	9.47	1614.63	-0.08	448.51	9.48	1997.66	0.12	554.91
9.97	661.79	-0.49	183.83	9.97	1604.45	-0.07	445.68	9.97	1986.78	0.14	551.88

Shearing Rate 0.0275 mm/min											
Normal Stress 160 kPa				Normal Stress 480 kPa				Normal Stress 750 kPa			
Horizontal Displacement (mm)	Shear Force (kN)	Vertical Displacement (mm)	Shear Stress (kPa)	Horizontal Displacement (mm)	Shear Force (kN)	Vertical Displacement (mm)	Shear Stress (kPa)	Horizontal Displacement (mm)	Shear Force (kN)	Vertical Displacement (mm)	Shear Stress (kPa)
0.00	0.00	0.00	0.00	0.00	0.00	0.00	0.00	0.00	0.00	0.00	0.00
0.50	462.20	-0.02	128.39	0.50	526.27	0.02	146.19	0.50	582.45	0.03	161.79
1.00	619.84	-0.11	172.18	1.00	1013.40	0.02	281.50	1.00	1303.92	0.07	362.20
1.50	635.11	-0.20	176.42	1.50	1235.81	0.00	343.28	1.50	1602.70	0.08	445.19
1.99	610.53	-0.25	169.59	1.99	1358.69	-0.03	377.41	1.99	1806.32	0.09	501.76
2.49	599.30	-0.27	166.47	2.49	1423.64	-0.06	395.46	2.49	1948.16	0.09	541.16
2.99	592.98	-0.28	164.72	2.99	1454.89	-0.09	404.14	2.99	2039.79	0.08	566.61
3.49	594.38	-0.29	165.11	3.49	1463.67	-0.11	406.57	3.49	2083.68	0.07	578.80
3.99	600.00	-0.30	166.67	3.99	1456.64	-0.13	404.62	3.99	2103.16	0.06	584.21
4.49	603.51	-0.31	167.64	4.49	1449.62	-0.14	402.67	4.49	2097.72	0.05	582.70
4.99	603.51	-0.32	167.64	4.99	1435.93	-0.16	398.87	4.99	2090.70	0.05	580.75
5.49	608.25	-0.33	168.96	5.49	1421.89	-0.17	394.97	5.48	2085.96	0.05	579.43
5.98	614.57	-0.34	170.71	5.98	1407.49	-0.18	390.97	5.98	2081.92	0.06	578.31
6.48	621.07	-0.34	172.52	6.48	1395.56	-0.18	387.65	6.48	2078.06	0.06	577.24
6.98	606.67	-0.35	168.52	6.98	1381.16	-0.18	383.66	6.98	2067.88	0.06	574.41
7.48	615.45	-0.35	170.96	7.48	1363.96	-0.18	378.88	7.48	2057.87	0.06	571.63
7.98	612.29	-0.35	170.08	7.98	1354.83	-0.18	376.34	7.98	2035.93	0.06	565.54
8.48	615.45	-0.36	170.96	8.48	1337.63	-0.18	371.56	8.48	2017.15	0.08	560.32
8.98	618.96	-0.36	171.93	8.98	1324.29	-0.17	367.86	8.97	2000.82	0.08	555.78
9.47	621.94	-0.36	172.76	9.47	1307.79	-0.16	363.27	9.47	1988.89	0.09	552.47
9.97	624.05	-0.36	173.35	9.97	1300.41	-0.15	361.23	9.97	1985.38	0.09	551.49

Shearing Rate 0.005 mm/min											
Normal Stress 160 kPa				Normal Stress 480 kPa				Normal Stress 750 kPa			
Horizontal Displacement (mm)	Shear Force (kN)	Vertical Displacement (mm)	Shear Stress (kPa)	Horizontal Displacement (mm)	Shear Force (kN)	Vertical Displacement (mm)	Shear Stress (kPa)	Horizontal Displacement (mm)	Shear Force (kN)	Vertical Displacement (mm)	Shear Stress (kPa)
0.00	0.00	0.00	0.00	0.00	0.00	0.00	0.00	0.00	0.00	0.00	0.00
0.50	199.77	0.00	55.49	0.50	688.12	0.01	191.15	0.50	1112.93	0.04	309.15
1.00	444.12	-0.04	123.37	1.00	1077.83	-0.01	299.40	1.00	1602.34	0.02	445.10
1.50	640.38	-0.11	177.88	1.50	1311.30	-0.05	364.25	1.50	1920.43	0.00	533.45
1.99	753.60	-0.19	209.33	1.99	1444.36	-0.09	401.21	1.99	2118.09	-0.02	588.36
2.49	794.85	-0.26	220.79	2.49	1517.73	-0.13	421.59	2.49	2223.76	-0.05	617.71
2.99	791.69	-0.31	219.91	2.99	1539.50	-0.16	427.64	2.99	2268.00	-0.07	630.00
3.49	782.21	-0.35	217.28	3.49	1540.03	-0.19	427.79	3.49	2286.96	-0.08	635.27
3.99	777.30	-0.38	215.92	3.99	1532.48	-0.21	425.69	3.99	2266.77	-0.11	629.66
4.49	781.16	-0.39	216.99	4.49	1511.06	-0.23	419.74	4.49	2222.01	-0.12	617.22
4.99	796.96	-0.40	221.38	4.99	1490.00	-0.24	413.89	4.99	2164.60	-0.12	601.28
5.48	818.90	-0.41	227.47	5.49	1471.04	-0.25	408.62	5.49	2127.21	-0.13	590.89
5.98	844.36	-0.41	234.54	5.98	1446.11	-0.26	401.70	5.98	2085.96	-0.13	579.43
6.48	873.85	-0.41	242.74	6.48	1423.29	-0.27	395.36	6.48	2062.61	-0.13	572.95
6.98	885.78	-0.42	246.05	6.98	1406.09	-0.27	390.58	6.98	2028.91	-0.12	563.59
7.48	897.90	-0.42	249.42	7.48	1382.57	-0.27	384.05	7.48	2013.99	-0.11	559.44
7.98	915.98	-0.42	254.44	7.98	1367.47	-0.27	379.85	7.98	1994.15	-0.10	553.93
8.48	921.59	-0.42	256.00	8.48	1355.71	-0.27	376.59	8.48	1981.87	-0.09	550.52
8.98	924.75	-0.42	256.88	8.98	1350.09	-0.26	375.03	8.98	1973.97	-0.08	548.32
9.48	926.51	-0.42	257.36	9.47	1341.66	-0.26	372.68	9.47	1965.72	-0.06	546.03
9.97	924.23	-0.42	256.73	9.97	1335.87	-0.25	371.08	9.97	1953.78	-0.04	542.72

APPENDIX D

Results of direct shear tests on moist (8% water content) samples with bulk density of 1850 kg/m^3 (Averages from the three test results)

Shearing Rate 0.5 mm/min											
Normal Stress 160 kPa				Normal Stress 480 kPa				Normal Stress 750 kPa			
Horizontal Displacement (mm)	Shear Force (kN)	Vertical Displacement (mm)	Shear Stress (kPa)	Horizontal Displacement (mm)	Shear Force (kN)	Vertical Displacement (mm)	Shear Stress (kPa)	Horizontal Displacement (mm)	Shear Force (kN)	Vertical Displacement (mm)	Shear Stress (kPa)
0.00	0.00	0.00	0.00	0.00	0.00	0.00	0.00	0.00	0.00	0.00	0.00
0.50	360.91	-0.03	100.25	0.50	511.35	0.03	142.04	0.50	735.17	0.05	204.21
1.01	501.35	-0.10	139.26	1.00	780.46	0.06	216.79	1.00	1195.44	0.11	332.07
1.51	540.84	-0.18	150.23	1.50	937.39	0.09	260.39	1.50	1374.49	0.16	381.80
2.01	566.30	-0.23	157.30	2.00	1039.21	0.11	288.67	2.00	1502.64	0.21	417.40
2.51	610.89	-0.26	169.69	2.51	1118.20	0.14	310.61	2.50	1619.02	0.26	449.73
3.01	651.08	-0.27	180.86	3.01	1186.66	0.16	329.63	3.00	1718.55	0.31	477.38
3.52	682.15	-0.27	189.49	3.51	1246.35	0.19	346.21	3.50	1809.83	0.35	502.73
4.02	708.49	-0.28	196.80	4.01	1295.15	0.21	359.76	4.00	1890.23	0.39	525.06
4.52	729.90	-0.28	202.75	4.52	1336.93	0.22	371.37	4.51	1956.94	0.43	543.59
5.02	748.86	-0.29	208.02	5.02	1370.98	0.24	380.83	5.00	2018.73	0.46	560.76
5.52	764.66	-0.29	212.41	5.52	1395.56	0.25	387.65	5.51	2062.61	0.49	572.95
6.02	779.93	-0.29	216.65	6.02	1413.11	0.26	392.53	6.01	2092.46	0.51	581.24
6.52	791.34	-0.30	219.82	6.52	1423.64	0.27	395.46	6.51	2111.42	0.53	586.50
7.03	799.42	-0.30	222.06	7.03	1425.05	0.28	395.85	7.01	2120.54	0.55	589.04
7.53	799.77	-0.30	222.16	7.53	1425.40	0.28	395.94	7.51	2117.03	0.57	588.06
8.03	801.87	-0.30	222.74	8.03	1421.54	0.29	394.87	8.01	2110.54	0.60	586.26
8.53	803.28	-0.31	223.13	8.53	1414.87	0.30	393.02	8.51	2117.03	0.62	588.06
9.03	796.26	-0.31	221.18	9.03	1411.00	0.31	391.95	9.01	2117.03	0.65	588.06
9.53	789.24	-0.31	219.23	9.53	1399.94	0.33	388.87	9.51	2110.54	0.67	586.26
10.04	780.46	-0.31	216.79	10.03	1334.99	0.43	370.83				

Shearing Rate 0.05 mm/min											
Normal Stress 160 kPa				Normal Stress 480 kPa				Normal Stress 750 kPa			
Horizontal Displacement (mm)	Shear Force (kN)	Vertical Displacement (mm)	Shear Stress (kPa)	Horizontal Displacement (mm)	Shear Force (kN)	Vertical Displacement (mm)	Shear Stress (kPa)	Horizontal Displacement (mm)	Shear Force (kN)	Vertical Displacement (mm)	Shear Stress (kPa)
0.00	0.00	0.00	0.00	0.00	0.00	0.00	0.00	0.00	0.00	0.00	0.00
0.50	412.17	-0.02	114.49	0.50	635.46	0.11	176.52	0.50	631.95	0.07	175.54
1.00	491.69	-0.07	136.58	1.00	777.30	0.19	215.92	1.00	1009.89	0.18	280.53
1.50	524.87	-0.13	145.80	1.50	875.95	0.25	243.32	1.50	1184.20	0.26	328.95
1.99	554.71	-0.17	154.09	2.00	955.82	0.30	265.51	2.00	1320.60	0.33	366.83
2.49	584.55	-0.19	162.38	2.49	1027.45	0.35	285.40	2.50	1432.60	0.39	397.94
2.99	609.66	-0.21	169.35	2.99	1090.11	0.39	302.81	3.00	1527.39	0.44	424.27
3.49	631.95	-0.22	175.54	3.49	1144.53	0.43	317.93	3.49	1615.51	0.50	448.75
3.99	654.77	-0.23	181.88	3.99	1186.66	0.45	329.63	3.99	1689.24	0.54	469.23
4.49	673.73	-0.24	187.15	4.49	1221.77	0.47	339.38	4.49	1752.08	0.58	486.69
4.99	688.12	-0.24	191.15	4.99	1244.24	0.49	345.62	4.99	1806.32	0.62	501.76
5.49	700.41	-0.24	194.56	5.49	1260.39	0.50	350.11	5.49	1852.49	0.65	514.58
5.98	708.84	-0.25	196.90	5.98	1270.57	0.51	352.94	5.99	1885.84	0.69	523.85
6.48	716.21	-0.25	198.95	6.48	1270.92	0.52	353.03	6.49	1906.56	0.71	529.60
6.98	719.72	-0.25	199.92	6.98	1270.04	0.53	352.79	6.99	1918.32	0.73	532.87
7.48	722.88	-0.26	200.80	7.48	1263.90	0.54	351.08	7.49	1920.95	0.75	533.60
7.98	719.72	-0.26	199.92	7.98	1255.12	0.56	348.65	7.99	1915.69	0.77	532.14
8.48	716.21	-0.26	198.95	8.48	1237.57	0.57	343.77	8.49	1913.93	0.79	531.65
8.98	710.94	-0.26	197.48	8.98	1223.53	0.59	339.87	8.99	1903.40	0.82	528.72
9.48	702.17	-0.26	195.05	9.48	1232.30	0.62	342.31	9.49	1901.64	0.84	528.23
9.97	691.63	-0.26	192.12	9.98	1302.34	0.74	361.76	9.99	1896.38	0.86	526.77

Shearing Rate 0.0275 mm/min											
Normal Stress 160 kPa				Normal Stress 480 kPa				Normal Stress 750 kPa			
Horizontal Displacement (mm)	Shear Force (kN)	Vertical Displacement (mm)	Shear Stress (kPa)	Horizontal Displacement (mm)	Shear Force (kN)	Vertical Displacement (mm)	Shear Stress (kPa)	Horizontal Displacement (mm)	Shear Force (kN)	Vertical Displacement (mm)	Shear Stress (kPa)
0.00	0.00	0.00	0.00	0.00	0.00	0.00	0.00	0.00	0.00	0.00	0.00
0.50	414.28	-0.03	115.08	0.50	531.89	0.05	147.75	0.50	606.15	0.07	168.37
1.00	486.25	-0.09	135.07	1.00	793.45	0.09	220.40	1.00	982.68	0.19	272.97
1.50	528.91	-0.13	146.92	1.50	905.44	0.13	251.51	1.50	1162.61	0.28	322.95
1.99	559.98	-0.16	155.55	2.00	988.30	0.16	274.53	2.00	1296.38	0.36	360.10
2.49	584.20	-0.19	162.28	2.49	1059.39	0.18	294.28	2.49	1413.11	0.42	392.53
2.99	606.15	-0.22	168.37	2.99	1121.36	0.21	311.49	2.99	1513.70	0.48	420.47
3.49	630.19	-0.23	175.05	3.49	1179.64	0.24	327.68	3.49	1608.49	0.54	446.80
3.99	656.53	-0.24	182.37	3.99	1227.04	0.27	340.84	3.99	1689.24	0.59	469.23
4.49	679.35	-0.25	188.71	4.49	1265.30	0.28	351.47	4.49	1761.21	0.63	489.22
4.99	699.18	-0.25	194.22	4.99	1293.74	0.30	359.37	4.99	1817.03	0.66	504.73
5.49	716.21	-0.26	198.95	5.49	1314.81	0.31	365.22	5.49	1861.27	0.69	517.02
5.98	731.66	-0.26	203.24	5.98	1332.01	0.31	370.00	5.98	1889.35	0.72	524.82
6.48	742.54	-0.26	206.26	6.48	1339.38	0.31	372.05	6.48	1908.14	0.73	530.04
6.98	746.75	-0.26	207.43	6.98	1339.38	0.32	372.05	6.98	1915.34	0.75	532.04
7.48	750.62	-0.27	208.50	7.48	1336.40	0.32	371.22	7.48	1914.81	0.76	531.89
7.98	750.97	-0.27	208.60	7.98	1330.25	0.33	369.52	7.98	1905.15	0.78	529.21
8.48	754.83	-0.27	209.67	8.48	1323.58	0.34	367.66	8.48	1906.03	0.79	529.45
8.98	750.97	-0.27	208.60	8.98	1314.81	0.35	365.22	8.98	1902.52	0.81	528.48
9.48	746.58	-0.28	207.38	9.48	1306.03	0.36	362.79	9.48	1891.11	0.83	525.31
9.98	742.54	-0.28	206.26	9.97	1292.16	0.37	358.93	9.97	1917.18	0.93	532.55

Shearing Rate 0.005 mm/min											
Normal Stress 160 kPa				Normal Stress 480 kPa				Normal Stress 750 kPa			
Horizontal Displacement (mm)	Shear Force (kN)	Vertical Displacement (mm)	Shear Stress (kPa)	Horizontal Displacement (mm)	Shear Force (kN)	Vertical Displacement (mm)	Shear Stress (kPa)	Horizontal Displacement (mm)	Shear Force (kN)	Vertical Displacement (mm)	Shear Stress (kPa)
0.00	0.00	0.00	0.00	0.00	0.00	0.00	0.00	0.00	0.00	0.00	0.00
0.50	334.93	-0.02	93.04	0.50	679.00	0.08	188.61	0.50	695.67	0.11	193.24
1.00	470.10	-0.08	130.58	1.00	851.03	0.13	236.40	1.00	953.37	0.21	264.82
1.50	518.90	-0.14	144.14	1.50	957.23	0.18	265.90	1.50	1119.25	0.29	310.90
1.99	564.89	-0.19	156.91	1.99	1047.63	0.21	291.01	1.99	1247.75	0.36	346.60
2.49	617.03	-0.21	171.40	2.49	1123.12	0.25	311.98	2.49	1360.97	0.42	378.05
2.99	661.44	-0.22	183.73	2.99	1184.56	0.28	329.04	2.99	1457.52	0.47	404.87
3.49	698.30	-0.22	193.97	3.49	1241.08	0.31	344.74	3.49	1541.78	0.52	428.27
3.99	728.15	-0.23	202.26	3.99	1292.51	0.33	359.03	3.99	1619.37	0.57	449.83
4.49	752.72	-0.23	209.09	4.49	1328.50	0.34	369.03	4.49	1685.73	0.61	468.26
4.99	775.19	-0.24	215.33	4.99	1352.72	0.34	375.76	4.99	1737.69	0.64	482.69
5.48	792.75	-0.24	220.21	5.48	1372.74	0.35	381.32	5.48	1773.50	0.67	492.64
5.98	808.02	-0.24	224.45	5.98	1386.78	0.35	385.22	5.98	1796.32	0.69	498.98
6.48	819.43	-0.24	227.62	6.48	1391.34	0.35	386.48	6.48	1811.77	0.71	503.27
6.98	836.98	-0.25	232.50	6.98	1388.18	0.35	385.61	6.98	1813.87	0.72	503.85
7.48	846.29	-0.25	235.08	7.48	1390.29	0.34	386.19	7.48	1805.62	0.74	501.56
7.98	854.54	-0.26	237.37	7.98	1386.43	0.34	385.12	7.98	1803.69	0.76	501.03
8.48	857.52	-0.26	238.20	8.48	1374.49	0.35	381.80	8.48	1796.67	0.77	499.07
8.98	866.82	-0.26	240.78	8.98	1368.87	0.35	380.24	8.98	1787.54	0.79	496.54
9.47	872.62	-0.27	242.39	9.47	1356.23	0.36	376.73	9.47	1807.11	0.84	501.98
9.97	870.34	-0.27	241.76	9.97	1349.92	0.36	374.98	9.97	1937.98	0.98	538.33

APPENDIX E

Results of direct shear tests on moist (8% water content) samples with bulk density of 1700 kg/m^3 (Averages from the three test results)

Shearing Rate 0.5 mm/min											
Normal Stress 160 kPa				Normal Stress 480 kPa				Normal Stress 750 kPa			
Horizontal Displacement (mm)	Shear Force (kN)	Vertical Displacement (mm)	Shear Stress (kPa)	Horizontal Displacement (mm)	Shear Force (kN)	Vertical Displacement (mm)	Shear Stress (kPa)	Horizontal Displacement (mm)	Shear Force (kN)	Vertical Displacement (mm)	Shear Stress (kPa)
0.00	0.00	0.00	0.00	0.00	0.00	0.00	0.00	0.00	0.00	0.00	0.00
0.50	302.46	0.01	84.02	0.50	415.16	0.07	115.32	0.50	581.22	0.10	161.45
1.00	401.29	0.00	111.47	1.00	612.29	0.19	170.08	1.00	876.13	0.25	243.37
1.50	433.76	-0.02	120.49	1.50	726.39	0.30	201.78	1.50	1039.73	0.37	288.81
2.00	459.57	-0.03	127.66	2.00	819.96	0.40	227.77	2.00	1176.30	0.47	326.75
2.50	479.23	-0.06	133.12	2.50	901.06	0.49	250.29	2.51	1293.04	0.55	359.18
3.01	493.80	-0.08	137.17	3.00	974.26	0.57	270.63	3.01	1397.49	0.63	388.19
3.51	507.84	-0.10	141.07	3.50	1042.89	0.63	289.69	3.51	1496.14	0.70	415.59
4.01	521.53	-0.12	144.87	4.00	1102.93	0.69	306.37	4.01	1590.58	0.76	441.83
4.51	532.42	-0.14	147.89	4.51	1159.10	0.75	321.97	4.51	1678.35	0.83	466.21
5.01	541.19	-0.16	150.33	5.01	1215.80	0.80	337.72	5.01	1760.33	0.90	488.98
5.51	547.87	-0.18	152.18	5.51	1264.43	0.86	351.23	5.51	1839.85	0.95	511.07
6.01	553.48	-0.20	153.75	6.01	1310.59	0.90	364.05	6.01	1906.03	1.00	529.45
6.51	555.24	-0.22	154.23	6.51	1343.42	0.93	373.17	6.51	1953.95	1.04	542.77
7.01	557.52	-0.24	154.87	7.01	1366.24	0.96	379.51	7.01	1986.43	1.08	551.79
7.51	556.64	-0.26	154.62	7.51	1380.28	0.99	383.41	7.51	2006.62	1.11	557.39
8.01	556.64	-0.28	154.62	8.01	1387.31	1.01	385.36	8.01	2018.90	1.14	560.81
8.51	554.71	-0.30	154.09	8.51	1394.33	1.03	387.31	8.51	2023.64	1.17	562.12
9.01	554.54	-0.32	154.04	9.01	1408.37	1.04	391.21	9.01	2055.24	1.19	570.90
9.51	551.73	-0.33	153.26	9.51	1410.48	1.07	391.80	9.51	2071.04	1.21	575.29
10.01	526.10	-0.30	146.14	10.01	1415.04	1.10	393.07	10.01	2073.32	1.24	575.92

Shearing Rate 0.05 mm/min											
Normal Stress 160 kPa				Normal Stress 480 kPa				Normal Stress 750 kPa			
Horizontal Displacement (mm)	Shear Force (kN)	Vertical Displacement (mm)	Shear Stress (kPa)	Horizontal Displacement (mm)	Shear Force (kN)	Vertical Displacement (mm)	Shear Stress (kPa)	Horizontal Displacement (mm)	Shear Force (kN)	Vertical Displacement (mm)	Shear Stress (kPa)
0.00	0.00	0.00	0.00	0.00	0.00	0.00	0.00	0.00	0.00	0.00	0.00
0.50	339.32	-0.03	94.26	0.50	503.80	0.02	139.95	0.50	523.99	0.13	145.55
1.00	411.65	-0.08	114.35	1.00	753.60	0.09	209.33	1.00	854.54	0.27	237.37
1.50	437.10	-0.12	121.42	1.50	863.31	0.15	239.81	1.50	1035.70	0.40	287.69
2.00	455.53	-0.16	126.54	2.00	942.66	0.20	261.85	2.00	1177.01	0.50	326.95
2.50	468.35	-0.20	130.10	2.50	1018.14	0.25	282.82	2.50	1299.53	0.58	360.98
3.00	480.11	-0.23	133.36	3.00	1090.11	0.30	302.81	3.00	1401.70	0.65	389.36
3.50	490.29	-0.27	136.19	3.50	1153.31	0.35	320.36	3.50	1497.90	0.72	416.08
4.00	506.96	-0.29	140.82	4.00	1207.73	0.39	335.48	4.00	1589.53	0.79	441.54
4.50	525.75	-0.31	146.04	4.50	1256.53	0.43	349.04	4.50	1682.57	0.84	467.38
5.00	545.58	-0.32	151.55	5.00	1303.40	0.47	362.05	5.00	1766.48	0.90	490.69
5.50	564.02	-0.33	156.67	5.50	1342.89	0.50	373.03	5.49	1828.79	0.95	508.00
6.00	578.94	-0.33	160.82	6.00	1374.49	0.53	381.80	5.99	1870.92	0.99	519.70
6.50	590.70	-0.34	164.08	6.50	1395.56	0.55	387.65	6.49	1912.53	1.02	531.26
7.00	597.72	-0.34	166.03	7.00	1413.64	0.57	392.68	6.99	1935.87	1.06	537.74
7.50	606.15	-0.34	168.37	7.50	1433.82	0.59	398.28	7.49	1954.66	1.09	542.96
8.00	614.40	-0.35	170.67	8.00	1443.83	0.61	401.06	7.99	1989.76	1.12	552.71
8.50	618.78	-0.35	171.88	8.50	1448.75	0.62	402.43	8.49	2025.75	1.15	562.71
9.00	618.78	-0.35	171.88	9.00	1446.46	0.63	401.80	8.99	2047.69	1.17	568.80
9.50	618.96	-0.35	171.93	9.50	1446.46	0.65	401.80	9.49	2060.51	1.19	572.36
10.00	619.31	-0.35	172.03	10.00	1444.88	0.66	401.36	9.99	2067.53	1.21	574.31

Shearing Rate 0.0275 mm/min											
Normal Stress 160 kPa				Normal Stress 480 kPa				Normal Stress 750 kPa			
Horizontal Displacement (mm)	Shear Force (kN)	Vertical Displacement (mm)	Shear Stress (kPa)	Horizontal Displacement (mm)	Shear Force (kN)	Vertical Displacement (mm)	Shear Stress (kPa)	Horizontal Displacement (mm)	Shear Force (kN)	Vertical Displacement (mm)	Shear Stress (kPa)
0.00	0.53	0.00	0.15	0.00	0.00	0.00	0.00	0.00	0.00	0.00	0.00
0.50	374.78	-0.04	104.11	0.50	528.56	0.08	146.82	0.50	572.27	0.12	158.96
1.00	444.12	-0.09	123.37	1.00	734.47	0.17	204.02	1.00	899.30	0.27	249.81
1.50	470.98	-0.14	130.83	1.50	849.80	0.24	236.05	1.50	1065.54	0.39	295.98
2.00	486.78	-0.19	135.22	2.00	940.03	0.31	261.12	2.00	1206.85	0.49	335.24
2.50	499.06	-0.23	138.63	2.50	1017.79	0.36	282.72	2.50	1323.58	0.57	367.66
3.00	514.51	-0.27	142.92	3.00	1088.53	0.41	302.37	3.00	1437.69	0.64	399.36
3.50	531.54	-0.30	147.65	3.50	1154.71	0.45	320.75	3.50	1537.04	0.71	426.96
4.00	547.34	-0.32	152.04	4.00	1211.76	0.49	336.60	4.00	1630.96	0.77	453.04
4.50	565.24	-0.35	157.01	4.50	1260.04	0.52	350.01	4.50	1715.57	0.83	476.55
5.00	588.06	-0.36	163.35	4.99	1295.15	0.55	359.76	5.00	1790.17	0.89	497.27
5.50	607.90	-0.37	168.86	5.50	1322.36	0.57	367.32	5.50	1853.02	0.92	514.73
6.00	626.33	-0.38	173.98	5.99	1341.14	0.59	372.54	6.00	1904.63	0.96	529.06
6.50	637.39	-0.38	177.05	6.49	1358.34	0.61	377.32	6.50	1945.00	0.99	540.28
7.00	651.79	-0.38	181.05	6.99	1368.87	0.62	380.24	7.00	1980.11	1.02	550.03
7.50	664.07	-0.39	184.47	7.49	1370.63	0.63	380.73	7.50	2004.69	1.04	556.86
8.00	669.34	-0.39	185.93	7.99	1364.49	0.64	379.02	8.00	2032.42	1.06	564.56
8.50	673.73	-0.40	187.15	8.49	1370.63	0.66	380.73	8.50	2056.47	1.08	571.24
9.00	665.48	-0.40	184.86	8.99	1369.23	0.67	380.34	9.00	2081.57	1.09	578.21
9.50	664.07	-0.40	184.47	9.49	1369.23	0.68	380.34	9.50	2088.95	1.10	580.26
10.00	662.32	-0.40	183.98	9.99	1372.38	0.69	381.22	9.99	2095.62	1.12	582.12

Shearing Rate 0.005 mm/min											
Normal Stress 160 kPa				Normal Stress 480 kPa				Normal Stress 750 kPa			
Horizontal Displacement (mm)	Shear Force (kN)	Vertical Displacement (mm)	Shear Stress (kPa)	Horizontal Displacement (mm)	Shear Force (kN)	Vertical Displacement (mm)	Shear Stress (kPa)	Horizontal Displacement (mm)	Shear Force (kN)	Vertical Displacement (mm)	Shear Stress (kPa)
0.00	0.00	0.00	0.00	0.00	0.00	0.00	0.00	0.00	0.00	0.00	0.00
0.50	426.57	-0.06	118.49	0.50	483.27	0.03	134.24	0.50	657.40	0.10	182.61
1.00	524.52	-0.13	145.70	1.00	790.46	0.06	219.57	1.00	952.84	0.23	264.68
1.50	549.45	-0.19	152.62	1.50	939.15	0.09	260.87	1.49	1129.26	0.32	313.68
2.00	588.06	-0.22	163.35	1.99	1050.79	0.11	291.89	1.99	1263.02	0.39	350.84
2.50	636.34	-0.24	176.76	2.49	1136.28	0.13	315.63	2.49	1378.53	0.45	382.92
3.00	675.84	-0.26	187.73	2.99	1201.23	0.14	333.68	2.99	1491.23	0.51	414.23
3.50	706.20	-0.28	196.17	3.49	1256.00	0.15	348.89	3.49	1601.82	0.56	444.95
4.00	735.52	-0.30	204.31	3.99	1301.29	0.16	361.47	3.99	1703.28	0.61	473.13
4.50	763.26	-0.31	212.02	4.49	1355.71	0.17	376.59	4.49	1798.07	0.65	499.46
5.00	794.50	-0.33	220.69	4.99	1380.28	0.17	383.41	4.99	1870.57	0.69	519.60
5.50	813.28	-0.33	225.91	5.48	1393.45	0.17	387.07	5.48	1938.86	0.72	538.57
6.00	833.47	-0.34	231.52	5.98	1396.08	0.17	387.80	5.98	1993.28	0.75	553.69
6.50	844.36	-0.34	234.54	6.48	1396.08	0.17	387.80	6.48	2042.08	0.77	567.24
7.00	839.97	-0.35	233.32	6.98	1392.92	0.17	386.92	6.98	2073.67	0.78	576.02
7.50	830.31	-0.35	230.64	7.48	1390.47	0.17	386.24	7.48	2095.97	0.78	582.21
8.00	837.33	-0.35	232.59	7.98	1385.20	0.17	384.78	7.98	2116.15	0.79	587.82
8.50	824.69	-0.35	229.08	8.48	1371.51	0.20	380.97	8.48	2119.67	0.79	588.80
8.99	818.02	-0.36	227.23	8.98	1375.90	0.20	382.19	8.97	2120.54	0.79	589.04
9.49	805.74	-0.36	223.82	9.47	1364.49	0.21	379.02	9.47	2124.58	0.80	590.16
9.99	790.46	-0.36	219.57	9.97	1361.85	0.22	378.29	9.97	2120.19	0.80	588.94